U.PORTO

FACULDADE DE CIÊNCIAS
UNIVERSIDADE DO PORTO

MSc

2.º
CICLO

FCUP
UM

2020

U.PORTO

Probiotic *Bacillus* spores as antigen delivery vehicles: towards the development of oral vaccines for aquaculture

Gabriela Catarina Chaves Gonçalves

FC

U.PORTO

FACULDADE DE CIÊNCIAS
UNIVERSIDADE DO PORTO

Universidade do Minho

# Probiotic *Bacillus* spores as antigen delivery vehicles: towards the development of oral vaccines for aquaculture

Gabriela Catarina Chaves Gonçalves

Dissertação de Mestrado apresentada à
Faculdade de Ciências da Universidade do Porto,
Universidade do Minho
Tecnologia e Ciência Alimentar

2020

# Probiotic *Bacillus* spores as antigen delivery vehicles: towards the development of oral vaccines for aquaculture

Gabriela Catarina Chaves Gonçalves

Mestrado em Tecnologia e Ciência Alimentar

Departamento de Química e Bioquímica

2020

**Orientador**

Cláudia R. Serra, Investigadora, CIIMAR

**Coorientador**

Filipe Coutinho, Investigador, CIIMAR

Universidade do Minho


Todas as correções determinadas pelo júri, e só essas, foram efetuadas.

O Presidente do Júri,

Porto, _____/_____/_____

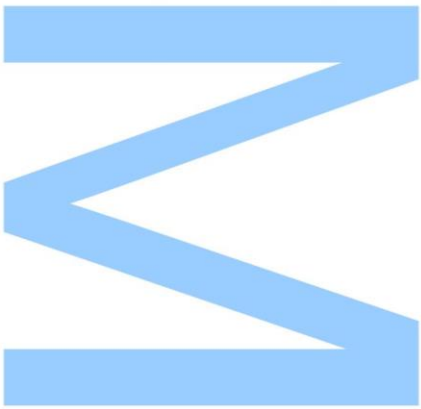

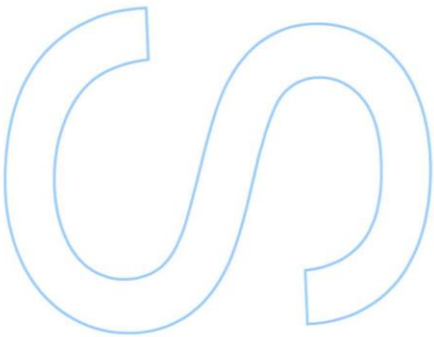

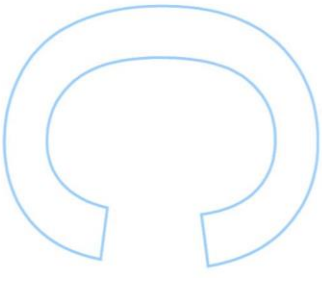

*Se podes olhar, vê. Se podes ver, repara.*

José Saramago

# Acknowledgments

Firstly, I want to thank all NUTRIMU group for welcoming me in such a positive way. Everyone was so supportive and always helped me when I was in need. This experience would not have been the same without all the motivation from Professor Aires. I very much enjoyed the conversations, support and all the funny moments.

To my supervisors, I want to thank all the knowledge passed and all the help in my work. Cláudia, I cannot explain how thankful I am for all your help. I sincerely learned a lot with your expertise. Thank you so much for the patience when I thought there was no solutions, for coming up with several alternative strategies and for being so available.

I would like to thank Professor António Paulo Carvalho for providing us the zebrafish larvae needed to complete this work in such a short notice. To Professor Fernando and the members of the laboratory, thank you for your availability in using several equipment and for the good mood in receiving so many visits from me.

I would also like to thank Eduardo Gomez-Casado from the National Agricultural and Food Research and Technology Institute (INIA), Patricia Diaz-Rosales and Carolina Tafalla Piñeiro from Animal Health Research Center (CISA-INIA) for the experimental assistance.

Rafaela, I would not be able to finish this work without all your help and friendship. Thank you for all your teaching moments, for the patience you had and for being able to help me calm down in not a few existential crises.

To my group of friends, Rúben, Alice, Sara, Sofia, Ana, Daniela, I would like to thank for all your support and patience in hearing my problems and for the long year friendship that never failed me. Also to Cláudia Sofia, thank you for being an incredible friend and laboratory partner, for all the coffee breaks and the help.

To João, for all the patience, attention and for never failing to impress me. You are one of a kind, and I cannot put in words how much you contributed for my achievements and happiness.

And last but definitely not least, to my beloved family. Thank you for the constant support, love and for all the advices you give me! To my mother, thanks for the love and for helping me accomplish my goals.

# Resumo

No setor da aquacultura, a procura por métodos profiláticos mais eficientes é uma tendência. Os métodos mais tradicionais requerem um manuseamento individual dos peixes, trazendo como consequências o stress, o aumento da mortalidade, e nem sempre uma imunização eficaz. Por outro lado, a incorporação de probióticos na alimentação de peixes continua a crescer, dado que os benefícios são diversos e incluem a proteção contra patogéneos e a modulação da imunidade. *Bacillus subtilis* é um probiótico capaz de formar esporos, estruturas altamente resistentes que conseguem sobreviver ao ambiente hostil do trato gastrointestinal do peixe, e germinar. É possível expressar antigénios na superfície dos esporos de *B. subtilis*, ligando-os a proteínas presentes nas camadas protetoras mais superficiais dos esporos e induzir uma resposta imunológica, quando administrados oralmente em ratos.

Neste trabalho utilizamos a estirpe *B. subtilis* 168 como um veículo de apresentação de duas proteínas imunogénicas – VP2, uma proteína do vírus causador da necrose pancreática (IPNV) e OmpK, um antigénio comum a várias espécies bacterianas de *Vibrio* – e a proteína verde fluorescente, GFP. Os genes que codificam as três proteínas foram amplificados contendo uma cauda de 6 histidinas, e clonados em dois vetores, originando fusões translacionais, C-ou-N-terminal, a uma proteína da superfície do esporo– CotY. As fusões foram integradas no cromossoma de *B. subtilis* 168 através de um evento de crossover-duplo no locus *amyE*. A apresentação da VP2 à superfície dos esporos foi avaliada por western blot com um anticorpo anti-VP2, que reconheceu uma banda do tamanho esperado em duas das estirpes recombinantes. Duas bandas do tamanho esperado foram detetadas nos clones que apresentam as fusões C-terminais com GFP e OmpK, utilizando um anticorpo anti-HisTag. As estirpes com as fusões CotY-H6-GFP e H6-GFP-CotY exibiram fluorescência, confirmando a presença de GFP recombinante e funcional à superfície dos esporos. A resistência dos esporos ao calor e à lisozima, essenciais para a sua aplicação oral, foi também testada, revelando que as fusões criadas não comprometeram significativamente a estrutura dos mesmos.

Esporos contendo a versão C-terminal da fusão CotY-H6-OmpK reduziram significativamente a mortalidade de larvas de peixe-zebra expostas a infeção por *V. parahaemolyticus* e *V. anguillarum,* demonstrando o potencial de usar esporos recombinantes com antigénios, como veículos de vacinas orais em aquacultura.

Palavras-chave: Aquacultura, vacinas orais, *Bacillus subtilis*, esporos

# Abstract

Alternative prophylactic measures for infectious diseases are highly demanded when it comes to the aquaculture sector. The usual methods require individual handling of fish and result in stress-related pathologies, mortality and not always an efficient immunization. Simultaneously, the incorporation of probiotics in the fish feed has registered a continual growth, as the beneficial effects are several: protection against pathogens, nutritional benefit, modulation of the mucosal immunity, among others. *Bacillus subtilis* is a probiotic with interesting characteristics, since it can originate spores, highly resistant structures that can survive the gastrointestinal tract of fish and germinate. Antigens can be successfully expressed or displayed at the surface of *B. subtilis* spores if fused to spore coat and crust proteins, inducing an immunological response upon oral administration, as it was already shown in mice.

In this work, we used *B. subtilis* 168 as a delivery vehicle for the presentation of two immunogenic proteins – the VP2 protein, from infectious pancreatic necrosis virus (IPNV) and the OmpK protein, an antigen among *Vibrio* species – and the green fluorescent protein, GFP. The genes encoding for the three proteins were PCR amplified including a tail of 6 histidines, and successfully cloned into two selected vectors, resulting in a translational fusion to a crust protein – CotY, either C-or-N-terminally. The constructed fusions were integrated into the *B. subtilis* 168 chromosome as a result of a double-crossover recombination event at the *amyE* locus. The display of VP2 at the surface of the spores was first evaluated by a western blot analysis with an anti-VP2 antibody that recognized a band of the expected size in two recombinant strains. Using an anti-HisTag antibody, bands of the expected size were detected in the C-terminal fusions of GFP and of OmpK. The recombinant strains carrying both CotY-H6-GFP and H6-GFP-CotY fusions revealed fluorescence, demonstrating the display of a functional protein at the spores' surface. Testing the heat and lysozyme resistance properties of the recombinant spores, essential for their oral delivery, indicated that the display of the target proteins did not affect significantly the spore structure.

Spores containing the C-terminal fusion of CotY-H6-OmpK significantly reduced the mortality of zebrafish larvae exposed to infection by *V. parahaemolyticus* and *V. anguillarum*, demonstrating the potential of using recombinant spores with antigens as oral vaccine vehicles in aquaculture.

Key-words: Aquaculture, oral vaccines, *Bacillus subtilis*, spores

# Table of contents

# Tables list

# Figures list

# Abbreviations list

6His-Tag or H6 – 6 histidine tag

BHI – Brain Heart Infusion

Cfu – Colony forming units

DAPI – 4', 6-Diamidino-2-Phenylindole

$dH_2O$ – Deionized water

dNTPs – Deoxynucleotides triphosphate

Dpf – Days post fertilization

DSM – Difco sporulation medium

DTT – Dithiothreitol

FAO – Food and Agriculture Organization of the United Nations

GFP – Green fluorescence protein

GM – Growth Medium

GRAS – Generally regarded as safe

IPN – Infectious pancreatic necrosis

IPNV – Infectious pancreatic necrosis virus

LB – Luria Bertani

MCE – Mixed cellulose esters

MW – Molecular weight

MWM – Molecular weight marker

OD – Optical density

OMP – Outer membrane protein

PBS – Phosphate buffered saline

PC – Phase contrast

PCR – Polymerase chain reaction

PMSF – Phenylmethylsulfonyl fluoride

RBS – Ribosome binding site

Rpm – Rotations per minute

TAE – Tris – acetate EDTA

WHO – World Health Organization

# 1. Introduction

## 1.1. Aquaculture: an overview

Aquaculture is the process of farming aquatic organisms, which include fish, plant species, crustaceans and mollusks, among others. These farming can occur in both coastal and inland areas, involving activities that enhance the production of the target species when compared with the traditional fishing (Lucas, 2015).

According to a 2020 report of the Food and Agriculture Organization of the United Nations (FAO), the aquaculture sector continues to grow and registered the highest value so far with a production of about 82 million tons of food fish in 2018, which represents 46% of the global fish production (FAO, 2020).

The average fish consumption has increased at an average rate of 3,1% per year, per capita between 1961 and 2017, derived not only from the technologic developments in the sector that allowed the reduction of fish waste, but also due to the rise of awareness of the nutritional and health benefits of fish consumption. This statistics show that fish consumption is increasing at a higher rate than the registered on the remaining animal protein sources (e.g. poultry or swine), which translates in a higher demand of fish supply for human consumption, that has been accomplished with the increase production of aquaculture fish (FAO, 2020).

## 1.2. Diseases in aquaculture

The high demand for fish food resulted in a large-scale intensive type of aquaculture, which has been associated with increasing disease outbreaks among fish and other species produced, bearing severe consequences for the industry profitability and sustainability. Several factors can impact the spread of diseases in aquaculture environments, namely high stocking density, poor water quality, fluctuations in water temperature or introduction of exogenous species (Bayliss et al., 2017). The occurrence of viral and bacterial outbreaks and the presence of parasites constitutes a limiting factor when it comes to the rentability of fish farming. If not properly handled, transfer of infected fish, or contaminated equipment or water, can spread these diseases from pond to pond or from aquafarm to aquafarm.

### 1.2.1. Viral diseases

Several viral pathogens are known to affect aquaculture fish, including the infectious pancreatic necrosis virus (IPNV), infectious salmon anemia virus (ISAV), viral hemorrhagic septicemia virus (VHSV), infectious hematopoietic necrosis virus (IHNV) and channel catfish virus (CCV) (Crane et al., 2011; Kibenge, 2019). These viruses affect fish and crustaceans and can remain viable for weeks, depending on aquatic parameters including temperature, and physicochemical composition (Oidtmann et al., 2018).

#### 1.2.1.1. Infectious pancreatic necrosis

One of the most problematic viral infection is the infectious pancreatic necrosis, a highly contagious disease, caused by IPNV. IPNV belongs to the *Birnaviridae* family and the *Aquabirnavirus* genera. Aquabirnavirus virions have non-enveloped icosahedral symmetry, and their genome consists in two segments (A and B) of linear double-stranded RNA. Segment A encodes a polyprotein that is processed to originate two structural proteins, VP2 and VP3 and a protease (VP4) that is responsible for the cleavage of the polyprotein, among other nonstructural proteins, like VP5 (Balasuriya et al., 2017). VP2 forms the outer capsid and contains the main antigenic sites that trigger antibodies (Lvov et al., 2015), while the inner capsid contains the protein VP3, which is related with the RNA and contains group-specific antigenic elements. Segment B encodes a RNA polymerase, VP1, that exists bonded to the segmented genome ($VP_g$) (Balasuriya et al., 2017). The IPN disease has a high rate of mortality in the young salmonids farmed in freshwater, namely trout and Atlantic salmon. Infected fish appear a darker coloration, swollen abdomen and decolored gills, as well as several lesions in the internal organs (L. Zhu et al., 2017).

### 1.2.2. Bacterial diseases

Among bacterial diseases outbreaks, there is a large group of pathogenic bacteria that can cause illness in different fish species, namely salmonids, turbot, seabass or seabream, but only a small group is responsible for the manifestation of diseases that have a severe impact on marine fish cultures. Some examples of these diseases are vibriosis, photobacteriosis or furunculosis, caused by Gram-negative bacteria belonging to the genera *Vibrio*, *Photobacterium* and *Aeromonas*, respectively, and streptococcosis and mycobacteriosis, caused by members of the Gram-positive genera *Streptococcus* and *Mycobacterium* (Austin et al., 2016; Toranzo et al., 2005). Vibriosis in particular,

caused by members of the genus *Vibrio*, is responsible for massive mortalities in cultured shrimp, fish and shellfish, leading to severe economic losses.

#### 1.2.2.1. Vibriosis

Vibriosis is the term used when referring to a hemorrhagic septicemia after an infection caused by *Vibrio* spp. and is frequently associated with an increase of the water temperature and salinity. In diseased fish and shellfish, the pathogen can be found in the gills and skin, in the gastrointestinal tract and in other internal organs (Ina-Salwany et al., 2019). Infected fish frequently appear lethargic and underweighted, with dark ulcerative lesions and red spots along the laterals of the fish; the eyes can show opacity and can also appear ulcerated (Frans et al., 2011).

*Vibrio* spp. are curved-rod-shaped (comma-like) facultatively anaerobic Gram-negative bacteria that belong to the *Vibrionaceae* family. The majority possess flagella that allows for motility. Their genome is commonly composed by two circular chromosomes (Mohamad et al., 2019). These bacteria are ubiquitous microorganisms in aquatic environments, such as estuaries, coastal waters or sediments, water columns and even in aquatic plants. Their optimal growth temperature varies between 15ºC and 30ºC depending on the strain and normally require salt for growing (Thompson et al., 2004), although capable of surviving in adverse conditions (Takemura et al., 2014).

Within this group of bacteria, some species can be considered as normal fish-colonizers, since their presence does not cause negative effects depending on environmental factors and their host (Raszl et al., 2016), while other species are important fish opportunistic pathogens that cause several consequences in fish farming. Some examples of the later are *V. anguillarum*, *V. parahaemolyticus*, *V. harveyi*, *V. salmonicida* or *V. vulnificus* (Deng et al., 2020). In the case of *V. anguillarum*, a classification into 23 serotypes that exhibit different levels of pathogenicity (O1 – O23) is currently accepted, although only serotypes O1, O2 and O3 are known to cause disease in fish. Serotype O1 also possesses a virulence plasmid that encodes a system that sequesters iron. (Frans et al., 2011).

*Vibrio* spp. have several strategies that contribute to their pathogenicity, including quorum-sensing, a mechanism dependent on the cell-density, that allows the bacteria to communicate and coordinate their behavior (Girard, 2019). Vibrios secrete polysaccharides in the form of capsule or slime to adhere to the host surface, among other molecules like cytotoxins and adhesion factors, and their flagella contribute to the infection of the host (Ina-Salwany et al., 2019). *Vibrio* spp. also produce proteases to

penetrate tissues and hemolysins that cause the cellular lysis of the host and consequence hemorrhagic septicemia (L. Zhang et al., 2013). Other virulence factors include the lipopolysaccharides (LPS), the formation of biofilm, and in some strains, the presence of bacteriophages that enhance their virulence (X. H. Zhang et al., 2020).

## 1.3. Disease control strategies in aquaculture

To overcome losses in aquaculture due to bacterial or viral diseases, several methods have been used, especially in the line of prevention, rather treatment. Some of the most used approaches are dietary supplements, immunostimulants, vaccines, probiotics, prebiotics, antimicrobial molecules, water disinfection and in-feed antibiotics (Assefa et al., 2018).

### 1.3.1. Vaccines

Over the past 30 years, fish vaccination has been studied and several vaccines were developed successfully, with the first vaccine being developed against *Aeromonas salmonicida* (Gudding et al., 2013). Vaccines can be classified as killed (the infectious agent is killed and it is used as an antigen), attenuated (the pathogen loses virulence but it is not killed), DNA (contains one or several genes from the pathogen), recombinant vector (the immunogenic element of the pathogen is expressed in another host), synthetic peptide (short sequences used as antigens) and subunit vaccines (the immunogenic element of the pathogen is used as vaccine). Vaccines can be administrated by oral via, when incorporated into the feed, by immersion of the fish in a concentrated vaccine solution, or by injection, which is the most used vaccination method due to its high efficiency. However, vaccination through injection presents important disadvantages including the stress caused to the fish, the difficulties in handling each fish, and the need for specific-equipment (Assefa et al., 2018).

### 1.3.2. Control of infectious pancreatic necrosis

Fish persistently carrying the IPNV contribute to the horizontal transmission of the virus in the same environment, while infected eggs result in a vertical transmission. Control strategies are based in disinfection and sanitization of the equipment when an outbreak occurs, and the use of vaccines in farmed fish (Balasuriya et al., 2017). Inactivated vaccines are available and involve intraperitoneal injection in each individual: *Alpha Jects® 1000* developed in Norway and *Birnagen Forte* in Chile. The VP2 and VP3

proteins are target antigens involved in the production of antibodies by the host so a few subunit vaccines are available containing these antigens, for example *Norvax®Minova - 6* manufactured in The Netherlands that is an injectable vaccine; an oral subunit vaccine, is also commercialized in Canada and in the United States of America (Ma et al., 2019).

Besides the existence of commercial vaccines, IPN continues to be a disease that bears high mortality among fish in aquaculture. Experimental vaccines have been developed focusing on the orally administrated vaccines (Dhar et al., 2014). Oral DNA vaccines encoding for the *vp2* gene and encapsulated in nanoparticles were developed and revealed to be effective in decreasing the mortality in IPNV challenges (Ahmadivand et al., 2017; Reyes et al., 2017). A recombinant vaccine using the probiotic *Lactobacillus casei* as a delivery vehicle for the presentation of the VP2 protein produced immune responses in rainbow trout (Min et al., 2012).

### 1.3.3. Control of vibriosis

For a long time, antibiotics were commonly used as a treatment to bacterial diseases in cultured fish, including vibriosis outbreaks. The use of antibiotics contributed to its accumulation in the aquatic environment and to the development of antibiotic resistances and the consequence ineffectiveness of the used antibiotics (Frans et al., 2011). Due to these critical consequences, the use of antibiotics has been highly regulated and other strategies to combat vibriosis were adopted (Jun et al., 2003).

Several commercial vaccines are currently available, some examples are: *Vibrogen 2*, an inactivated *V. anguillarum-ordalii* vaccine administrated through immersion, *AquaVac Vibrio Oral*, also an inactivated vaccine in this case orally administrated and *Lipogen Forte*, an injectable vaccine. These vaccines have the limitation of offering protection against some serotypes from *V. anguillarum* and *V. ordalii* among several *Vibrio* spp. that cause diseases (Ina-Salwany et al., 2019).

The development of vaccines against vibriosis has been focusing in using antigens that are common among *Vibrio* spp., thus enhancing the chances of obtaining a more effective and versatile vaccine. Outer membrane proteins (Omp) have been identified as immunogenic proteins that are common among some vibrios (L. Li et al., 2019). Some experimental vaccines have been developing using these proteins as a target: vaccination of Orange-spotted groupers with a recombinant protein OmpK resulted in higher tolerance to Vibrio infections (N. Li et al., 2010). A subunit vaccine involving an OmpK and OmpU fusion resulted in a protective effect against *V. harveyi* infection and showed potential against other *Vibrio* species (Nguyen et al., 2018). Other antigens have

been studied as potential vaccines candidates with promising results like TolC, an Omp from *V. harveyi* (Z. Zhu et al., 2019).

### 1.3.4. Probiotics

Probiotics are defined as “live microorganisms which when administered in adequate amounts confer a health benefit on the host”, accordingly to the FAO and the World Health Organization (WHO) (Hill et al., 2014).

Probiotics used in humans must be considered as GRAS (generally recognized as safe), instigate or maintain a health benefit or a favorable health condition, which is assessed in terms of safety considering the long-term or chronic effects. In the case of probiotics used in animals, the priority is the manifestation of fast effects, which concern the performance and health of the animal and its environment (Singh et al., 2011). Several studies suggest that incorporating probiotics in the fish feed offers nutritional benefits, protection against pathogenic microorganisms and promotes the development of immune responses (Fečkaninová et al., 2017; Newaj-Fyzul et al., 2014). Probiotics can have several functions: exhibit an antagonistic activity, produce antimicrobial compounds to compete for nutrients uptake, produce enzymes that help the host external metabolism, compete for colonization of the mucosal gut surface, blocking pathogen attachment and modulate the mucosal immunity when in contact to pathogens. Various probiotics are used in aquaculture, and some examples are strains of *Bacillus*, *Enterococcus*, *Lactococcus* and *Lactobacillus* (Banerjee et al., 2017).

#### 1.3.4.1. *Bacillus* probiotics

*Bacillus* species are rod-shaped, aerobic or facultative anaerobic, Gram-positive bacteria. An interesting characteristic about *Bacillus* species is the capacity to originate biological structures called endospores (or spores for simplification) by a process in which the cells divide asymmetrically originating two genetically identical cells. Sporulation occurs under unfavorable conditions for the species survival, originating metabolically dormant cells. Bacterial spores are the most resistant biological structure known, resisting desiccation, extreme temperatures, UV and γ-radiation, toxic agents, among other insults (Tan et al., 2014).

*B. subtilis* is by far the best characterized *Bacillus* species, and it has been classified as GRAS, since it is non-harmful to animals and humans. This bacteria is commonly used as a probiotic, including in aquaculture, with several beneficial effects like the

improvement of feed assimilation and water quality (Olmos et al., 2019), as well as immunomodulation, among others (Kuebutornye et al., 2019).

In laboratory conditions, *B. subtilis* takes 8 to 10 hours to initiate the sporulation process, triggered by the deterioration of the environmental conditions, namely starvation and desiccation, by high population density and other cell-cycle signals (de Hoon et al., 2010; Errington, 1993). This results in the phosphorylation of the transcriptional regulator, Spo0A, that activates the transcription of several key sporulation genes (Errington, 2003). The sporulation process (**Figure 1**) begins through an asymmetrical division located at one of the poles of the cell, originating two different compartments: a small compartment called prespore and a larger one called mother cell, separated by a septum with a thin peptidoglycan wall (Higgins et al., 2012).

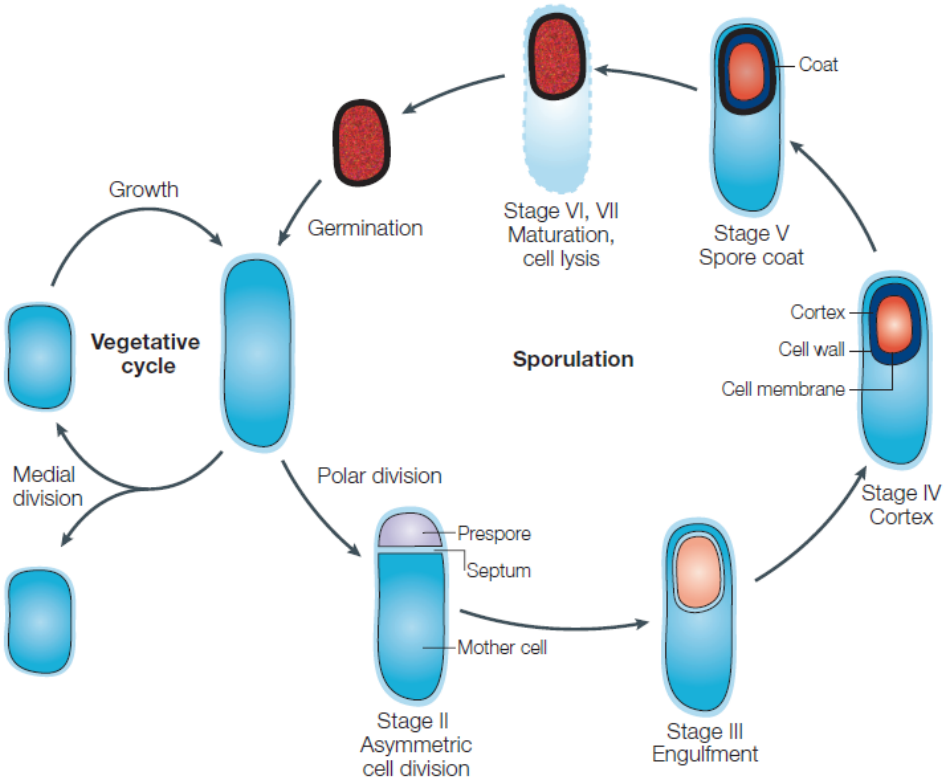


**Figure 1.** Schematic representation of the sporulation process in *Bacillus subtilis*. Retrieved from Errington, 2003.

The onset of the septum involves a period of chromosomal asymmetry: approximately 1/3 of one of the chromosomes is trapped within the prespore while 2/3 remain on the mother cell and are later transferred to the inside of the prespore through a DNA transporter present in the septum (Errington et al., 2005). After this division, the prespore is engulfed by the mother cell, a process that implicates the enzymatic digestion of the

septum wall and the migration of the membrane around the prespore, which becomes a free protoplast inside the mother cell (de Hoon et al., 2010).

Next, several protective layers are assembled around the core of the spore, with the spore cortex (mainly formed by peptidoglycan) being synthesized between the two prespore membranes, as well as the protective proteinaceous coat. The lysis of the cell occurs when the spore is mature to release this resistance form of life to the environment. When the environmental conditions become favorable again, spores enter the germination stage, originating a functional vegetative cell (de Hoon et al., 2010; Henriques et al., 2007; Higgins et al., 2012; Setlow, 2006).

*B. subtilis* spores are composed by several outer layers that protect the inner layers and the core containing the chromosome, from enzymatic, chemical and physical damage (**Figure 2**). For example, the proteinaceous multilayered coat acts as a permeability barrier, protecting the spore from the action of enzymes, such as lysozyme, avoiding the degradation of the peptidoglycan inner cortex, and thus protecting spores from predation (Setlow, 2014). The inner membrane is highly impermeable, restricting the access of chemicals to the spore chromosome. Also, the core's low water content (25 to 55% of wet weight), the presence of dipicolinic acid complexed with $Ca^{2+}$ together with acid-soluble spore proteins (SASPs) bound to DNA, guarantee spore dormancy while protecting it from desiccation, wet and dry heat, UV and γ-radiation (Setlow, 2014).

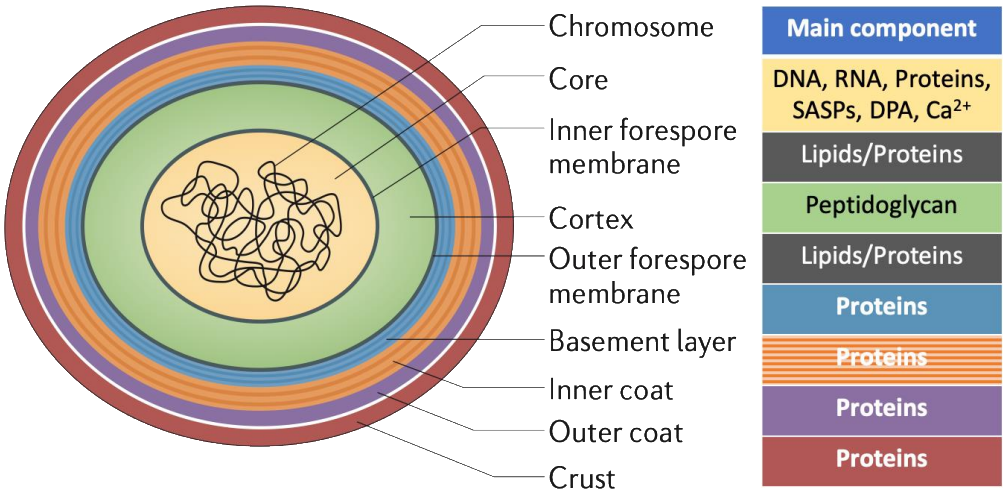


**Figure 2.** Schematic representation of a *B. subtilis* spore. The structure is composed by an outerlayer, the crust, followed by the coat, an outer membrane, the cortex, an inner layer and the core, where the chromosome is located. Adapted from McKenney, 2013.

The multilayer spore coat contains at least 70 identified proteins, and it can be divided in at least 4 layers: under coat, inner coat, outer coat and a glycoprotein layer named crust (Plomp et al., 2014). Some proteins are crucial for the assembly of the spore coat and were named morphogenetic proteins, which include SpoIVA, SpoVM, SpoVID, SafA and CotE. The assembly of the spore coat is dependent on several interactions between these morphogenetic proteins and other proteins that contribute to the composition of each layer (McKenney et al., 2013).

## 1.4. *Bacillus subtilis* spores as a vehicle for oral vaccination: towards the development of SporoVaccines for aquaculture

Several studies indicate that antigens can be successfully displayed at the surface of *B. subtilis* spores if fused to spore coat proteins. Different recombinant proteins were able to induce an immunological response upon oral administration in mice, showing improved immunization rates in comparison with oral immunization with soluble antigens, since they are most likely degraded in the gastrointestinal tract (Das et al., 2016; Duc et al., 2007; Duc et al., 2003; Lega et al., 2016; Mauriello et al., 2004).

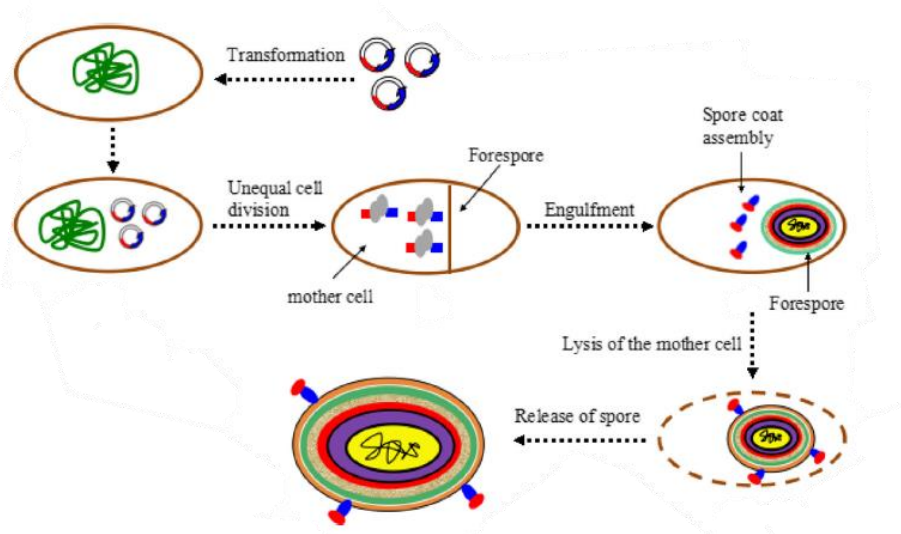


**Figure 3.** Schematic representation of the display of recombinant proteins in *B. subtilis* spores' surface through the chromosomal integration method. Adapted from Wang, 2017.

Two methods can be used for the display at the spore surface: chromosomal integration of recombinant proteins (**Figure 3**) (Hinc et al., 2010; Liu et al., 2019) or adsorption of the purified target protein through a combination of electrostatic and hydrophobic interaction (Isticato et al., 2014; Isticato et al., 2013; Lanzilli et al., 2018). This later

method is still under development and absorption rates appear to be higher in mutants that present an altered outermost layer (Sirec et al., 2012).

To successfully display a recombinant protein (**Figure 3**) at the surface of the spore, different properties must be considered including the chosen anchor protein, the site of insertion of the fusion, the possibility of a linker peptide between the anchor and the target protein to display (Lin et al., 2020). Several proteins from the spore coat and crust have been used as anchor motifs (**Table 1**), including CotB, CotC, CotE, CotG, CotX, CotZ, CotY, OxdD and CgeA (H. Wang et al., 2017).

**Table 1.** Examples of protein display at the surface *B. subtilis* spores

| Anchor coat protein* | Protein displayed | Reference |
|---|---|---|
| CotG | Haloalkane dehalogenase, DdhA from *Rhodococcus rhodochrous.* The protein retained its enzymatic activity. | (F. Wang et al., 2019) |
| CotB<br>CotC<br>CotG | Urease, UreA, from *Helicobacter acinonychis.* UreA was displayed on the surface when fused to CotB. The fusion with CotC resulted in the most efficient expression of UreA. The fusion with CotG appeared to be partially processed. | (Hinc et al., 2010) |
| CotC | Paramyosin, CsPmy, from *Clonorchis sinensis.* CsPmy maintained its immunogenicity, and the administration of recombinant spores elicited an immune response in mice. | (Sun et al., 2018) |
| OxdD | Endogenous Phytase, Phy, from *Bacillus subtilis.* The recombinant spores showed phytase activity. | (Potot et al., 2010) |
| CotC | Outside capsid protein, VP4, from grass carp reovirus. The administration of recombinant spores resulted in protection of the fish against the virus. | (Jiang et al., 2019) |
| CotC | Outer membrane protein, OmpC, from *Salmonella* serovar Pullorum. Oral immunization with recombinant spores induced protection in mice against a *Salmonella* challenge. | (Dai et al., 2018) |
| CotC | Ag85B and CFP10, from *Mycobacterium tuberculosis.* Mice immunized with recombinant spores induced specific immune response. | (Das et al., 2016) |

* CotB, CotC and CotG are outer coat proteins; OxdD is an inner coat protein.

## 1.5. Zebrafish larvae as a model of infection

Zebrafish larvae have been recently used as a model to study bacterial infections, the innate immune system of invertebrates and also inflammatory processes, since larvae only possess an innate immunity system during the first three weeks upon fertilization

(Lam et al., 2004). Infection of zebrafish larvae has several advantages including the possibility of immersion rather than injection with the bacteria, as well as the capacity of real time observations, since larvae are transparent in early life stages (Varas et al., 2017). Larvae were also used to study the interaction with probiotics, which resulted in a decreased state of inflammation (Rendueles et al., 2012). Zebrafish larvae were used to study the model of infection of the bacteria *V. anguillarum*, one of the pathogen agents that cause vibriosis in fish. The infection resulted in the suppression of several innate immune genes and culminated in total mortality within 96 hours post infection (Oyarbide et al., 2015). Other studies were able to test the protective effect of two probiotic candidate yeasts, antibacterial compounds, and phage therapy against infection with *V. anguillarum*, elucidating the potential of the use of larvae to study vaccine candidates (Caruffo et al., 2016; Silva et al., 2014; L. Zhang et al., 2017).

## 1.6. Objectives of this study

Due to the resistance properties of *B. subtilis* spores, described earlier in this thesis, that translate to their suitability to be use as oral display systems (e.g. resistance to incorporation into fish feed; resistance to passage through the gut), the development of a recombinant spore carrying antigens against the major fish diseases, for use in fish aquaculture is an attractive goal. Ideally, would be to build a ProbioSporoVaccine using a probiotic strain isolated from the fish gut, as a way of maximizing its efficacy on the host.

Thus, the aim of this project was to use a probiotic *B. subtilis* strain (FI99), previously isolated from the gut of European seabass and characterized in the laboratory of the present work, as a delivery vehicle for the presentation of target antigens. The VP2 protein from IPNV, and the OmpK protein from *Vibrio* spp. were chosen as the antigen targets since both are immunogenic proteins from pathogens that cause severe disease outbreaks in aquaculture environments. By translationally fusing the genes encoding the target antigens to the genes of three different coat proteins: CotB, CotC and CotY, either N-or-C-terminally, this work aimed at assess the antigenic potential of the recombinant spores by measuring their ability to modulate the immune response and the survival of zebrafish larvae upon a challenge.

# 2. Material and Methods

## 2.1. General methods

Luria-Bertani (LB) (Fisher BioReagents) medium was used for the routine growth and transformations of *Bacillus subtilis* and *Escherichia coli* strains. Brain Heart Infusion (BHI) (Becton Dickinson) medium was used for the growth of *Vibrio vulnificus*, *V. anguillarum* and *V. parahaemolyticus*. All routine incubations were performed at 37ºC overnight with agitation at 140 rpm when cultured in liquid medium. For *B. subtilis* strains, and when appropriate, chloramphenicol (5 µg $mL^{-1}$) was used, and ampicillin (100 µg $mL^{-1}$) was used for *E. coli* strains.

## 2.2. Plasmids and strains construction

The bacterial strains, plasmids and oligonucleotide primers used in this work are listed in **Table 2**, **Table 3** and **Table 4**, respectively.

### 2.2.1. DNA extraction

A single colony from *B. subtilis* and *V. vulnificus* (**Table 2**) was inoculated in 5 mL of LB or BHI, respectively, and grown overnight at 37ºC with agitation. 2 mL of each culture were centrifugated at 13000 rpm for 10 min and the pellet was resuspended in 500 µL of SET buffer (20% saccharose, 20 mM Tris pH=8 and 10 mM EDTA), followed by an incubation at 37ºC for an hour with 100 mM of RNase and 500 mM of freshly prepared lysozyme (Sigma), which degrades RNA and promotes cellular lysis. A second incubation at 37ºC for 2 hours was carried out after adding 120 mM of proteinase K along with 0,5% of sarkosyl to denature proteins by cleavage of the peptide bonds. After the incubation, 560 µL of phenol: chloroform: isoamyl-alcohol (25:24:1) were added, mixed, and the sample centrifuged at 8000 rpm for 10 min. The aqueous fraction, which has the DNA, was then mixed with the same volume of chloroform: isoamyl alcohol (24:1) and centrifuged at 8000 rpm for 10 min. The aqueous fraction was then removed to a new Eppendorf and 20 µL were dialyzed against MiliQ water in a 0.025 µm mixed cellulose esters (MCE) membrane filter (Millipore) for 30 min. The dialyzed DNA was then transferred into a new Eppendorf and stored at -20ºC.

**Table 2.** Bacterial strains used in this work.

| Bacterial strain | Relevant genotype / phenotype [a] | Source, Reference or construction [b] |
|---|---|---|
| *E. coli* DH5α | fhuA2Δ(argF-lacZ)U169 phoA glnV44 Φ80 Δ(lacZ)M15 gyrA96 recA1 relA1 endA1 thi-1 hsdR17 | Commercial strain (Nzytech Lda. MB004) |
| *B. subtilis* 168 | trpC2 | A.O.Henriques (Kunst et al., 1997) |
| *B. subtilis* FI99 | Fish isolate with probiotic properties | NUTRIMU collection (Serra et al. 2019) |
| *Vibrio vulnificus* LMG 13545, ATCC 27562 | Type Strain, Biohazard group 2 | BCCM/LMG |
| *Vibrio anguillarum* DSM 21597, ATCC 19264 | Type Strain, Biohazard group 2 | DSMZ |
| *Vibrio parahaemolyticus* LMG 2850, ATCC 17802 | Type Strain, Biohazard group 2 | BCCM/LMG |
| CRS203 | *cotB-vp2*, $Ap^R$ | This study: *E. coli* DH5α x pGG1 |
| CRS204 | *cotC-vp2*, $Ap^R$ | This study: *E. coli* DH5α x pGG2 |
| CRS205 | $P_{cotYZ}$-*cotY-vp2*, $Ap^R$ | This study: *E. coli* DH5α x pGG3 |
| CRS207 | $P_{cotYZ}$- *vp2-cotY*, $Ap^R$ | This study: *E. coli* DH5α x pGG4 |
| CRS210 | $P_{cotYZ}$-*cotY-6His-vp2*, $Ap^R$ | This study: *E. coli* DH5α x pGG5 |
| CRS211 | $P_{cotYZ}$-*6His-vp2-cotY*, $Ap^R$ | This study: *E. coli* DH5α x pGG6 |
| CRS212 | $P_{cotYZ}$-*cotY-6His-gfp*, $Ap^R$ | This study: *E. coli* DH5α x pGG7 |
| CRS213 | $P_{cotYZ}$-*6His-gfp-cotY*, $Ap^R$ | This study: *E. coli* DH5α x pGG8 |
| CRS214 | $P_{cotYZ}$-*cotY-6His-ompK*, $Ap^R$ | This study: *E. coli* DH5α x pGG9 |
| CRS215 | $P_{cotYZ}$-*6His-ompK-cotY*, $Ap^R$ | This study: *E. coli* DH5α x pGG10 |
| CRS206 | amyE::$P_{cotYZ}$-*cotY-vp2*, $Cm^R$ | This study: *B. subtilis* 168 x pGG3 |
| CRS208 | amyE::$P_{cotYZ}$-*vp2-cotY*, $Cm^R$ | This study: *B. subtilis* 168 x pGG4 |
| CRS216 | amyE::$P_{cotYZ}$-*cotY-6His-vp2*, $Cm^R$ | This study: *B. subtilis* 168 x pGG5 |
| CRS217 | amyE::$P_{cotYZ}$-*6His-vp2-cotY*, $Cm^R$ | This study: *B. subtilis* 168 x pGG6 |
| CRS218 | amyE::$P_{cotYZ}$-*cotY-6His-gfp*, $Cm^R$ | This study: *B. subtilis* 168 x pGG7 |
| CRS219 | amyE::$P_{cotYZ}$-*6His-gfp-cotY*, $Cm^R$ | This study: *B. subtilis* 168 x pGG8 |
| CRS220 | amyE::$P_{cotYZ}$-*cotY-6His-ompK*, $Cm^R$ | This study: *B. subtilis* 168 x pGG9 |
| CRS221 | amyE::$P_{cotYZ}$-*6His-ompK-cotY*, $Cm^R$ | This study: *B. subtilis* 168 x pGG10 |

[1] Antibiotic resistance indicated: Ap – ampicillin, Cm – chloramphenicol, Km – kanamycin.
[2] Bacterial strains were obtained from bacterial collections (BCCM/LMG, Belgian Coordinated Collections of Microorganisms, Laboratory of Microbiology, Department of Biochemistry and Microbiology, Faculty of Sciences of Ghent University, Ghent, Belgium; DSMZ, DSM Collection, German Collection of Microorganisms and Cell Cultures, Braunschweig, Germany; from our laboratory stocks (NUTRIMU collection) or kindly supplied by A. O. Henriques (Instituto de Tecnologia Química e Biológica António Xavier, Universidade Nova de Lisboa, Portugal).

**Table 3.** Plasmids used in this work.

| Plasmid | Relevant genotype | Source or construction |
|---|---|---|
| pMCV1.4 VP2015 | *neo km vp2* | Tafalla Lab (CISA-INIA) |
| pMS157 | *bla km gfp* | (Steil et al., 2005) |
| pDG364 | *bla cat* | (Cutting, 1990) |
| p1CSV-CotY-C | *bla amyE3´ $P_{cotYZ}$-cotY-rfp cat amyE5´* | (Bartels et al., 2018) |
| p1CSV-CotY-N | *bla amyE3´ $P_{cotYZ}$-rfp-cotY cat amyE5´* | (Bartels et al., 2018) |
| pGG1 | *$Ap^R$ $Cm^R$ cotB-vp2* | This study |
| pGG2 | *$Ap^R$ $Cm^R$ cotC-vp2* | This study |
| pGG3 | *bla amyE3´ $P_{cotYZ}$-cotY-vp2 cat amyE5´* | This study |
| pGG4 | *bla amyE3´ $P_{cotYZ}$-vp2-cotY cat amyE5´* | This study |
| pGG5 | *bla amyE3´ $P_{cotYZ}$-cotY-6His-vp2 cat amyE5´* | This study |
| pGG6 | *bla amyE3´ $P_{cotYZ}$-6His-vp2-cotY cat amyE5´* | This study |
| pGG7 | *bla amyE3´ $P_{cotYZ}$-cotY-6His-gfp cat amyE5´* | This study |
| pGG8 | *bla amyE3´ $P_{cotYZ}$-6His-gfp-cotY cat amyE5´* | This study |
| pGG9 | *bla amyE3´ $P_{cotYZ}$-cotY-6His-ompK cat amyE5´* | This study |
| pGG10 | *bla amyE3´ $P_{cotYZ}$-6His-ompK-cotY cat amyE5´* | This study |

## 2.2.2. Amplification of target genes

### 2.2.2.1. Amplification of cotB, cotC and vp2 for cloning into pDG364

To obtain the different gene fusions, the sequences of *cotB* and *cotC* genes were retrieved from the genome of *B. subtilis* 168, available at the Subtilist World-Wide Web Server (http://genolist.pasteur.fr/SubtiList/). Sequences were exported with an excess of nucleotides to include both promoters and copied to the SnapGene Viewer 5.0.8 Software for further analysis and design of primers. In the case of *cotB*, only the sequence encoding the first 275 amino acids from the start codon was used for the polymerase chain reaction (PCR), since the C-terminus of CotB is constituted by a 27 amino acid sequence that results in genetic instability (Isticato R., 2004).

To amplify the *cotB* and *cotC* sequences, two sets of primers were designed based on oligonucleotides cotB-up, cotB-dn, cotC-up, and cotC-dn used in Hinc et al., 2010. Three nucleotides were added between the restriction site of HindIII and the 5´-end of cotB-up, originating cotB-263F to assure the cleavage efficiency (**Table 4**). Four nucleotides were added to the 3'-end of cotC-up to increase the primer stability, originating cotC-23F (**Table 4**). The restriction original sites present in both cotB-dn and cotC-dn were

eliminated. 14 or 12 nucleotides were added to allow the overlapping with the 5'-end of the *vp2* sequence, which originated cotB-vp2+826R and cotC-vp2+354R (**Table 4**).

Oligonucleotides vp2-cotB-2F and vp2-cotC-1F (**Table 4**), were designed to include 15 nucleotides from the 3'-end of *cotB* or *cotC* target sequences. Oligonucleotide vp2+1417R (**Table 4**) was designed to anneal to the bottom strand of the 3'-end of the vp2 sequence and contain a recognition site for the restriction endonuclease HindIII.

To obtain an 1112 bp fragment of *cotB*, oligonucleotides cotB-263F, annealing at nucleotides –263 to –244 from the start codon and cotB-vp2+826R, annealing at nucleotides 804 to 825 were used as primers in a PCR.

Oligonucleotides cotC-23F, annealing at nucleotide –23 to –1 from the start codon of *cotC* and cotC-vp2+354R, annealing at nucleotide 327 to 354 were used as primers to amplify the *cotC* sequence, eliminating the stop codon at the end of the sequence and originating a fragment of 399 bp (**Table 4**).

Two fragments of 1443 bp from the *vp2* sequence were obtained (*vp2B* and *vp2C*), using two sets of primers: oligonucleotides vp2-cotB-2F annealing at nucleotides –2 to 21 from the start codon of the *vp2* sequence, and vp2+1417R, annealing at nucleotides 1395 to 1317, to amplify a fragment with 15 nucleotides that overlaps with the 3'-end of the *cotB* sequence and oligonucleotides vp2-cotC-1F annealing at nucleotides –1 to 21 from the start codon of the *vp2* sequence, and vp2+1417R to amplify a fragment that overlaps with the 3'-end of the *cotC* sequence (**Table 4**).

**Table 4.** List of oligonucleotide primers used in this study. Native or introduced restriction sites are indicated in different colors (NgoMIV, XbaI, AgeI, SpeI) or underlined (HindIII). Length in DNA bases and the melting temperature (Tm) at 50 nM of NaCl are indicated.

| Primer name | Sequence (5'-3') | Length (bases) | Tm (ºC) |
|---|---|---|---|
| cotB-263F | ACCCAAGCTTACGGATTAGGCCGTTTGTC | 29 | 63.7 |
| cotC-23F | ACCCAAGCTTTGTAGGATAAATCGTTTGGGCC | 32 | 63.4 |
| cotB-vp2+826R | TTGTTTGTGTTCATGGATGATTGATCATCTGAAGA | 35 | 59.8 |
| cotC-vp2+354R | GTTTGTGTTCATGTAGTGTTTTTTATGCTTTTTATACTC | 39 | 57.6 |
| vp2-cotB-2F | GATGATCAATCATCCATGAACACAAACAAGGCAAC | 35 | 61.2 |
| vp2-cotC-1F | CATAAAAAACACTACATGAACACAAACAAGGCAAC | 35 | 59.1 |
| vp2+1417R | GACCCAAGCTTCCTCGAGGGATCCTTATGCCAT | 33 | 66.4 |
| cotY-vp2-F | GATCGAATTCGCGGCCGCTTCTAGAAAGGAGGTGGCCGGCATGAACACAAACAAGGCAACCGCA | 64 | 92.0 |
| cotY-vp2-R | AGCTCTGCAGCGGCCGCTACTAGTATTAACCGGTTGCCATTGGAAACAGCGTGGACAGT | 59 | 72.9 |
| 6His-vp2-F | ATGCATCACCATCACCATCACATGAACACAAACAAGGCAACCGCA | 45 | 69.1 |
| 6His-SpoVec-F | GATCGAATTCGCGGCCGCTTCTAGAAAGGAGGTGGCCGGCATGCATCACCATCACCATCAC | 61 | 91.0 |
| 6His-gfp-F | ATGCATCACCATCACCATCACATGAGTAAAGGAGAAGAACTTTTC | 45 | 64.5 |
| gfp-SpoVec-R | AGCTCTGCAGCGGCCGCTACTAGTATTAACCGGTTTTGTATAGTTCATCCATGCCATG | 58 | 69.8 |
| 6His-ompK-F | ATGCATCACCATCACCATCACGACGGCGATATCCACAAAAACGAT | 45 | 68.3 |
| ompK-SpoVec-R | AGCTCTGCAGCGGCCGCTACTAGTATTAACCGGTCTTGTAAGTTACTGCGACGTAGTG | 58 | 70.4 |
| amyE-F | CGGTTTGAAAGGAGGAAGCGGAAGAATG | 28 | 61.4 |
| amyE-R | CAAAGCCAGGCTGATTCTGACCGGGCAG | 28 | 66.6 |

The preparation of PCR reactions was carried out on ice, using Phusion™ High-Fidelity DNA Polymerase (Thermo Scientific™) accordingly to the manufacturer's instructions. Briefly, a single 50 µL reaction contained 1x Phusion™ HF buffer, 0.2 mM of deoxyribonucleotides triphosphate (dNTPs), 0.5 µM of each primer and 1U of Phusion™ High-Fidelity DNA Polymerase. For the amplification of *cotB* and *cotC*, 3 µL of chromosomal DNA from *B. subtilis* 168 was used as template, whereas for the amplification of *vp2B and vp2C*, a dilution of 1:10 was done to pMCV1.4 VP2015 (**Table 3**) prior to the use of 3 µL as template. All reactions were performed in a T100 Thermal Cycler (Bio-Rad), with an initial denaturation step performed at 98ºC for 30s, followed by 34 cycles of denaturation at 98ºC for 10s, annealing at the 59ºC (for *cotB*), 57ºC (for *cotC*), 61ºC (for *vp2B*) or 59ºC (for *vp2C*) for 30s, extension at 72ºC for 30s (for *cotB*),15s (for *cotC*) or 45s (for *vp2B* and *vp2C*) and a final cycle of extension during 10 min at 72ºC. 5 µL of each PCR reaction were loaded in a 1% agarose gel stained with 4% of GreenSafe Premium (NzyTech), along with 5 µL of GeneRuler DNA Ladder Mix (Thermo Scientific). The electrophoresis was carried out at a constant voltage of 100V in 1x Tris-Acetate-EDTA (TAE) buffer. The gel was visualized in a Gel-Doc XR$^+$ System, using the Image Lab Software (Bio-Rad).

Before further use, PCR products (*cotB*, *cotC, vp2B,* and *vp2C*) were purified using the illustra™ GFX™ PCR DNA and Gel Band Purification Kit (GE Healthcare) accordingly to the manufacturer's instructions. 5 µL of each purified product were visualized for DNA integrity on a 1% agarose gel as previously described.

To obtain a translational fusion of *cotB* and *cotC* with *vp2*, two overlapping PCRs were carried out, in the same conditions described previously. As DNA templates, 3 µL of the purified *cotB* or *cotC* PCR products*,* and 2 µL of the purified *vp2B* or *vp2C* PCR products were used. Two fusions were obtained: *cotB-vp2* (2528 bp) and *cotC-vp2* (1815 bp). Both overlapping PCRs were carried out as previously described, and consisted of an initial denaturation step performed at 98ºC for 30s, followed by 34 cycles of denaturation at 98ºC for 10s, annealing at 63ºC for 30s, extension at 72ºC 78s, and a final cycle of extension during 10 min at 72ºC. 5 µL of each overlapping PCR were visualized for DNA integrity on a 1% agarose gel as previously described.

Each purified PCR reaction was sent to STAB VIDA (https://www.stabvida.com/pt) for sequencing with the same set of primers used for the overlapping PCR reaction.

#### 2.2.2.2. Amplification of *vp2* and *6His-vp2* for cloning into p1CSV-CotY-C and p1CSV-CotY-N

A set of primers was designed following the indications included in the Supplemental Material of *Sporobeads: The Utilization of the Bacillus subtilis Endospore Crust as a Protein Display Platform* (Bartels et al., 2018). Oligonucleotides cotY-vp2-F and cotY-vp2-R (**Table 4**) were designed to anneal to the 5'-end and 3'-end of the *vp2* gene and include an overhang sequence containing the necessary restriction sites for cloning into the chosen vectors.

A second version of the same target sequence was constructed aiming to facilitate the detection of the viral protein in the spore's coat. For that, oligonucleotide 6His-vp2-F was designed to anneal to the top strand of the *vp2* sequence, containing a sequence of nucleotides that translate into six histidines (6His-tag), N-terminally. Oligonucleotide 6His-SpoVec-F (**Table 4**) anneals to the sequence encoding the 6His-tag and contains the necessary restriction sites for cloning into the chosen vectors.

Plasmid pMCV1.4 VP2015 (**Table 3**) was used as template to PCR amplify a 1475 bp fragment (*vp2*), using oligonucleotides cotY-vp2-F annealing at nucleotides –1 to 24 from the start codon of the *vp2* sequence, and cotY-vp2-R, annealing at nucleotides 1376 to 1401 as primers (**Table 4**). A fragment of 1456 bp was amplified by PCR using oligonucleotide primers 6His-vp2-F, which anneals at nucleotides –1 to 24 from the start codon of the *vp2* sequence, and cotY-vp2-R (**Table 4**). After purification carried out as previously described, the fragment was used as template for a second PCR with oligonucleotides 6His-SpoVec-F and CotY-vp2-R as primers (**Table 4**), resulting in a 1496 bp fragment (*6His-vp2*).

PCRs were carried out as previously described and consisted of an initial denaturation step performed at 98ºC for 30s, followed by 34 cycles of denaturation at 98ºC for 10s, annealing at 72ºC (*vp2*) or 70ºC (*6His-vp2*) for 30s, extension at 72ºC for 45s and a final extension at 72ºC for 10 min. 5 µL of each PCR were resolved on a 1% agarose and purified as described before.

#### 2.2.2.3. Amplification of *6His-gfp* and *6His-ompK* for cloning into p1CSV-CotY-C and p1CSV-CotY-N

Oligonucleotides 6His-gfp-F and 6His-ompK-F (**Table 4**) were designed to anneal to the top strand of each target gene, containing a sequence of nucleotides that translate into six histidines, N-terminally. Oligonucleotides gfp-SpoVec-R and ompK-SpoVec-R (**Table**

**4**) anneal to 3'-end of the target genes and include an overhand sequence that contains the necessary restriction sites for cloning into the chosen vectors.

A plasmid containing the *gfp* sequence, pMS157 (**Table 3**), was used as the template of a PCR using oligonucleotides 6His-gfp-F that anneals at nucleotides –1 to 24 from the start codon of the *gfp* sequence, and gfp-SpoVec-R (**Table 4**), which anneals at nucleotide 693 to 714, resulting in the amplification of a 769 bp fragment encoding a 6His-tag N-terminally. After purification carried out as previously described, the fragment was used as template for a second PCR with oligonucleotides 6His-SpoVec-F and gfp-SpoVec-R as primers (**Table 4**), resulting in an 809 bp product (*6His-gfp*).

The amplification of *ompK* started at position 73 to eliminate the sequence encoding for the signal peptide (first 60 nucleotides) and to initiate at a common region of the sequences of each protein selected among the *Vibrio* spp. considered in this work. DNA extracted from *Vibrio vulnificus* (**Table 2**) (as described in section 2.2.1) was used as template of a PCR, performed with oligonucleotides 6His-ompK-F, which anneals at nucleotides 73 to 92 from the start codon and ompK-SpoVec-R (**Table 4**), annealing at nucleotides 785 to 803, resulting in a 787 bp fragment encoding a 6His-tag N-terminally. After purification carried out as previously described, the fragment was used as template for a second PCR with oligonucleotides 6His-SpoVec-F and ompK-SpoVec-R as primers (**Table 4**), originating an 827 bp product (*6His-ompK*).

PCRs were carried out as previously described 2.2.2.1 and consisted of an initial denaturation step performed at 98ºC for 30s, followed by 34 cycles of denaturation at 98ºC for 10, extension at 72ºC for 24s (initial fragments containing encoding 6His-tag) or 26s (*6His-gfp* and *6His-ompK*), and a final extension step at 72ºC for 10 min.5 µL of each PCR were loaded in a 1% agarose and purified as previously described.

## 2.2.3. Cloning into plasmid vectors

### 2.2.3.1. Cloning of *cotB-vp2* and *cotC-vp2* into pDG364

To obtain the two translational fusions of VP2 to two different coat proteins – CotB or CotC – the purified inserts (*cotB-vp2* and *cotC-vp2*) and the vector pDG364 (**Table 3**) were digested with the restriction endonuclease HindIII (Thermo Scientific).

Digestions of both inserts and pDG364 were separately carried out with HindIII in a 30 µL reaction mix containing 1x Buffer R, 10U of HindIII, nuclease-free water, and 20 µL of *cotB-vp2* or *cotC-vp2* or pDG364, and incubated at 37ºC for 30 min. The restriction enzyme was heat-inactivated at 80ºC for 20 min and the reaction mix was purified using the illustra™ GFX™ PCR DNA and Gel Band Purification Kit accordingly to the

manufacturer's instructions. 5 µL of each purified sample were loaded in a 1% agarose gel as previously described, to confirm the size of inserts and to assure the successful digestion.

To avoid self-ligation of the digested pDG364, a 40 µL reaction of dephosphorylation was carried out containing 1U Anza™ Alkaline Phosphatase (Invitrogen), 1x Anza™ 10x Buffer and 30 µL of digested pDG364, incubated at 37ºC during 15 min followed by heat-inactivation of the enzyme at 80ºC for 5 min.

A ligation reaction of 10 µL was prepared with 4 µL of the target digested insert, 2 µL of digested pDG364, 1x T4 DNA Ligase Buffer, 1U of T4 DNA Ligase (Thermo Scientific), nuclease-free water, and incubated at 4ºC overnight.

#### 2.2.3.2. Cloning of *vp2*, *6His-vp2*, *6His-gfp* and *6His-ompK* into p1CSV-CotY-C and p1CSV-CotY-N

To obtain the different translational fusions of VP2, 6His-VP2, 6His-GFP and 6His-ompK to a crust protein – CotY – the inserts (*vp2*, *6His-vp2*, *6His-gfp* and *6His-ompK*) were sequentially digested with the appropriate restriction endonucleases along with the chosen vectors – p1CSV-CotY-C and p1CSV-CotY-N (**Table 3**). All digestions were carried out in a final volume of 30 µL.

For the N-terminal variants, each insert, and the vector p1CSV-CotY-N were firstly digested with Anza™ XbaI (Invitrogen). Reactions were carried out containing 1x Anza™ Buffer, 10U of Anza™ XbaI, nuclease-free water, and 20 µL of *vp2*, *6His-vp2*, *6His-gfp* or *6His-ompK* or 15 µL of p1CSV-CotY-N and incubated at 37ºC for 2h. After the first digestion, each reaction was dialyzed against MiliQ water in a 0.025 µm MCE membrane filter for 30 min and transferred to a new Eppendorf. The second digestion of the inserts was carried out with AgeI (Thermo Scientific). The reactions contained 1x Buffer O, 10U of AgeI, nuclease-free water, and 20 µL of the purified insert digested with XbaI, and incubated at 37ºC for 2,5h. The reaction was again dialyzed against MiliQ water, transferred to a new Eppendorf, and stored at -20ºC. The second digestion of the vector was carried out with NgoMIV (New England BioLabs), and contained 1x CutSmart Buffer®, 10U of NgoMIV, nuclease-free water, and 20 µL of the purified digested vector, and incubated at 37ºC for 2h. This reaction was also dialyzed against MiliQ water, transferred to a new Eppendorf, and stored at -20ºC.

For the C-terminal variants, each insert was firstly digested with NgoMIV. Reactions were carried out containing 1x CutSmart Buffer®, 10U of NgoMIV, nuclease-free water, and 20 µL of *6His-vp2*, *6His-gfp* or *6His-ompK* and incubated at 37ºC for 2h. After that, each

reaction was dialyzed against MiliQ water in a 0.025 µm MCE membrane filter for 30 min and transferred to a new Eppendorf. The second digestion of the inserts was carried out with SpeI (Thermo Scientific). The reactions contained 1x Buffer Tango, 10U of SpeI, nuclease-free water, and 20 µL of the purified insert digested with NgoMIV and incubated at 37ºC for 2h. The reaction was again dialyzed against MiliQ water, transferred to a new Eppendorf, and stored at -20ºC. The first digestion of the vector p1CSV-CotY-C was carried out with SpeI and contained 1x Buffer Tango, 10U of SpeI, nuclease-free water and 15 µL of p1CSV-CotY-C and incubated at 37ºC for 2,5h. After that, the reaction was dialyzed against MiliQ water and transferred to a new Eppendorf. The second digestion was carried out with AgeI, and reaction contained 1x Buffer O, 10U of AgeI, nuclease-free water, and 20 µL of the purified digested vector, and incubated at 37ºC for 2,5h. The reaction was finally dialyzed against MiliQ water, transferred to a new Eppendorf, and stored at -20ºC.

5 µL of each insert and vector digested were loaded in a 1% agarose gel as previously described, to confirm the size of inserts and to assure successful digestion.

A ligation reaction of 10 µL was prepared with 4 µL of each digested insert (*vp2*, *6His-vp2*, *6His-gfp* and *6His-ompK)*, 2 µL of each digested vector, 1x T4 DNA Ligase Buffer, and 1U of T4 DNA Ligase and incubated at 4ºC overnight.

### 2.2.4. Transformation of *E. coli* competent cells

*E. coli* DH5α competent cells (NZYTech) stored at -80ºC, were thawed on ice for about 5 min and mixed gently. To each ligation reaction tube, 90 µL of competent cells were added and the tubes were gently tapped and incubated on ice for 30 min. Cells were heat-shocked for 40 sec in a 42ºC water bath and thawed on ice for 2 min. 900 µL of LB medium were added to each tube and incubated at 37ºC and 200 rpm for 1 hour. To obtain the maximum number of colonies, a pellet was obtained from the cells and 800 µL of the supernatant was removed. The same steps were carried out in a negative control tube containing only competent cells. The pellet was resuspended in the remaining supernatant. 10 µL and 90 µL of the transformed cells were spread on LB agar plates containing 100 µL $mL^{-1}$ of ampicillin and incubated overnight at 37ºC.

### 2.2.5. Screening of *E. coli* recombinant colonies and plasmid purification

Recombinant colonies were screened by colony PCR and restriction enzyme digestion. For the colony PCR, 5 colonies of each transformation were chosen based on their apparent size and shape, in the case of transformation using pDG364 (**Table 3**) and replated to fresh LB plates containing 100 µg $mL^{-1}$ ampicillin. In the case of the colonies obtained from the transformation using plasmids p1CSV-CotY-C or p1CSV-CotY-N (**Table 3**), negative transformants present a pink coloration versus potential positive transformants, which are white. A bit of each colony was resuspended in 25 µL of nuclease-free water, heated at 99ºC for 10 min, and used as DNA template for a colony-PCR with the same oligonucleotide primers used to amplify each insert. PCR reactions were prepared on ice, using NzyTaq Polymerase (NzyTech) accordingly to the manufacturer's instructions. Briefly, a single reaction was carried out in 25 µL, containing 1x Reaction buffer, 0.5 mM of dNTPs, 0.5 µM of each primer, 4 mM of $MgCl_2$, and 1.25 U of NZYTaq DNA polymerase. Reactions were submitted to an initial denaturation step performed at 95ºC for 120s, followed by 34 cycles of denaturation at 95ºC for 60 s, annealing at 60ºC (*cotB-vp2* and *cotC-vp2*), 68ºC (*vp2*) or 72ºC (*6His-vp2*, *6His-gfp* and *6His-ompK*) for 60s, extension at 72ºC for 120s (*vp2* and *6His-vp2*), 90s (*cotB-vp2* and *cotC-vp2*) or 50s (*6His-gfp* and *6His-ompK*), and a final cycle of extension during 10 min at 72ºC. 5 µL of each overlapping PCR reaction were resolved in a 1% agarose gel as described previously.

The positive colonies were inoculated in 5 mL of LB with 100 µg $mL^{-1}$ of ampicillin and incubated overnight at 37ºC and 140 rpm. A pellet was obtained from 2 mL of the cultures and used to extract plasmids applying the boiling method already established in the laboratory. The pellet was resuspended in 360 µL of STET (8% saccharose, 0,5% Triton X-100, 10 mM Tris-HCl pH=8 and 50 mM EDTA pH=8), 24 µL of lysozyme and 10 µL of RNase (both at 10mg $mL^{-1}$), incubated for 5 min at 37ºC and 1 min at 100ºC and centrifugated at 13000 rpm for 10 min. The sediment was removed, and the DNA was precipitated with cold isopropanol followed by a centrifugation at 13000 rpm for 15 min. The supernatant was removed, and the sediment was washed with ice-cold 70% ethanol and centrifugated at 13000 rpm for 5 min. The remaining pellet was dried at room temperature for at least 15 min by inversion of the Eppendorf, before being resuspended in 20 µL of nuclease-free water.

Each extracted plasmid was used for a digestion reaction using enzymes HindIII (in transformations with pDG364 backbone), HindIII and SpeI (in p1CSV-CotY-C

backbone), HindIII and AgeI (in p1CSV-CotY-N backbone), or HindIII and PstI (in p1CSV-CotY-C and p1CSV-CotY-N backbones) to confirm its structure. One positive colony containing each plasmid was selected based on the PCR and structural digestions results, inoculated in 5 mL of LB medium with 100 µg $mL^{-1}$ of ampicillin and incubated overnight at 37ºC and 140 rpm. Plasmids obtained are listed in **Table 3**.

A stock of *E. coli* derivatives containing pGG1 (*cotB-vp2)*, pGG2 (*cotC-vp2)*, pGG3 (*cotY-vp2)*, pGG4 (*vp2-cotY)*, pGG5 (*cotY*-6His-*vp2)*, pGG6 (*6His-vp2-cotY)*, pGG7 (*cotY-6His-gfp)*, pGG8 (*6His-gfp-cotY)*, pGG9 (*cotY-6His-ompK)*, pGG10 (*6His-ompK-cotY)* were stored in 30% of glycerol at -80ºC, creating strains CRS203, CRS204, CRS205, CRS207, CRS210, CRS211, CRS212, CRS213, CRS214 and CRS215 (**Table 2**).

Plasmids pGG1, pGG2, pGG3, pGG4, pGG5, pGG6, pGG7, pGG8, pGG9 and pGG10 were extracted and purified using the GenElute™ Plasmid Miniprep Kit (Sigma), accordingly to the manufacturer's instructions.

In the case of plasmids pGG3 to pGG10, 3 µL of each plasmid was used as template for a PCR to amplify the *amyE* region with primers *amyE*-F and *amyE*-R (**Table 4**) and verify that the translational fusion had occurred. PCR reactions were prepared on ice, using MyTaq™ DNA Polymerase (Bioline) accordingly to the manufacturer's instructions. Briefly, a single reaction was carried out in 25 µL, containing 1x MyTaq Reaction buffer, 0.2 µM of each primer and 2.5 U of using MyTaq™ DNA Polymerase. Reactions were submitted to an initial denaturation step performed at 95ºC for 60s, followed by 34 cycles of denaturation at 95ºC for 15 s, annealing at 56ºC for 15s and extension at 72ºC for 180s. 5 µL of each PCR product with were loaded in a 1% agarose gel and purified as described in 2.2.2.1. Each purified PCR reaction was sent to STAB VIDA (https://www.stabvida.com/pt) for sequencing (**Figures S1**, **S2**, **S3**, **S4**, **S5**, **S6**, **S7** and **S8** from Supplementary material).

### 2.2.6. Transformation of *B. subtilis* 168 and FI99

For integration into *B. subtilis* 168 and FI99 chromosome, each plasmid was linearized with ScaI (Thermo Scientific). This restriction endonuclease cuts the *bla* gene, linearizing the plasmid without compromising the integration region, that occurs at the homologous portions of the *amyE* gene through a double crossover event. Linearizations occurred in 30 µL reactions containing 1x Sca Buffer, 10U of ScaI, nuclease-free water, and 20 µL of each plasmid at 37ºC for 2,5h. If not immediately used, the reactions were then stored at -20ºC.

#### 2.2.6.1. Development of competence using the GM1/GM2 method

The GM1/GM2 method consists in the use of two different growth media – Growth Medium 1 (GM1) and Growth Medium 2 (GM2) to induce competence development in *B. subtilis*. GM1 consists in 240 mL of B&W salts (1,24% $K_2HPO_4$, 0,76% $KH_2PO_4$, 0,1% tri-sodium citrate, 0,6% $(NH_4)_2SO_4$, pH=6,7), 2,5 mL of 100 mM of $MgSO_4$, 2,5 mL of 50% glucose, 2,5 mL of 10% of yeast extract, 2,5 mL of 5x B&W aminoacids (2,5 mg $mL^{-1}$ of L-tryptophan, L- arginine, L- lysine, L- methionine, L- histidine, L-valine, L- threonine, L-aspartic acid and glycine), 2,5 mL of 10 mg $mL^{-1}$ L-tryptophan and 625 µL of 20 mg $mL^{-1}$ L-methionine. The medium was sterilized by filtration prior to use and stored at 4ºC. GM2, prepared just prior to use, consists in 9,7 mL of GM1, 50 µL of 50 mM $CaCl_2$ and 250 µL of 1M $MgCl_2$.

A single colony of *B. subtilis* 168 or FI99 from an overnight plate was inoculated in 5 mL of GM1 and incubated at 37ºC and 150 rpm. After 5h, 500 µL of each culture were diluted in 4,5 mL of pre-warmed (at 37ºC) GM2 and incubated at 37ºC and 150 rpm for 2h. To sterile 50 mL conical falcons, 500 µL of each competent culture and 20 µL of the linearized plasmids were gently mixed, and the tubes incubated for 30 min at 37ºC and 180 rpm. One negative control, without adding linearized plasmid, was prepared for each strain. 200 µL of each transformation were plated in LB with 5 µg $mL^{-1}$ of chloramphenicol and incubated at 37ºC overnight.

#### 2.2.6.2. Development of competence using the MC method

Competence medium MC was developed by Rudner´s Lab. A 10x concentrated medium was prepared with 5,35 g of $K_2HPO_4$, 2,6 g of $KH_2PO_4$, 10 g of glucose, 0,44 g of $Na_3C_6H_5O_7 \cdot 2H_2O$, 0,5 mL of 1000x ferric ammonium citrate, 0,5 g of casein hydrolysate, 1,1 g of $C_5H_8KNO_4 \cdot H_2O$ and 50 mL of deionized water ($dH_2O$). The 10x MC medium was sterilized by filtration, distributed into 10 mL aliquots, and stored at -20ºC.

A single colony of *B. subtilis* 168 or FI99 from a fresh overnight plate was inoculated in 5 mL of 1x MC (100 mM potassium phosphate pH7; 3mM sodium citrate, 2% glucose, 22 mg $mL^{-1}$ ferric ammonium citrate, 0.1% casein hydrolysate and 0.2% potassium glutamate) supplemented with 3 mM $MgSO_4$ and 10 µL of 2 mg $mL^{-1}$ tryptophan, in sterile 50 mL conical falcon tubes, and incubated at 37ºC and 140 rpm. After 4h, 200 µL of each competent culture were added to 20 µL of the linearized plasmid in sterile 50 mL conical falcon tubes, gently mixed, and further incubated at 37ºC and 140 rpm for 2h. One negative control without linearized plasmid was prepared for each strain. 200 µL of each transformation (*B. subtilis* 168 x pGG5, *B. subtilis* 168 x pGG6, *B. subtilis* 168 x pGG7,

*B. subtilis* 168 x pGG8, *B. subtilis* 168 x pGG9, *B. subtilis* 168 x pGG10, *B. subtilis* 168, FI99 x pGG5, FI99 x pGG6, FI99 x pGG7, FI99 x pGG8, FI99 x pGG9, FI99 x pGG10 and FI99) were plated in LB with 5 µg $mL^{-1}$ of chloramphenicol and incubated at 37ºC overnight.

### 2.2.7. Screening of *B. subtilis* recombinant colonies

Recombinant strains of *B. subtilis* were screened by starch hydrolysis method and by PCR. First, 10 colonies of each transformation, based on their apparent size and shape, were replated to LB plates containing 1% starch and incubated at 37ºC overnight. A colony of parental strain *B. subtilis* 168 and FI99 were also plated and to be used as controls. Starch hydrolysis was evaluated by flooding the plates with Lugol's iodine ($I_2KI$ solution).

Four amylase-negative colonies from each transformation were chosen, inoculated in fresh LB plates containing 5 µg $mL^{-1}$ of chloramphenicol and incubated at 37ºC overnight. The next day, each colony was inoculated in liquid medium and incubated at 37ºC and 140 rpm. Stocks of CRS206 (CotY-VP2), CRS208 (VP2-CotY), CRS216 (CotY-H6-VP2), CRS217 (H6-VP2-CotY), CRS218 (CotY-H6-GFP), CRS219 (H6-GFP-CotY), CRS220 (CotY-H6-OmpK) and CRS221 (H6-OmpK-CotY) (**Table 2**) were stored in 30% of glycerol at -80ºC.

Chromosomal DNA was extracted from each strain as previously described in 2.2.1. To confirm that each fusion was successfully integrated into the *B. subtilis* chromosome, a PCR using oligonucleotides amyE-F and amyE-R (**Table 4**) as primers and the extracted DNA as template was carried out as described in 2.2.5.

5 µL of each PCR were loaded in a 1% agarose gel and purified as described in 2.2.2.1. Each purified PCR product was sent to STAB VIDA (https://www.stabvida.com/pt) for sequencing (**Figures S1**, **S2**, **S3**, **S4**, **S5**, **S6**, **S7** and **S8** from Supplementary material).

## 2.3. Growth curves, viable cell titer, heat and lysozyme resistance tests

A single fresh colony from strains *B. subtilis* 168, CRS206, CRS208 and CRS216 to CRS221 was inoculated in 5 mL of LB or LB with 5 µg $mL^{-1}$ of chloramphenicol when required, and incubated at 37ºC and 140 rpm overnight. The next day, the absorbance at 600 nm of each inoculum was measured and the Optical Density (OD) cultures adjusted to an $OD_{600nm}$= 0,05 in 10 mL of pre-warmed (37ºC) Difco Sporulation Medium

(DSM) broth supplemented with 1 mL of 1 M $Ca(NO_3)_2$, 0.01 M $MnCl_2$, 1 mM $FeSO_4$ and with 5 µg $mL^{-1}$ of chloramphenicol when required, and incubated at 37ºC and 150 rpm until the beginning of stationary phase (T0). Incubation was carried out for 24h from T0 at the same conditions.

For the establishment of the growth curve of each strain, samples were taken from the cultures and diluted (1:3) in DSM broth before $OD_{600nm}$ was measured, in 30 min intervals until T8. This experiment and the followings were repeated three times.

After the 24h incubation, 50 µL of each culture was diluted in 450 µL of B&W salts. Serial dilutions were prepared ($10^{-1}$ to $10^{-7}$) by adding 50 µL of the previous dilution to 450 µL of B&W salts. 100 µL of dilutions $10^{-6}$ and $10^{-7}$ were plated onto LB plates (with 5 µg $mL^{-1}$ of chloramphenicol when required) and incubated at 37ºC overnight. Dilutions $10^{-6}$ and $10^{-7}$ were incubated at 80ºC for 20 min and then plated as described previously. 1 mL of each culture was incubated with 250 µL of freshly prepared lysozyme at 10 mg $mL^{-1}$, at 37ºC for 20 min. The culture was then centrifuged at 4000 rpm for 5 min and the pellet was resuspended in 1 mL of B&W salts. Serial dilutions were prepared ($10^{-1}$ to $10^{-7}$) and plated onto LB plates, as previously described.

The next day, viable cell, heat resistant cells and lysozyme resistant cells were counted.

## 2.4. Induction of sporulation and spores purification

A fresh colony from strains *B. subtilis* 168, CRS206, CRS208 and CRS216 to CRS221 was inoculated in 20 mL of DSM broth (with 5 µg $mL^{-1}$ of chloramphenicol when required) and incubated at 37ºC and 150 rpm. Sporulating cultures were harvested after 24h and centrifugated at 10000g for 10 min at 4ºC and treated as described in Bartels et al., 2018 and Sun et al., 2018. The pellet was resuspended in 50 mM of Tris-HCl with 75 µg $mL^{-1}$ of lysozyme and incubated at 37ºC for 1h. Spores were centrifugated, washed 1x with cold $dH_2O$ with 1 mM of phenylmethylsulphonyl fluoride (PMSF), a protease inhibitor. After that, spores were centrifugated, resuspended in 0.05% SDS, and washed 3x with cold $dH_2O$ with 1 mM of PMSF. Spores were resuspended in 200 µL of nuclease-free water.

## 2.5. Western Blot analysis

5 µL of each spore suspension was diluted in 950 µL of $dH_2O$. The optical density at 580 nm was used to quantify the spores and calculate the µL necessary for the sample loading. All samples were equalized by adding $dH_2O$ to obtain a fixed volume. The same

volume of 2x Loading Buffer for Spores' Crust (10% glycerol, 10% 2-mercaptoethanol, 100 mM Dithiothreitol (DTT), 4% SDS, 0.05% bromophenol blue and 0.125 M Tris) or 2x Loading Buffer (10% glycerol, 10% 2-mercaptoethanol, 1 mM DTT, 4% SDS, 0.05% bromophenol blue and 0.125 M Tris) and samples were heated at 100ºC for 8 min.

Approximately 25 µL of each sample were loaded into a 10% or 15% denaturing polyacrylamide (with or without 6M of urea) gel along with 5 µL of the protein marker (Precision Plus Protein™ All Blue Prestained Protein Standards, BioRad), and spore coat proteins were separated at 25 mA per gel for 60 to 120 min.

One gel was stained with a staining solution (0.3% Coomassie R-250, 50% ethanol and 10% acetic acid) for 30 min, distained for 2h with a distaining solution (10% ethanol, 10% acetic acid) and stored in $dH_2O$ at 4ºC. The other gel was used to electrotransfer the separated spore coat proteins into a 0.2 µm nitrocellulose membrane (BioRad) at 100 V in cold transfer buffer (0.192 M glycine, 0.025 M Tris, 10% ethanol, pH=8.3) for 90 min. The membrane was then blocked with 10% of low-fat powder milk for 30 min, washed 3x with a solution consisting of 1x PBS (phosphate buffered saline), 0.5% low-fat powder milk and 0.1% Tween-20 and incubated with 1:1000 rabbit anti-VP2 polyclonal antibody or 1:1000 mouse 6His-tag monoclonal antibody (Thermo Scientific, catalogue number MA121315) overnight at 4ºC. The next day, the primary antibody solution was removed, the membrane washed 5x with the same solution and incubated with either 1:10000 goat anti-rabbit IgG (H+L) horseradish peroxidase (HRP) conjugated (Thermo Scientific, catalogue number 31466) or 1:10000 goat anti-mouse IgG (H+L) HRP conjugated (Thermo Scientific, catalogue number G21040) for 30 min. The membrane was then washed 3x for 15 min with slow agitation and incubated with the Clarity Western ECL Substrate (Bio-Rad) for 5 min in the dark. The membrane was then visualized in a ChemiDoc XRS Gel Imaging System (Bio-Rad) and analyzed with the Image Lab Software (Bio-Rad).

## 2.6. Phase-Contrast and Fluorescence microscopy

Sporulation was induced in cultures of strains *B. subtilis* 168, CRS218 and CRS219 as described in 2.3. Sporulating cultures, grown for 24h after the onset of sporulation or T0 in DSM, were observed by phase contract (PC) and fluorescence microcopy. 600 µL of each culture were removed and centrifuged at 6000 rpm for 30s, and the pellet was resuspended in 200 µL of 1x PBS. 2 µL of the DNA stain 4',6-diamidino-2-phenylindole dihydrochloride (DAPI, Sigma) were added to each sample. Samples incubated for 1 min at room temperature in the dark.

A microscope slide was prepared with a thin layer of 1.7% agarose in MiliQ water and 5 µL of each stained culture was placed on top of a microscope slide before observation by PC and fluorescence microscopy, using a Nikon Eclipse Ci-L microscope with a CoolLED's pE 300lite illumination system equipped with a 100x oil objective. Each culture was observed under the same filter conditions: exposure of 50 ms with FITC (green fluorescence) and 20 ms with DAPI (blue fluorescence). Images were captured using a DS-Ri2 and processed with the NIS-Elements BR v. 4.60.00 software.

## 2.7. Assessment of the protective effect on zebrafish larvae

Zebrafish larvae were produced by pair-wise mating of wild-type adults, collected and raised at 28ºC with natural photoperiod. Larvae from 5 days-post-fertilization (dpf) or above were fed twice a day. At the end of each assay, larvae were euthanized with an overdose of tricaine.

### 2.7.1. Toxicity test using spores from *B. subtilis* 168

A preliminary toxicity test (only one assay) was carried out to assess the toxicity potential of spores from *B. subtilis* 168. At 3 dpf, larvae were distributed into 6-well plates containing 10 larvae per well in Egg water (Instant Ocean® Salt). Serial dilutions from purified spores' suspension were carried out in different wells, from $10^8$ cfu $mL^{-1}$ to $10^4$ cfu $mL^{-1}$. A negative control without the spores' suspension was also included. Larvae survival was monitored for 72 hours.

### 2.7.2. Challenge with *V. anguillarum* and *V. parahaemolyticus*

At 3 dpf, larvae were distributed into 6-well plates containing 10 larvae per well in Egg water to acclimatize to the experimental conditions. 6 dpf larvae were treated for 2h with spores suspensions containing approximately $10^8$ cfu $mL^{-1}$ of each recombinant strain CRS220 (CotY-H6-OmpK) and CRS221 (H6-OmpK-CotY) or from the parental *B. subtilis* 168 strain. At 9 dpf larvae were then challenged by immersion during 12h with $3\times10^8$ cfu $mL^{-1}$ of *V. anguillarum* or $1\times10^8$ cfu $mL^{-1}$ of *V. parahaemolyticus* (following an established model of infection of zebrafish larvae developed in our laboratory). Cumulative mortalities were registered between 16 and 72h, and the dead larvae were removed and safely discarded. Control groups were included: (i) non-vaccinated larvae challenged with *V. anguillarum* or *V. parahaemolyticus*; (ii) non-inoculated larvae and (iii) larvae inoculated

with 1x PBS, since each bacterial inoculum was diluted in 1x PBS. The experiment was independently carried out 3 times.

The statistical analysis was done using the SPSS 26.0 software package for Windows. Survival data were analyzed using Kaplan–Meier and group differences were analyzed by the log-rank. Dunnett's test was performed for comparisons between treatments and the control. $p<0.05$ was considered significant.

# 3. Results

## 3.1. Fusion of viral and bacterial antigens to *B. subtilis* coat and crust proteins

Two coat carrier proteins (CotB and CotC) and one crust protein (CotY) were chosen as the carriers for the target antigens.

### 3.1.1. Display of viral VP2 at the surface of *B. subtilis* spores using the coat proteins CotB and CotC as carriers

To obtain a translational fusion of VP2 to coat proteins CotB and CotC, both *cot* genes were successfully amplified from the DNA of *B. subtilis* 168, originating two fragments of 1112 bp – *cotB* (**Figure 4A**) and 399 bp – *cotC* (**Figure 4B**). The promotor of each *cot* gene was included in the PCR amplification to guarantee the appropriate gene expression during sporulation. Amplification of the DNA coding for the VP2 protein and containing tails for *cotB* (*vp2B,* **Figure 4C**) and *cotC* (*vp2C,* **Figure 4D**) resulted in two fragments of 1443 bp. Since *cot* genes were amplified with an overhang from the 3'-end of the *vp2* sequence, and the *vp2* sequence was amplified with an overhang from the 5'-end of each *cot* gene, an overlapping PCR was effectively carried out to obtain two fusions – a fragment of 2528 bp resulted from *cotB-vp2* and 1815 bp from *cotC-vp2* (**Figure 4E**).

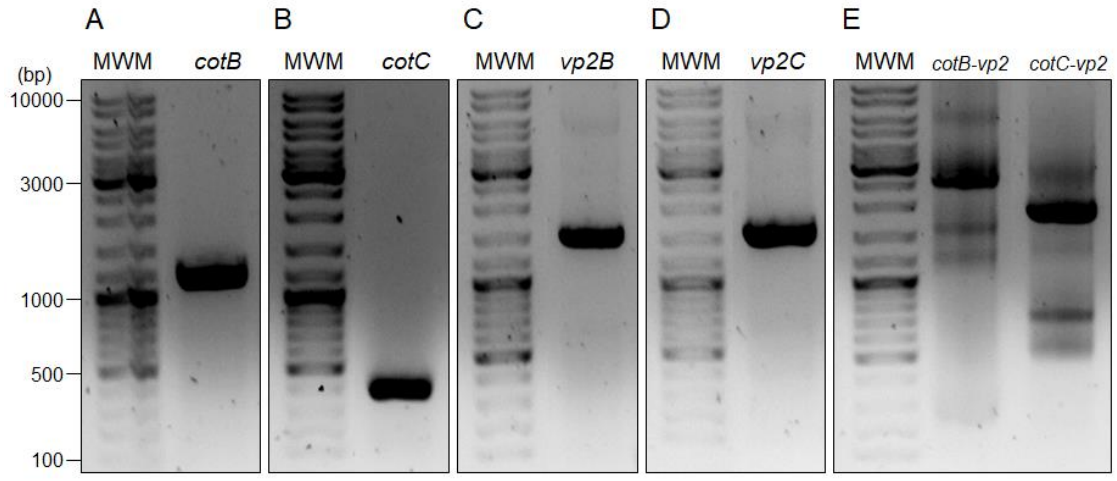


**Figure 4.** Gel electrophoresis of the PCR amplification of *cotB* (**A** – 1112 bp), *cotC* (**B** – 399 bp) from *B. subtilis* 168 chromosomal DNA, and *vp2* with tails for *cotB* (**C** – 1443 bp) or for *cotC* (**D** – 1443 bp). The overlapping PCR resulted in two fragments of 2528 bp (**E**, lane *cotB-vp2*) and 1815 bp (**E**, lane *cotC-vp2*). Molecular weight of representative bands of the molecular weight marker (MWM) are indicated in bp.

Each purified fusion was digested in both ends with HindIII (**Figure 5A**) and ligated to plasmid pDG364 (**Figure 5B; Table 3**), previously digested with the same restriction endonuclease (**Figure 5C**), before transforming *E. coli* DH5α competent cells. 5 colonies of each transformation were assessed for the presence of the fusions through a colony PCR (**Figure 6**). The presence of *cotB-vp2* was confirmed in 1 of the 5 colonies tested (**Figure 6**, lanes 3 to 7, only lane 7 appear correct), whilst *cotC-vp2* was present in 4 of the 5 colonies (**Figure 6**, lanes 10 to 14), since the amplified products had the same size as the original insert (**Figure 6**, lane 1 for *cotB-vp2* and lane 8 for *cotC-vp2*).

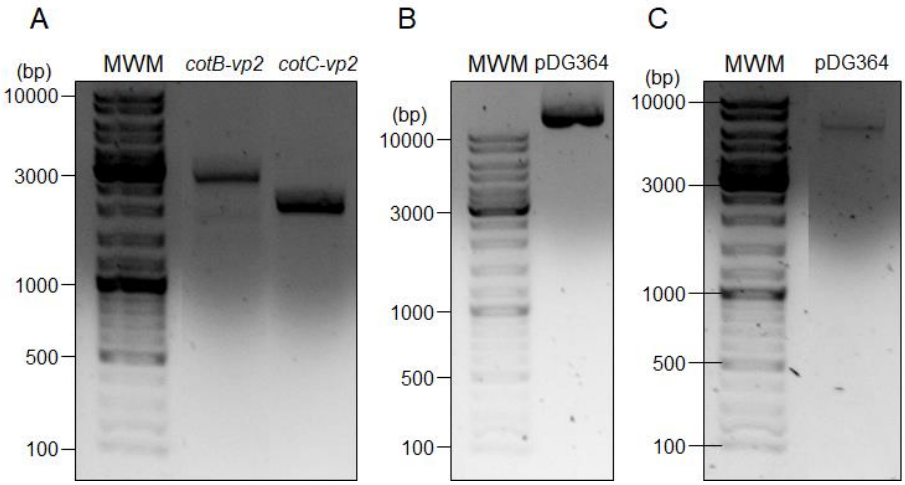


**Figure 5.** Gel electrophoresis of (**A**) the digestion reactions of fusions cotB-vp2 (2528 bp) and cotC-vp2 (1815 bp) with HindIII, which were ligated to (**B**) plasmid pDG364, previously digested with HindIII (**C** – 6257 bp).

One positive colony of each fusion was used for a manual plasmid preparation to extract the corresponding plasmids and confirm their structure by restriction analysis with HindIII. The restriction enzyme does not cut the backbone plasmid but cuts at the 5'-end and 3'-end of each insert, originating a band of the same size of the original inserts: 2528 bp for *cotB-vp2* and 1815 bp for *cotC-vp2* (**Figure 7A**). After confirming their correct structure, new plasmid extractions were prepared: plasmid containing the *cotB-vp2* fusion was named pGG1 (**Table 3**) and the corresponding *E. coli* strain, CRS203 (**Table 2),** while plasmid containing the *cotC-vp2* fusion was named pGG2 (**Table 3**), and the corresponding *E. coli* strain, CRS204 (**Table 2**).

Linearization of pGG2 with ScaI originated a single band that corresponds to the expected size (8074 bp) (**Figure 7B**), but linearization of pGG1 originated two unexpected bands, since ScaI is a single cutter in the target sequence. To re-confirm the presence of each fusion, a PCR was carried out to amplify fusions *cotB-vp2* and *cotC-vp2* from pGG1 and pGG2, respectively. A fragment of the expected size – 1815 bp –

was amplified only in the case of pGG2 (**Figure 7C**). Different approaches have been employed to confirm the correct structure of each plasmid, without success in the case of pGG1 and their employment in subsequent steps was not pursued. Instead, another strategy based on specifically dedicated plasmid vectors (Bartels et al., 2018) was chosen to display the VP2 antigen at the surface of *B. subtilis* spores.

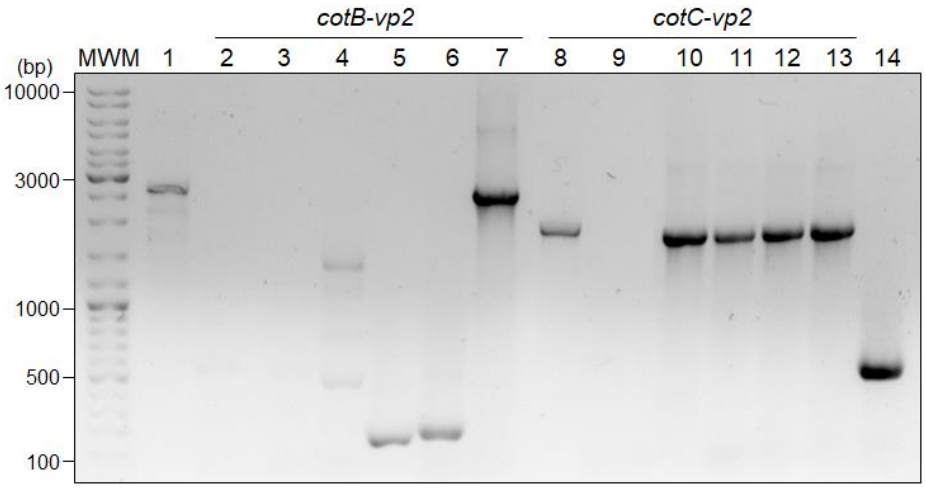


**Figure 6.** Gel electrophoresis of the colony PCR to assess the presence of the fusions *cotB-vp2* (1 – 2528 bp) and *cotC-vp2* (8 – 1815 bp). Non-transformed *E. coli* competent cells (lanes 2 and 9) were included. Of the five colonies tested for the presence of *cotB-vp2* (lanes 3 to 7), only one appear to have the same size as the fusion (lane 7). Four of the five colonies tested for the presence of *cotC-vp2* (lanes 10 to 14) appear to have the same size as the fusion (lanes 10 to 13).

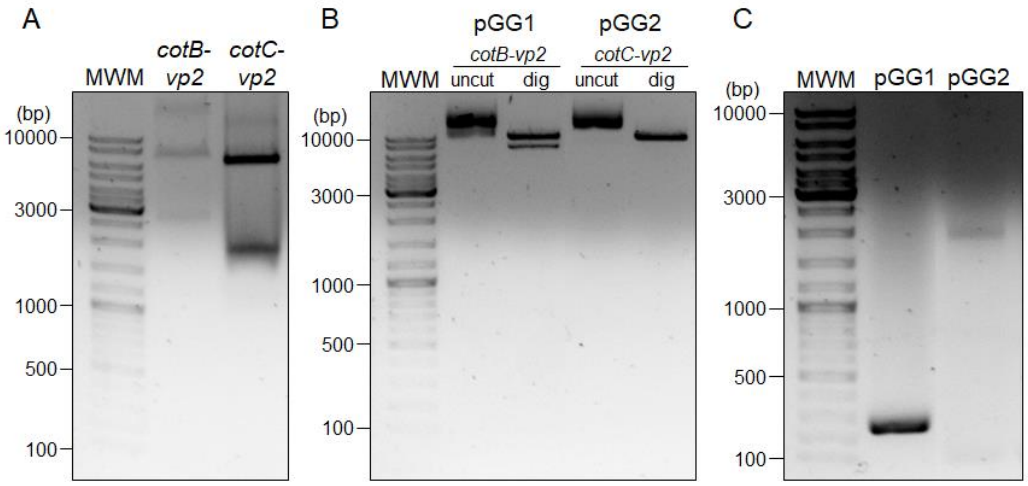


**Figure 7.** (**A**) Gel electrophoresis of (A) the extracted digested plasmids from positive colonies. Since the backbone plasmid is not cut by HindIII, the digestion with HindIII of positive plasmids originates a band with the same size of the inserts (2528 bp in plasmids containing *cotB-vp2* and 1815 bp in plasmids containing *cotC-vp2*). (**B**) New plasmids were extracted, containing the fusion *cotB-vp2* – pGG1 and *cotC-vp2* – pGG2. Digestion with ScaI was expected to originate a single band of 8785 bp in pGG1 and 8072 bp in pGG2 (confirmed). (**C**) PCR amplification of each fusion was only successful in the case of pGG2, originating a band of the expected size (1815 bp).

### 3.1.2. Display of viral VP2 at the surface of *B. subtilis* spores using the crust protein CotY as carrier

Vectors p1CSV-CotY-C and p1CSV-CotY-N (**Table 3**) allow C-terminal and N -terminal fusions to the crust CotY protein. A 1475 bp sequence encoding the VP2 protein was successfully amplified from pMCV1.4 VP2015 (**Table 3**), (**Figure 8A**) and the corresponding PCR product was sequentially digested with two sets of enzymes that allow the cloning in plasmids p1CSV-CotY-C and p1CSV-CotY-N. For the C-terminal one (**Figure 8B**), digestion was performed with NgoMIV and SpeI, resulting in the loss of the ribosome binding site (RBS) while the stop codon is still present after the AgeI cut site, allowing the translation to stop after the target gene. For the N-terminal one (**Figure 8C**), digestion was done with XbaI and AgeI, resulting in the presence of the RBS of the target gene and on the loss of the stop codon, allowing the translation to continue.

The vectors p1CSV-CotY-C and p1CSV-CotY-N were sequentially digested with SpeI and AgeI, and NgoMIV and XbaI, respectively. The double digestion results in the drop of the RFP-cassette of approximately 1.2 Kb (**Figure 8D and 8E**). The overhangs resulting from the insert digestion with NgoMIV or AgeI are compatible with the AgeI of p1CSV-CotY-C or with the NgoMIV of p1CSV-CotY-N. This results in a translational fusion of each target gene with *cotY*, linked by a sequence coding for two aminoacids (Thr-Gly).

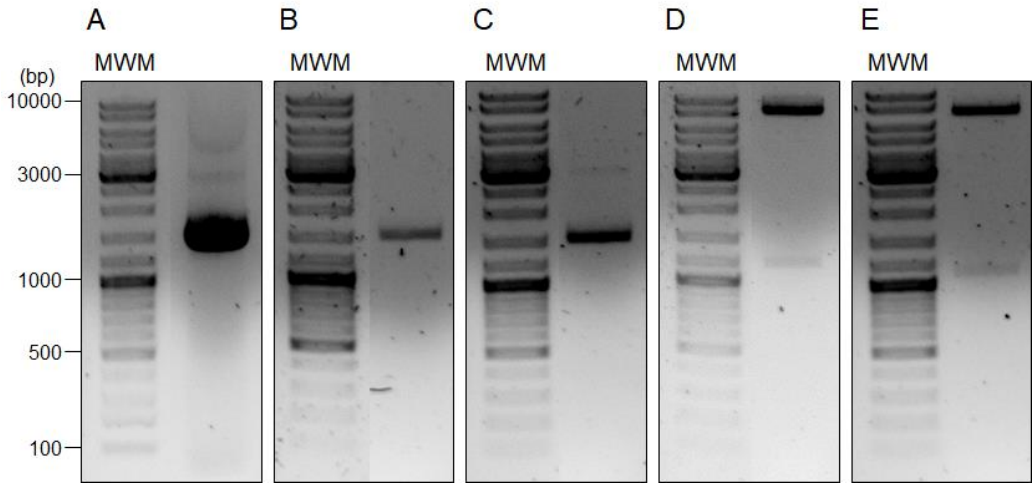


**Figure 8.** Gel electrophoresis of the *vp2* amplification (**A** – 1475 bp). This fragment was sequentially digested with NgoMIV and SpeI for cloning into p1CSV-CotY-C (**B**) and XbaI and AgeI for p1CSV-CotY-N (**C**). Vectors were also digested, resulting in the drop of the RFP-cassette of approximately 1.2 Kb – p1CSV-CotY-C was digested with SpeI and AgeI (**D**) and p1CSV-CotY-N with NgoMIV and XbaI (**E**).

After ligation and transformation into *E.coli* competent cells the presence of *vp2* insert was confirmed in 10 colonies tested (**Figure 9A** and **9B**), since the amplified products have the same size as the original insert (1475 bp). Plasmids from the PCR positive's colonies were extracted and their structure confirmed by restriction analysis (**Figure 10A** and **10B**). Positive clones originate a pattern of digestion constituted by two bands of 2128 bp and 6157 bp – colonies from lanes 1, 2, 4, 5, 7, 8, 9 and 10, in the case of *vp2* x p1CSV-CotY-C (**Figure 10A**), or 2127 bp and 6127 bp in colonies 1, 6 and 7, for *vp2* x p1CSV-CotY-N (**Figure 10B**).

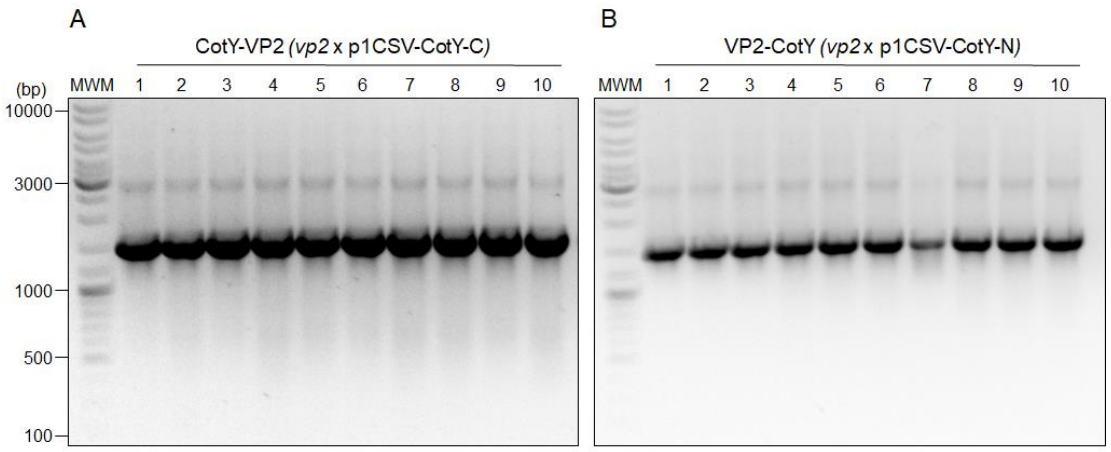


**Figure 9.** Gel electrophoresis of the colony PCR to assess the presence of the insert *vp2* after transformation of *E. coli* competent cells, to obtain the fusion *cotY-vp2* (**A**) and *vp2-cotY* (**B**). All colonies (lanes 1 to 10 in both panels) tested were positive for the presence of the insert, since the amplified products have the same size as the original digested inset (1475 bp).

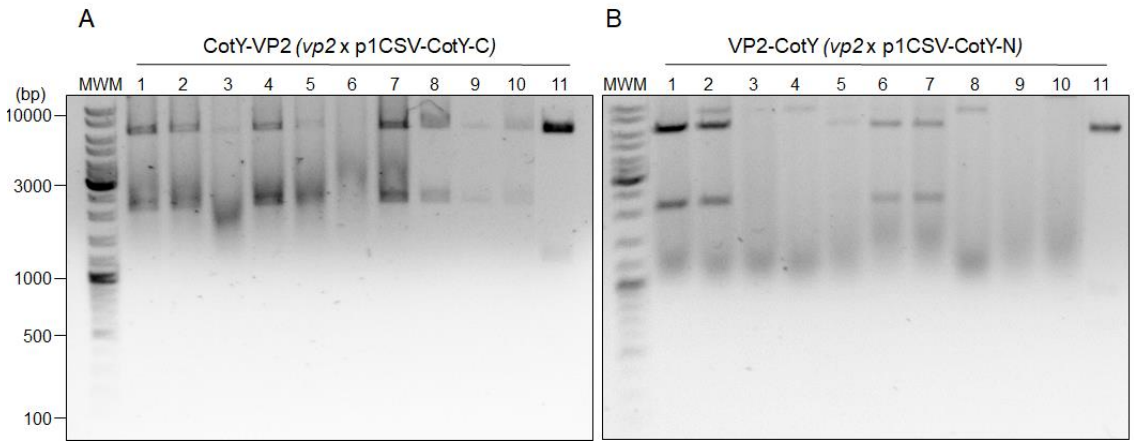


**Figure 10.** Gel electrophoresis of the extracted plasmids from positive colonies after digestion to confirm their structure. Positive colonies originate a pattern of two bands of approximately 6127 bp and 2128 or 2127 bp. (**A**) Colonies from lanes 1, 2, 4, 5, 7, 8, 9 and 10 from the C-terminal transformation are positive. (**B**) In the case of the N-terminal transformation, colonies 1, 6 and 7 were positive. In both panels, lanes 11 correspond to the digested backbone vector, which originate a different pattern of digestion since they possess multiple sites of digestion for HindIII.

One positive colony of each transformation was selected to create strain CRS205 (**Table 2**), that contained pGG3 (**Figure 11A** and **12A**, **Table 3**), and CRS207 (**Table 2**), containing pGG4 (**Figure 11B** and **12B**, **Table 3)**. Amplification of the insert DNA between the 2 flanking parts of *amyE* gene in each plasmid, which originated a band of 5178 bp in pGG3 and of 5177 bp in pGG4 (**Figure 13A**), and subsequent sequencing of each PCR product, revealed that *vp2* was successfully cloned in frame with *cotY* in both constructions. Linearized plasmids (**Figure 13B**) were used to transform competent cells of *B. subtilis* 168 and FI99, though the GM1-GM2 method. Integration was successful into *B. subtilis* 168 chromosome through a double-crossover event at the *amyE* locus (**Figure 14**).

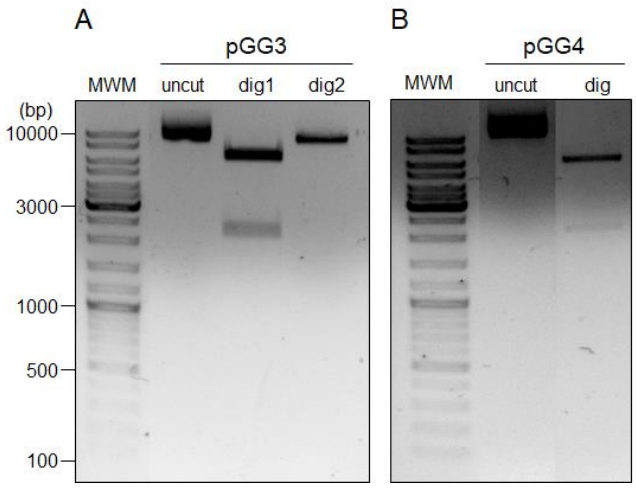


**Figure 11. (A)** Gel electrophoresis of the plasmid pGG3 (CotY-VP2) extracted from strain CRS205. Confirmation of the structure by digestion with HindIII and SpeI originated the same two band (lane dig1 – 6127 bp and 2128 bp) pattern expected. Digestion with ScaI (dig2) originated a band with the expected size of the linearized plasmid (8285 bp). (**B**) Gel electrophoresis of the plasmid pGG4 (VP2-CotY) extracted from strain CRS207. Confirmation of the structure by digestion with HindIII and AgeI originated the same two band (lane dig – 6127 bp and 2127 bp) pattern expected.

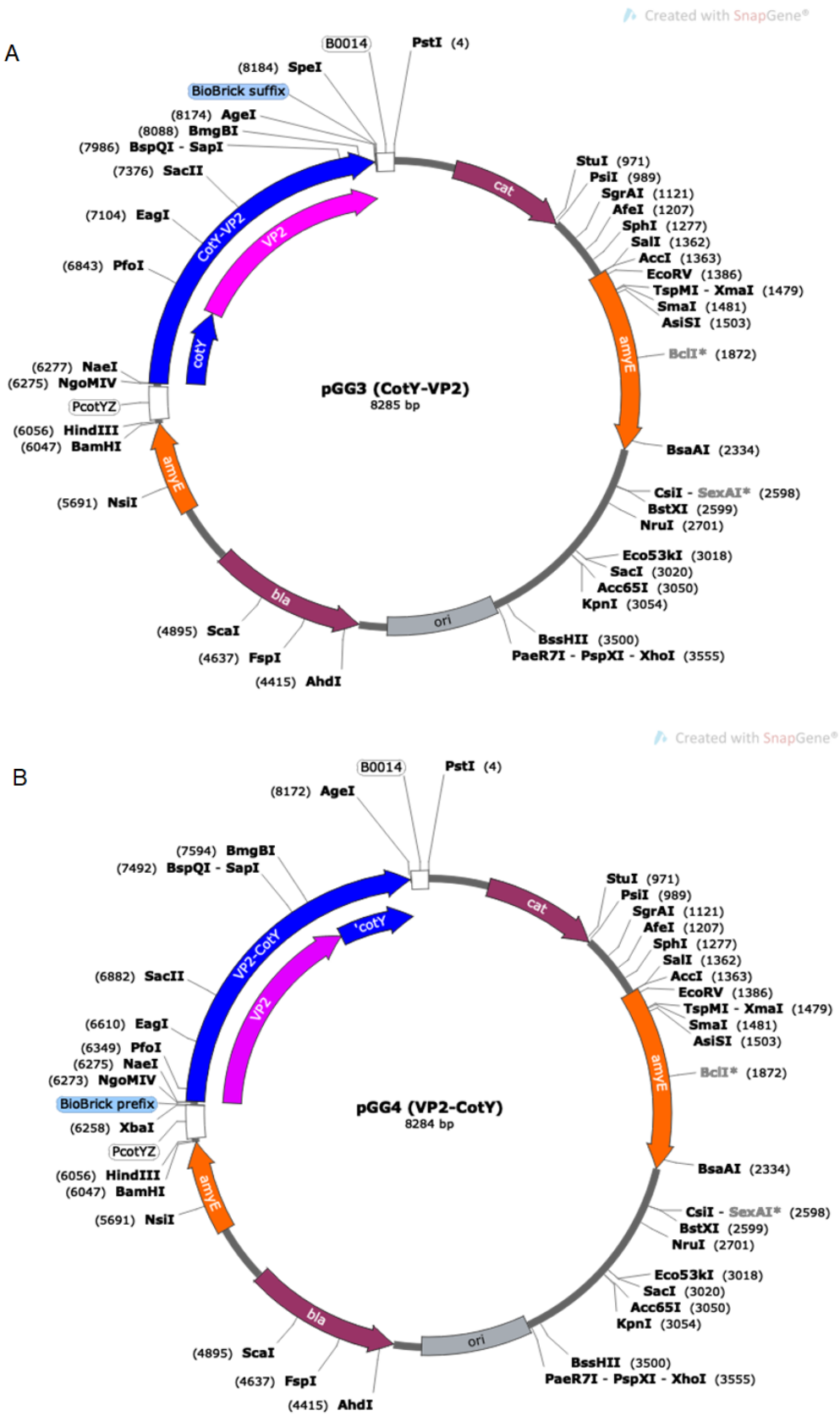


**Figure 12**. Schematic representation of **(A)** pGG3 and **(B)** pGG4 with the sites of restriction for unique cutters enzymes.

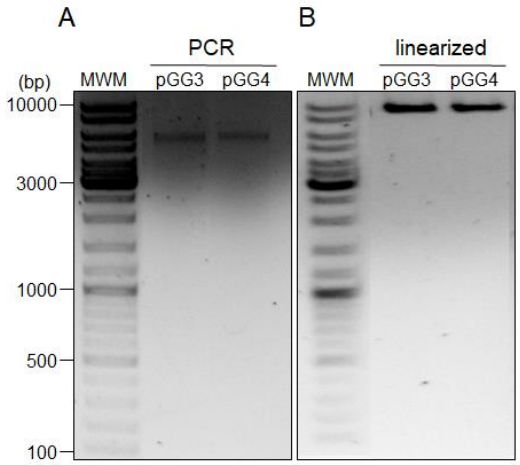


**Figure 13.** Gel electrophoresis of (**A)** the amplification of the insert DNA between the 2 flanking parts of *amyE* gene in each plasmid, which originated a band of 5178 bp in pGG3 and 5177 bp in pGG4. (**B**) Plasmids were linearized with ScaI prior to the transformation of *B. subtilis* 168, originating a pattern of band of 8285 bp (pGG3) or 8284 bp (pGG4).

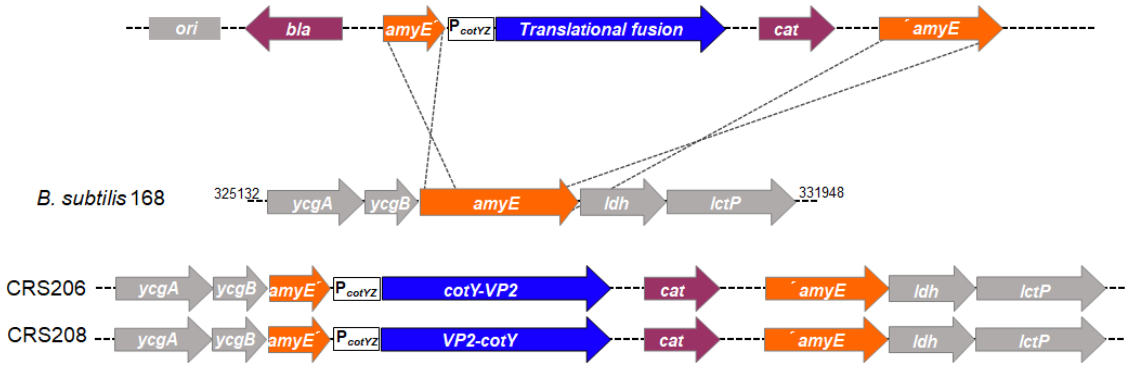


**Figure 14.** Schematic representation of a successful chromosomal integration of fusions *cotY-VP2* and *VP2-cotY* in *B. subtilis* 168, which occurs through a double-crossover event at the *amyE* locus, originating strains CRS206 and CRS208.

The resulting strains – CRS206 (CotY-VP2) and CRS208 (VP2-CotY) (**Table 2**, **Figure 14**) are chloramphenicol resistant, allowing for an initial selection of positive clones. No transformants were obtained in the background FI99. Chloramphenicol resistant colonies were inoculated in LB plates containing 1% starch along with a colony of the parental strain *B. subtilis* 168, which served as control since it retains the starch degradation capacity due to the intact *amyE* gene. Positive colonies, with a disrupted *amyE* gene, were not able to degrade the starch. To further confirm the genotype of the resulting strains, their chromosomal DNA was extracted and used as template for a PCR amplification of the *amyE* region. The PCR products had the same size as the expected bands – 5178 bp in CRS206, 5177 bp in CRS208 (**Figure 15B),** higher than that obtained for the parental strain *B. subtilis* 168 (**Figure 15A**) and coincident with the insertion of our target sequence. Sequencing of corresponding PCR products revealed a correct genotype of both CRS206 and CRS208 (**Table 2**).

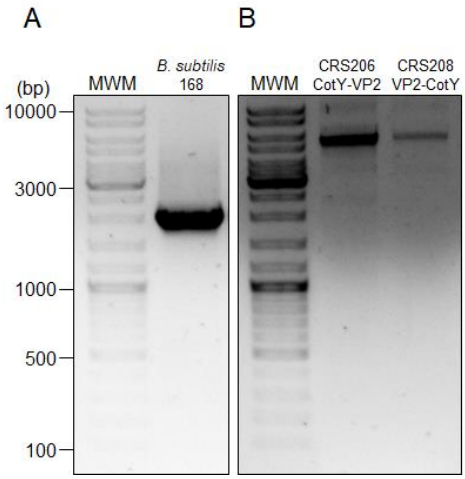


**Figure 15.** Gel electrophoresis of the PCR amplification of the *amyE* region. (**A**) The band originated using the parental strain DNA as template has a smaller size than the ones obtained using the recombinant strains. (**B**) Bands of 5178 bp and 5177 bp were obtained when using CRS206 and CRS208 chromosomal DNA as template, which results of the successful integration of each fusion.

Next, both strains CRS206 and CRS208 were induced to sporulate in DSM broth for 24h and their spores purified and quantified before analysis by SDS-PAGE (**Figure 16A**).

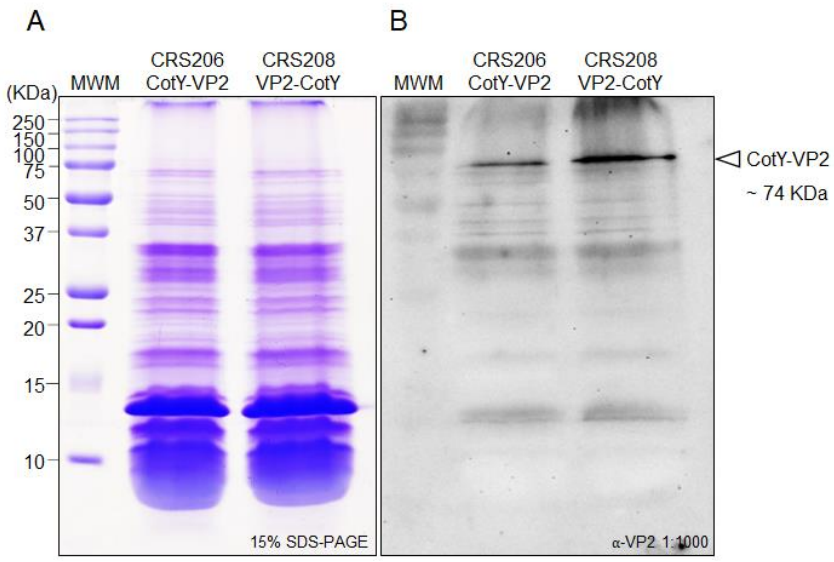


**Figure 16.** (**A**) Spores proteins from strains CRS206 and CRS208 were separated in a 15% acrylamide gel, revealing a similar pattern. (**B**) Western blot analysis using an anti-VP2 primary antibody (1:1000) detected a band of approximately 74KDa equivalent to the sum of the MW of CotY (18KDa) and VP2 (56KDa). Some sizes of the MWM are indicated in KDa.

Spores proteins were resolved on a 15% acrylamide gel and used for detection of recombinant CotY-VP2 using a VP2 specific antibody. A band of approximately 74KDa

equivalent to the sum of the MW of CotY (18KDa) and VP2 (56KDa) was detected on the corresponding western blot (**Figure 16B**). To further verify the display of VP2 at the surface of CRS206 and CRS208 spores, spores of parental *B. subtilis* 168 were also prepared and included on a western blot as before, but resolving proteins in a 10% acrylamide gel containing the 6M denaturant agent urea, to maximize denaturing conditions as a way of increasing the chances of detecting VP2, as it might form highly cross-linked structures with CotY and other coat proteins, like CotZ (J. Zhang et al., 1993) (**Figure 17A**). Again, a band of approximately 74KDa equivalent to the sum of the MW of CotY (18KDa) and VP2 (56KDa) could be detected on the corresponding western blot (**Figure 17B**).

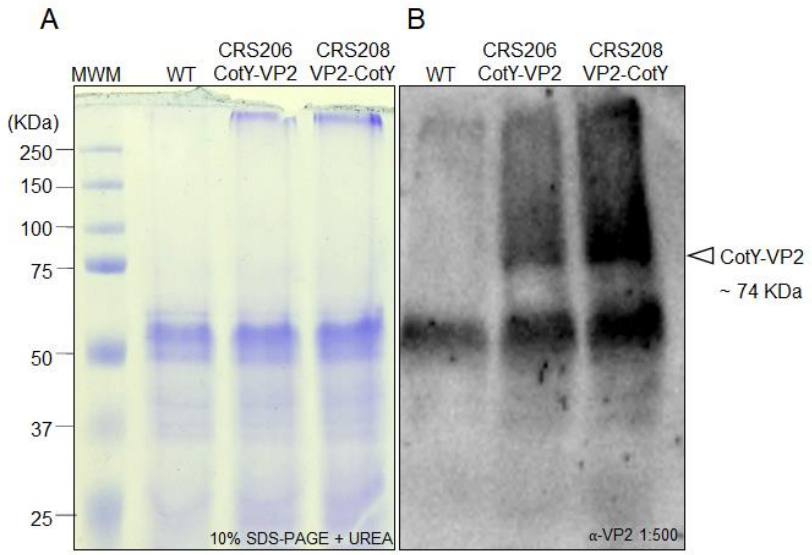


**Figure 17.** (**A**) Spores proteins from strains WT, CRS206 and CRS208 were separated in a 10% acrylamide gel with 6M of urea, revealing a similar pattern. (**B**) Western blot analysis using the anti-VP2 primary antibody (1:500) detected a band of approximately 74KDa equivalent to the sum of the MW of CotY (18KDa) and VP2 (56KDa), that was absent in the WT spores' proteins.

### 3.1.3. Display of GFP, bacterial OmpK and viral VP2 containing a 6His-tag at the surface of *B. subtilis* spores using the crust protein CotY as carrier

To be able to detect protein display at the surface of *B. subtilis* spores using an anti-HisTag antibody, one tag of 6 histidines was placed by PCR at the N-terminal ends of viral VP2, bacterial OmpK and the green fluorescence protein GFP. The 6 His-tag was introduced in the forward primers used to amplify the target genes from pMCV1.4-VP2015 (**Table 3**) in the case of VP2, pMS157 (**Table 3**) in the case of GFP and

chromosomal DNA of *V. vulnificus* (**Table 2**) in the case of OmpK, before re-amplification to add the sporovector tag (details in section 2.2.2.2 and 2.2.2.3 of Materials & Methods). A 1496bp DNA fragment was obtained for the *6His-vp2* **(Figure 18A**), an 809 bp for *6His-gfp* (**Figure 18B**) and an 827 bp fragment for *6His-ompK* (**Figure 18C**). The purified PCR products were digested to clone into plasmids p1CSV-CotY-C and p1CSV-CotY-N, essentially as previously described for the VP2 protein (**Figure 19A**, **19B** and **19C**), ligated to the corresponding vectors and transformed into *E. coli* competent cells

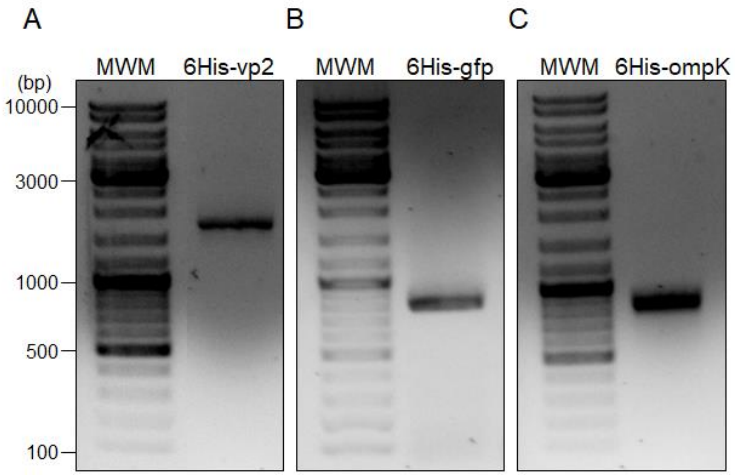


**Figure 18.** Gel electrophoresis of the PCR amplification of *6His-vp2* (**A** – 1496 bp), *6His-gfp* (**B** – 809 bp) and *6His-ompK* (**C** – 827 bp), using pMCV1.4-VP2015, pMS157 or DNA of *V. vulnificus*, respectively, as DNA template.

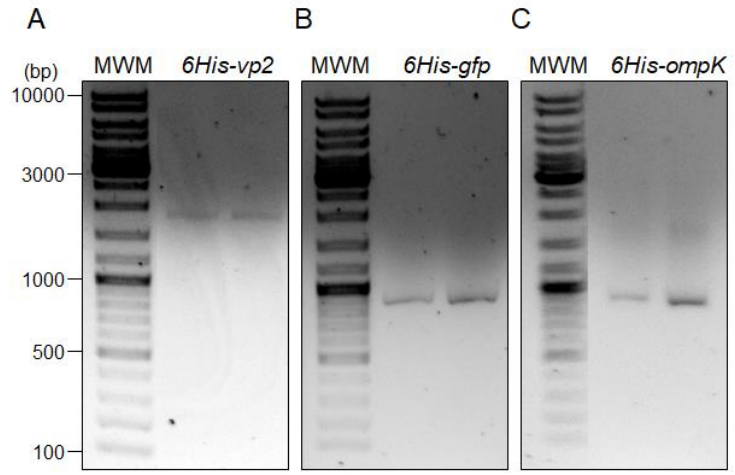


**Figure 19.** Gel electrophoresis of sequentially digested fragments (**A** – *6His-vp2*, **B** – *6His-gfp* and **C** – *6His-ompK*) with NgoMIV and SpeI for cloning into p1CSV-CotY-C and XbaI and AgeI for p1CSV-CotY-N.

The presence of *6His-vp2* was confirmed by PCR in 4 out of 5 clones from *6His-vp2* x p1CSV-CotY-C transformation (**Figure 20A**, Lanes 1 to 5) and in all 5 clones from *6His-vp2* x p1CSV-CotY-N transformation (**Figure 20A**, Lanes 6 to 10). Further verification

was done by restriction analysis with HindIII and PstI, with positive clones originating a pattern of digestion constituted by a band of 6052 bp and one additional band of 2254 bp (in the case of C-terminal clones, **Figure 20B**, Lane 1 and 2) or 2253 bp (N-terminal clones, **Figure 20B**, Lane 3 and 4, in which only nº 4 was correct).

The colony in lane 2 was selected to create strain CRS210 (**Table 2**), which was used for the extraction of pGG5 (**Figure 21** and **22A, Table 3**), whilst colony in lane 4 was used for strain CRS211 (**Table 2)** and plasmid pGG6 extraction (**Figure 21** and **22B**, **Table 3**).

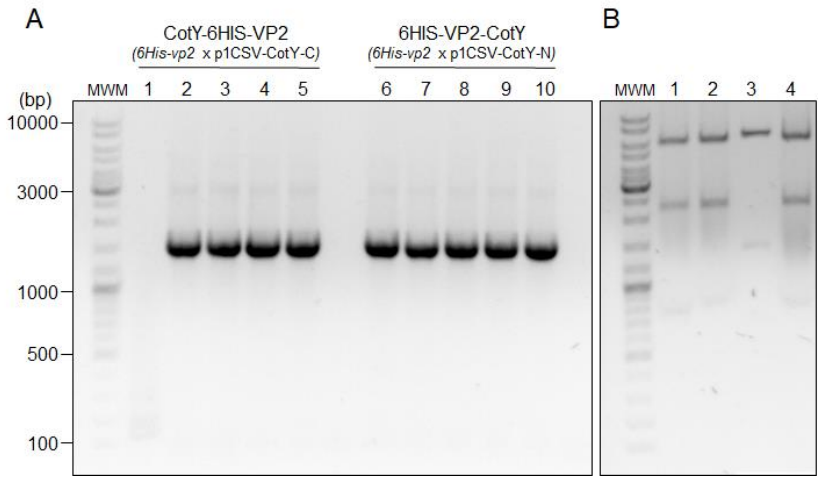


**Figure 20.** Gel electrophoresis of (**A**) the colony PCR to assess the presence of *6His-vp2* after transformation of *E. coli* competent cells. In the C-terminal transformation, four (lanes 2 to 5) of the five colonies tested were positive whilst all colonies tested for the N-terminal transformation were positive (lanes 6 to 10), since the product appear to be the same size of the original insert (1496 bp) (**B**). The extracted plasmids were digested with HindIII and PstI to confirm their structure, and positive colonies originated a pattern of two bands of approximately 6052 bp and 2254 bp in the case of C-terminal clones (lanes 1 and 2) or 2253 bp in N-terminal clones (lanes 3 and 4, only lane 4 was positive).

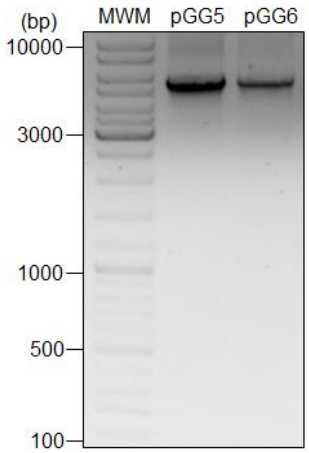


**Figure 21**. Gel electrophoresis of plasmids pGG5 (8306 bp) extracted from CRS210 and pGG6 (8305 bp) from CRS211.

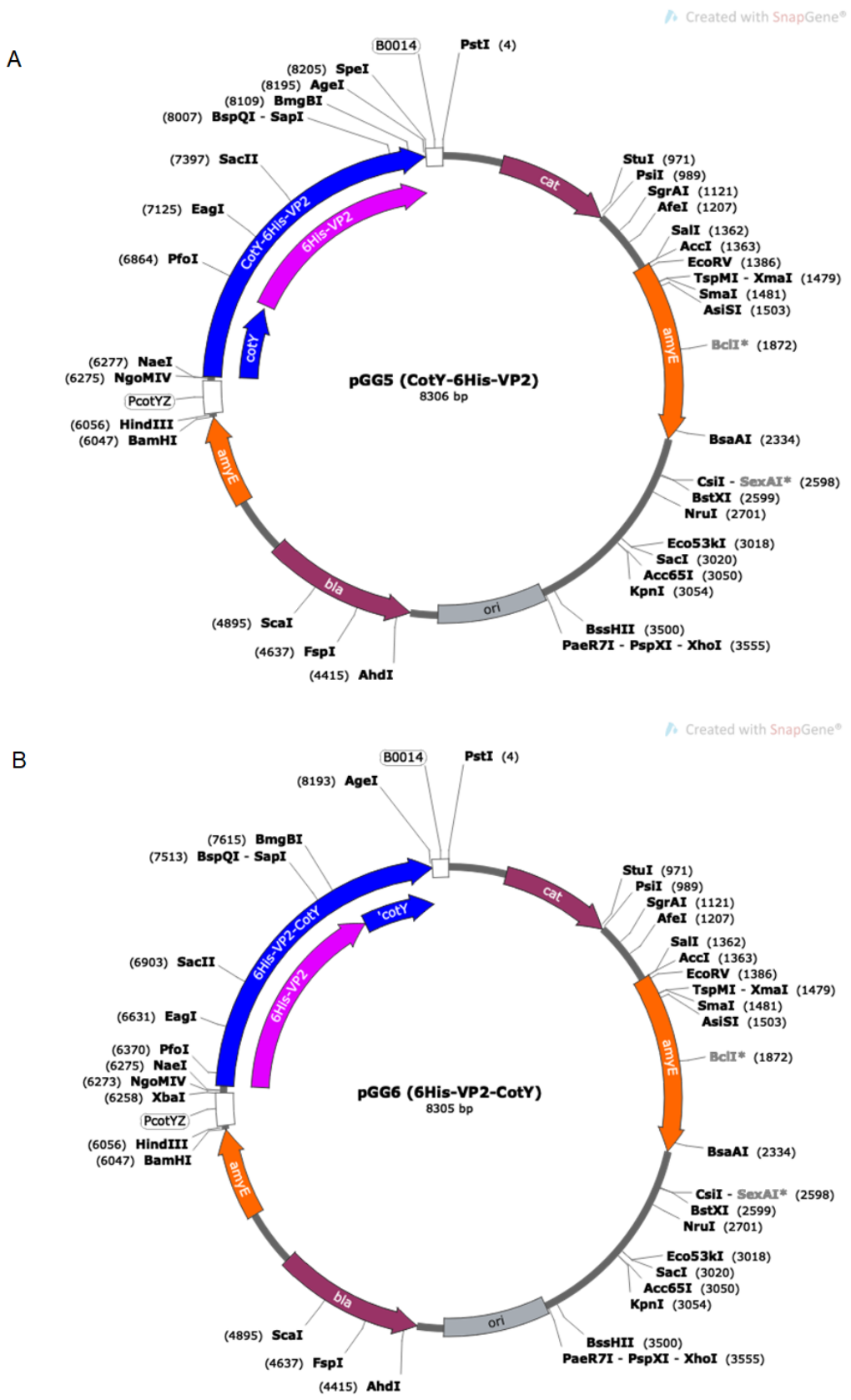


**Figure 22.** Schematic representation of **(A)** pGG5 and (**B)** pGG6 with the sites of restriction for unique cutters enzymes.

The presence of *6His-gfp* was confirmed by PCR (**Figure 23A**) and by restriction analysis with HindIII and PstI (**Figure 23B**) in all colonies tested of both clones *6His-gfp* x p1CSV-CotY-C and *6His-gfp* x p1CSV-CotY-N transformations. Positive clones originate a pattern of digestion constituted by two bands of 1567 bp (C-terminal clones) or 1566 bp (N-terminal clones) and 6052 bp (**Figure 23B**).

The colony in lane 2 was used to create strain CRS212 (**Table 2**) and for the extraction of pGG7 (**Figure 24** and **25A**, **Table 3**), whilst colony in lane 4 was used for strain CRS213 (**Table 2**) and plasmid pGG8 (**Figure 24** and **25B**, **Table 3**).

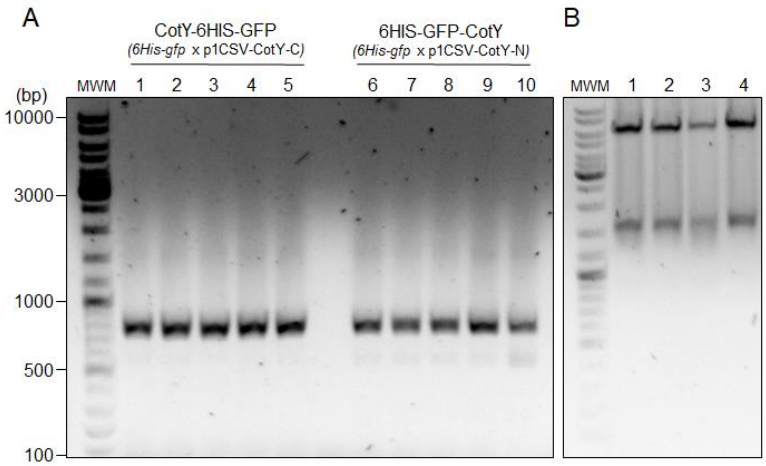


**Figure 23.** Gel electrophoresis of (**A**) the colony PCR to assess the presence of *6His-gfp* after transformation of *E. coli* competent cells. In the C-terminal transformation, the five (lanes 1 to 5) were positive which was also verified in the N-terminal transformation (lanes 6 to 10), since the product appear to be the same size of the original insert (809 bp) (**B**). The extracted plasmids were digested with HindIII and PstI to confirm their structure, and positive colonies originated a pattern of two bands of approximately 6052 bp and 1567 bp in the case of C-terminal clones (lanes 1 and 2) or 1566 bp in N-terminal clones (lanes 3 and 4).

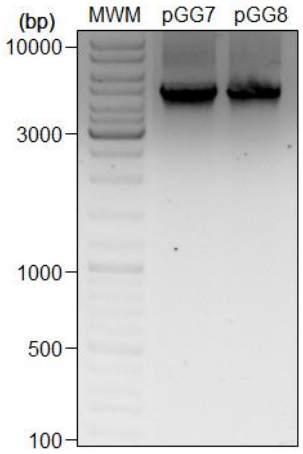


**Figure 24.** Gel electrophoresis of plasmids pGG7 (7619 bp) extracted from CRS212 and pGG8 (7618 bp) from CRS213.

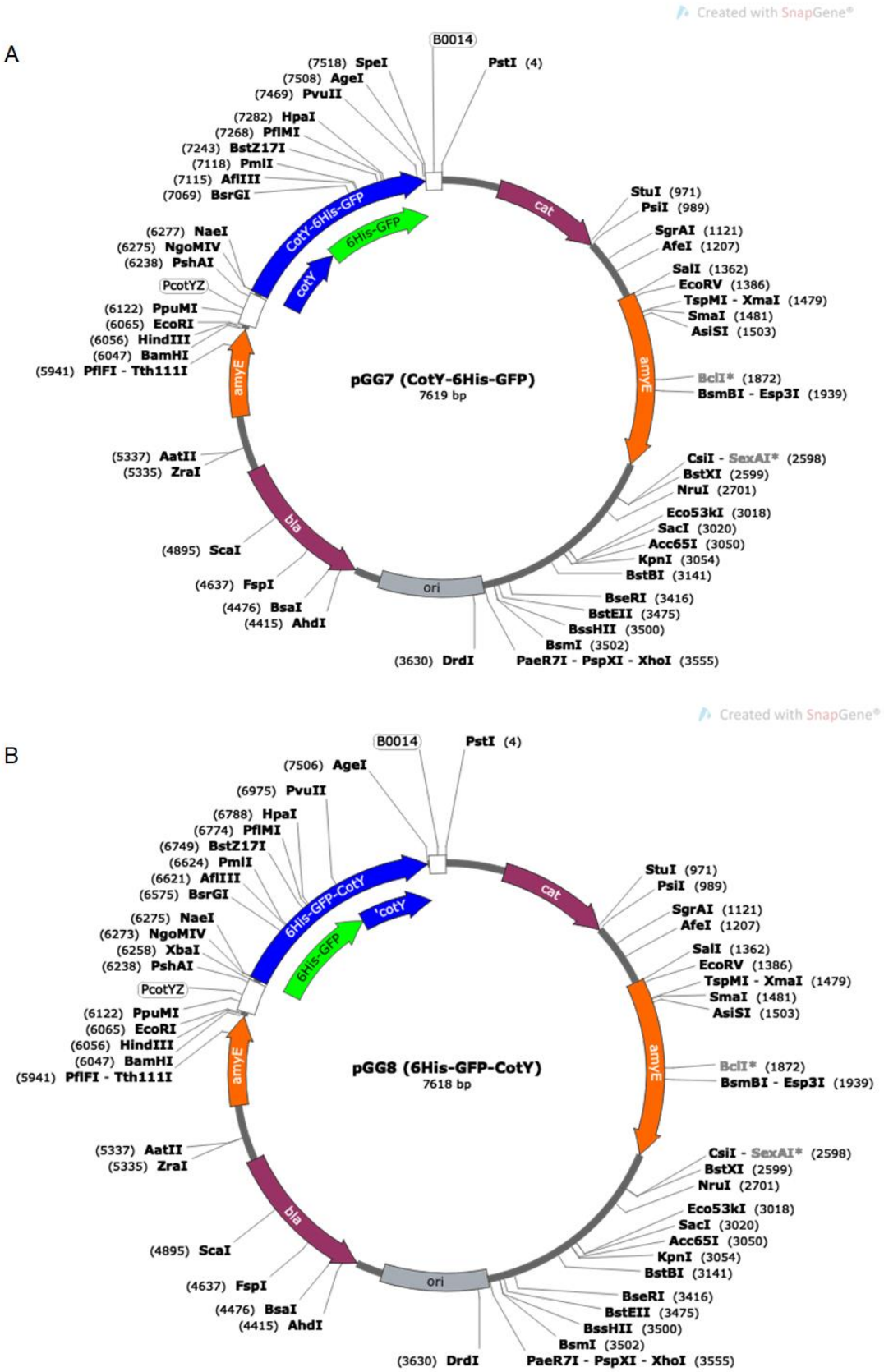


**Figure 25.** Schematic representation of **(A)** pGG7 and **(B)** pGG8 with the sites of restriction for unique cutters enzymes.

The presence of *6His-ompK* was confirmed by PCR (**Figure 26A**) and by restriction analysis with HindIII and PstI (**Figure 26B**) in all colonies tested of both clones *6His-ompK* x p1CSV-CotY-C and *6His-ompK* x p1CSV-CotY-N transformations. Positive clones originate a pattern of digestion constituted by two bands of 1585 bp (C-terminal clones) or 1584 bp (N-terminal clones) and 6052 bp (**Figure 26B**).

The colony in lane 1 originated strain CRS214 (**Table 2**), which was used for the extraction of pGG9 (**Figure 27** and **28A, Table 3**), whilst colony in lane 4 was used for strain CRS215 (**Table 2**) and plasmid pGG10 (**Figure 27** and **28B, Table 3**).

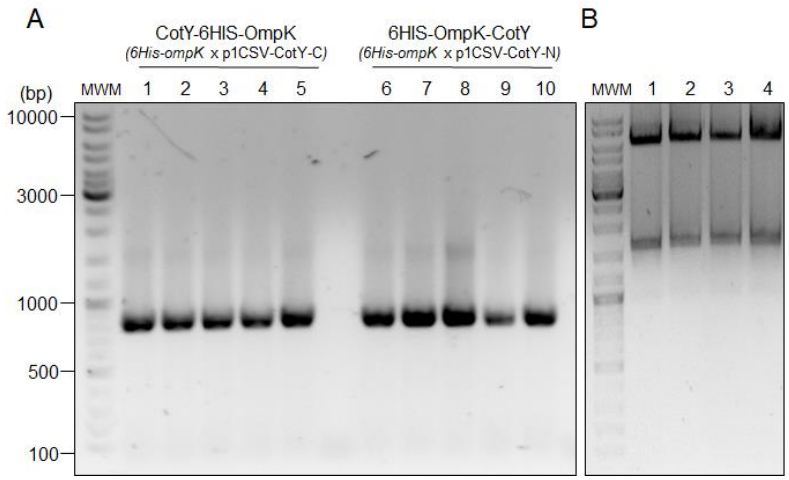


**Figure 26.** Gel electrophoresis of (**A**) the colony PCR to assess the presence of *6His-ompK* after transformation of *E. coli* competent cells. In the C-terminal transformation, the five (lanes 1 to 5) were positive, which was also verified in the N-terminal transformation (lanes 6 to 10), since the product appear to be the same size of the original insert (827 bp) (**B**). The extracted plasmids were digested with HindIII and PstI to confirm their structure and positive colonies originated a pattern of two bands of approximately 6052 bp and 1585 bp in the case of C-terminal clones (lanes 1 and 2) or 1584 bp in N-terminal clones (lanes 3 and 4).

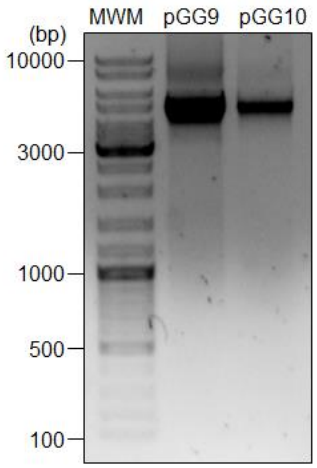


**Figure 27.** Gel electrophoresis of plasmids pGG9 (7637 bp) extracted from CRS214 and pGG10 (7636 bp) from CRS215.

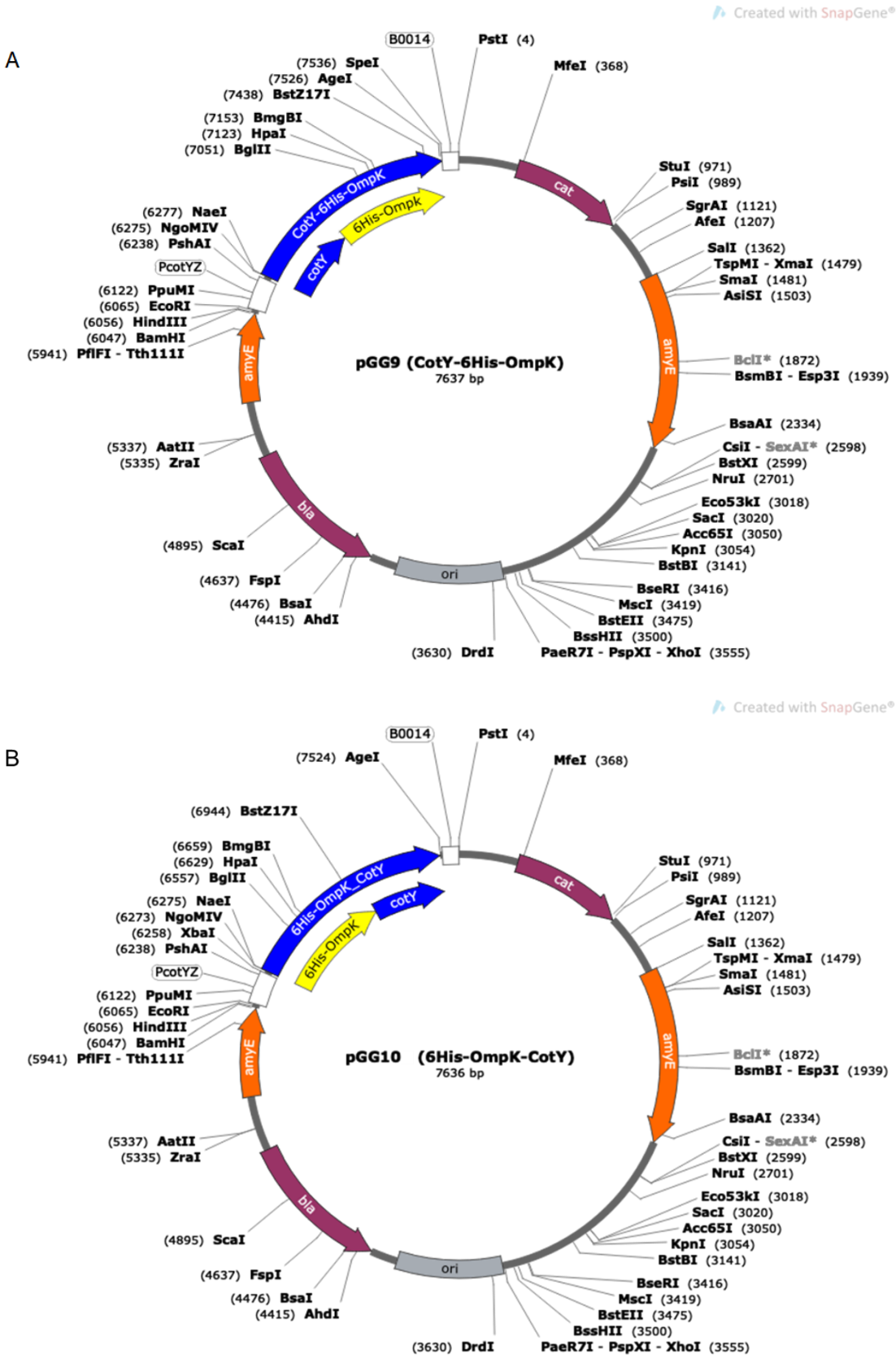


**Figure 28.** Schematic representation of **(A)** pGG9 and **(B)** pGG10 with the sites of restriction for unique cutters enzymes.

Each plasmid was successfully linearized with ScaI (**Figure 29A**) before transformation of *B. subtilis* 168 and FI99. A first attempt of transformation of *B. subtilis* 168 and strain FI99 with pGG5 to pGG10 was done using the GM1/GM2 method without success. Alternatively, competence of both *B. subtilis* 168 and strain FI99 was induce with competence medium MC.

Linearized plasmids pGG5 to pGG10 were integrated into *B. subtilis* 168 chromosome through a double-crossover event at the *amyE* locus (**Figure 30**). The resulting strains – CRS216, CRS217, CRS218, CRS219, CRS220 and CRS221 – are chloramphenicol resistant, allowing for an initial selection of positive clones. No transformants were obtained in the background FI99.

Chloramphenicol resistant colonies were inoculated in LB plates containing 1% starch along with a colony of *B. subtilis* 168, as negative control. Positive colonies were not able to degrade the starch, oppositely to the background strain *B. subtilis* 168.

The chromosomal DNA of each strain was extracted and used as template for a PCR amplification of the *amyE* region. The purified PCR products had the expected sizes – 5199 bp in CRS216, 5198 in CRS217, 4512 bp in CRS218, 4511 bp in CRS219, 4530 bp in CRS220 and 4529 bp in CRS221 (**Figure 29B** and **C)**, and revealed that each target was successfully cloned in frame with *cotY,* after sequencing.

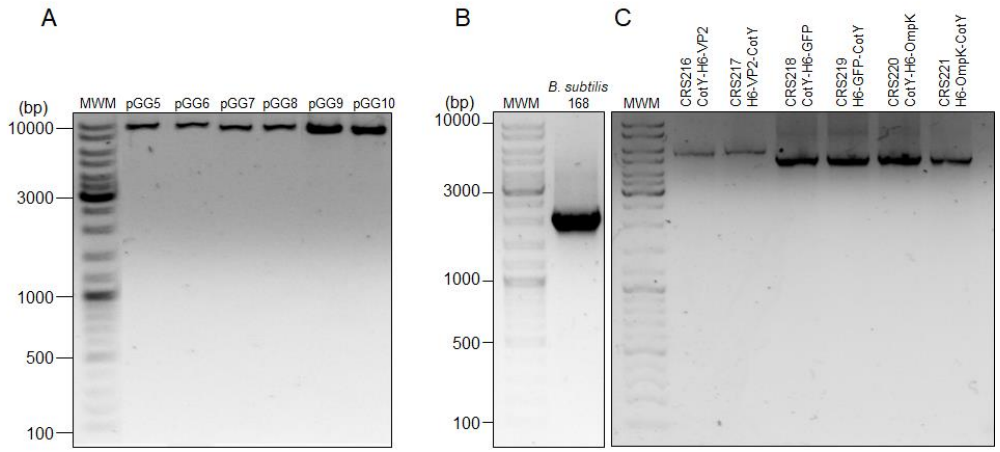


**Figure 29.** Gel electrophoresis of (**A**) the resulting linearization of pGG5, pGG6, pGG7, pGG8, pGG9 and pGG10 in the expected sizes. (**B**) PCR amplification of the *amyE* region using the parental strain as DNA template resulted in a band of smaller size than the ones obtained using the recombinant strains. (C) Bands of 5199 bp (CRS216), 5198 bp (CRS217), 4512 bp (CRS218), 4511 bp (CRS219), 4530 (CRS220) and 4529 (CRS221) indicate the successful integration of each fusion.

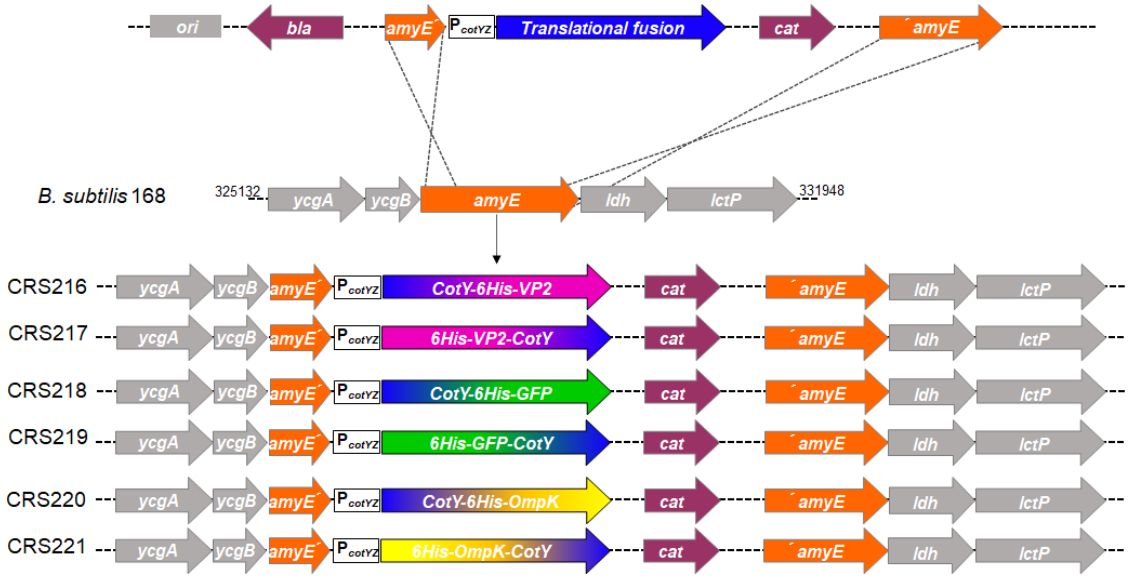


**Figure 30.** Schematic representation of a successful chromosomal integration of fusions *cotY-6His-VP2, 6His-VP2-cotY*, *cotY-6His-GFP, 6His-GFP-cotY, cotY-6His-OmpK* and *6His-OmpK-cotY* in *B. subtilis* 168, which occurs through a double-crossover event at the *amyE* locus, originating strains CRS216, CRS217, CRS218, CRS219, CRS220 and CRS221.

Purified spores from each strain were obtained after induction to sporulate in DSM broth for 24h. Spore coat proteins from strains CRS216, CRS217, CRS218, CRS219, CRS220 and CRS221 were separated in a 15% SDS-PAGE revealing a similar pattern to the proteins from the WT spores (**Figure 31A**). No bands reacting with the anti-HisTag antibody were present in the strains CRS216 (CotY-H6-VP2), CRS217 (H6-VP2-CotY), CRS219 (H6-GFP-CotY), CRS221 (H6-OmpK-CotY) and, as expected, in WT. The anti-HisTag antibody is recognizing bands of the expected sized in the case fusions CotY-H6-GFP (46 KDa) and CotY-H6-OmpK (45 KDa) (**Figure 31B**).

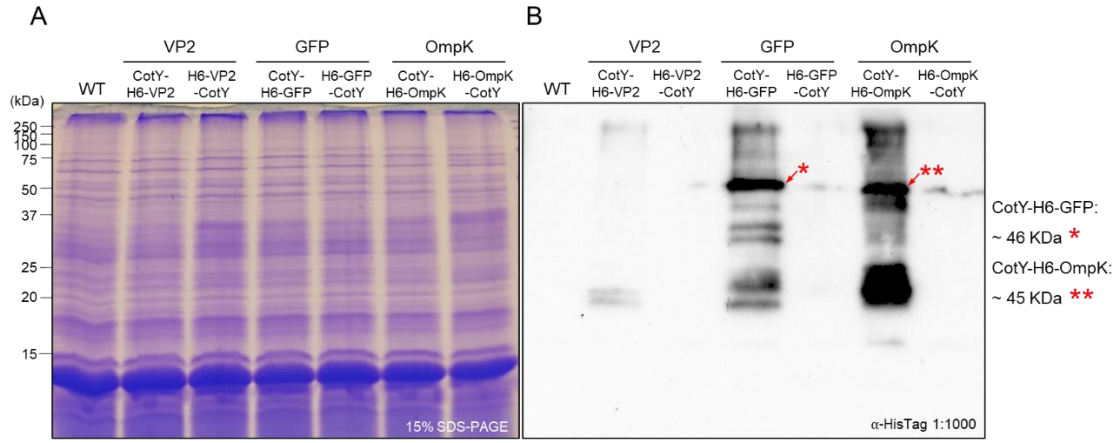


**Figure 31.** (**A**) Spores proteins from strains WT, CRS216 (CotY-H6-VP2), CRS217 (H6-VP2-CotY), CRS218 (CotY-H6-GFP), CRS219 (H6-GFP-CotY), CRS220 (CotY-H6-OmpK) and CRS221 (H6-OmpK-CotY) were separated in a 15% acrylamide gel, all revealing a similar pattern. (**B**) Western blot analysis using an anti-HisTag primary antibody (1:1000) detected two bands (indicated with red arrows) of approximately 46 KDa and 45 KDa equivalent to the sum of the MW of CotY (18 KDa) and H6-GFP (28 KDa) or H6-OmpK (27 KDa) in the C-terminal clones.

## 3.2. Observation of functional GFP at the surface of *B. subtilis* spores

Strains WT, CRS218 and CRS219 were grown in sporulation medium for 24h, stained with DNA-stain DAPI and observed by PC and fluorescence microscopy. Vegetative cells present as phase-dark in PC and exhibits blue fluorescence since DAPI enters the cell and stains the DNA. In sporulating cells, the developing spore becomes phase-bright in PC and the mother-cell continues phase dark. Free mature spores are phase-bright in PC, and DAPI does not enter the cell thus inhibiting the blue fluorescence signal.
Developing spores and free mature stores exhibit green fluorescence resulting from the expression of the functional protein GFP at their surface (**Figure 32)**. Spores from the strain CRS218 (fusion CotY-H6-GFP) have higher fluorescence intensity than spores from the strain CRS219 (fusion H6-GFP-CotY).

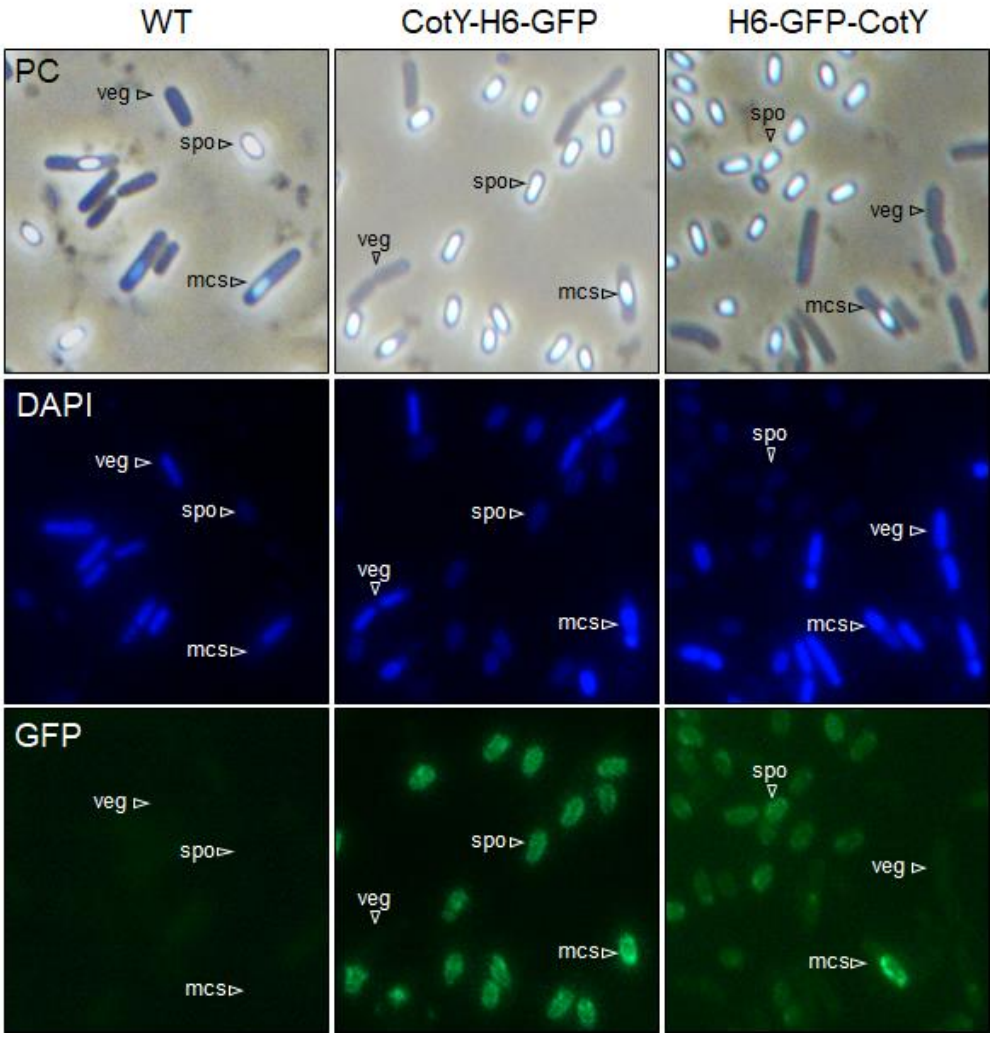


**Figure 32.** PC and fluorescence microscopy of 24h cultures of *B. subtilis* 168, CRS218 (CotY-H6-GFP) and CRS219 (H6-GFP-CotY), stained with DNA-stain DAPI. Vegetative cells (veg), sporulating cells (mother-cells) and free mature spores (spo) are indicated. Exposure time was the same for all samples.

## 3.3. Recombinant strains growth and viability evaluation

The parental strain *B. subtilis* 168 and its congenic derivatives CRS206, CRS208 and CRS216 to CRS221 were induced to sporulate by nutrient exhaustion in DSM broth. Bacterial growth and sporulation were monitored for the first 8h. The growth curves of each strain follow an identical behavior (**Figure 33**), and appear to enter the stationary phase around 4h after the initial inoculation, which corresponds to the beginning of sporulation (T0).

Quantification of cell titer before and after a heat treatment at 80ºC or an enzymatic treatment with lysozyme at T24 after the onset of sporulation, revealed that the number of viable cells of all cultures was similar to the control. *B. subtilis* 168 presented the higher percentage of sporulation, since 76% of the number of viable cells were heat resistant, and 73% were resistant to lysozyme (**Figure 34).** In general, recombinant strains presented a lower percentage of sporulation in comparison with WT strain. Strains CRS216, CRS217 and CRS221 presented the lowest percentage of heat and lysozyme resistant cells. The C-terminal or N-terminal type of fusion did not interfere significantly with the viability of sporulating cells.

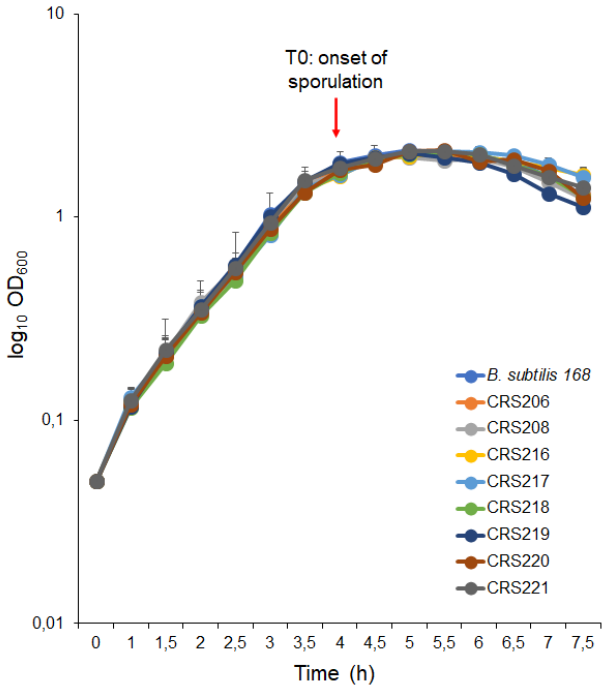


**Figure 33.** Growth curves of strain CRS206, CRS208, CRS216, CRS217, CRS218, CRS219, CRS220, CRS221 and *B. subtilis* 168 in DSM. Each culture started at an $OD_{600nm}$ of 0,05 and incubated at 37ºC and 150 rpm. $OD_{600nm}$ was measured at every 30 minutes for 8h. The sporulation onset is indicated with a red arrow, and occurred around 4h after initial inoculation. Data shown are the means of three independent experiments.

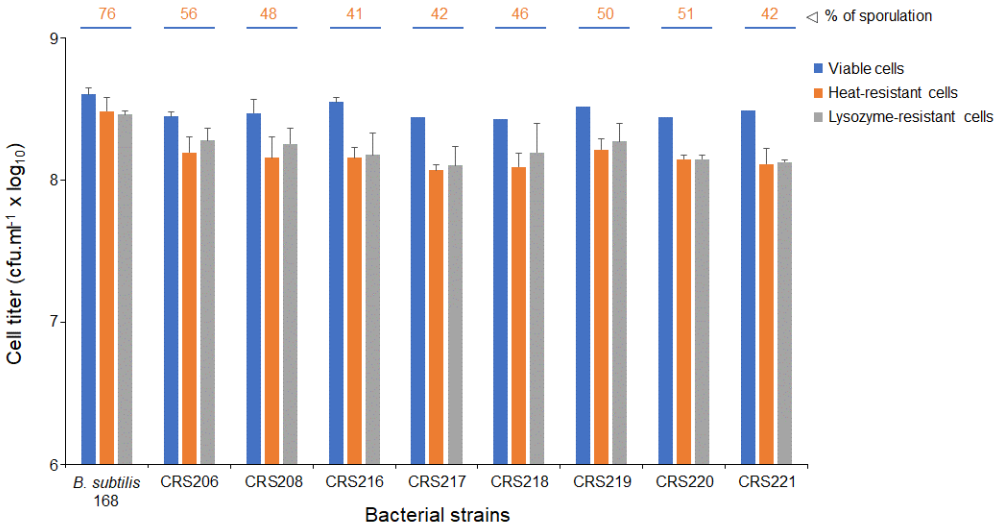


**Figure 34.** Titration of the number of cfu per milliliter of culture at T24 of recombinant strains CRS206, CRS208, CRS216, CRS217, CRS218, CRS219, CRS220 and CRS221 and WT, before (viable) and after (heat-resistant) a heat treatment and a lysozyme resistance test (lysozyme resistant). Data shown are the means of three independent experiments.

## 3.4. Recombinant spores immunomodulation potential

Challenge of zebrafish larvae with *V. anguillarum* revealed to be more deadly than the challenge with *V. parahaemolyticus*, revealing the different pathogenic character of both strains. Infection with *V. anguillarum* caused almost total mortality within 12 hours, while 40% of larvae were able to survive when exposed to *V. parahaemolyticus* (**Figure 35**). When previously treated (vaccinated) with spores from the WT strain *B. subtilis* 168 and CRS221 (H6-OmpK-CotY) no significantly reduction on larvae mortality was observed. On contrary, vaccination with spores exhibiting the fusion CotY-H6-OmpK (CRS220) induced a significant protective effect against both pathogens (**Figure 35**): larvae survival upon challenge with *V. parahaemolyticus* increased from 40 to 80% ($p$<0.05) and when challenged with *V. anguillarum* from 5 to 90% ($p$<0.001).

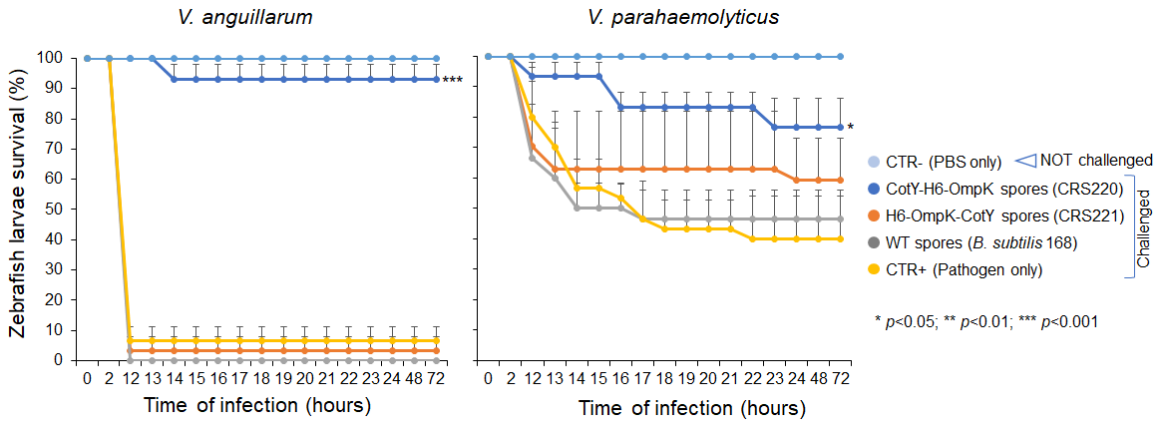


**Figure 35.** Zebrafish larvae were challenged with *V. anguillarum* and *V. parahaemolyticus* by immersion, three days after being vaccinated with spores from strains CRS220 (CotY-H6-OmpK), CRS221 (H6-OmpK-CotY) and WT (*B. subtilis* 168). Unvaccinated larvae (CTR+, pathogen only) and non-challenged larvae (CTR-, PBS only) were use as controls. Data shown are the means of three independent experiments. Significant differences area highlighted by a * ($p$<0.05) or *** ($p$<0.001).

# 4. Discussion

*Bacillus subtilis* have been extensively used in the aquaculture sector due to several beneficial effects, which include their role as probiotics, the improvement of the water quality, the increase in the assimilation of fish feed and the immunomodulation capacity (Nayak, 2020). *Bacillus* spp. are normal colonizers of the animal gastrointestinal tract, including aquatic organisms, and can sporulate, resulting in the most resistant form of life known so far. Spores can be ingested by terrestrial and aquatic organisms and are able to germinate, grow and resporulate (Tam et al., 2006). These characteristics make *Bacillus subtilis* the optimal delivery vehicle of antigens for the development of an oral vaccine to combat viral and bacterial diseases in aquaculture.

Although prophylactic measures against the pathogenic agents that cause the IPN and vibriosis are implemented in aquacultures, these diseases continue to be a concern worldwide due to the frequent outbreaks in fish farms and the high mortality associated (Jun et al., 2003; Ma et al., 2019). In this work, our focus was to develop an orally administrated vehicle of two selected immunogenic proteins, displaying each protein at the surface of spores of a domesticated *B. subtilis* laboratory strain and of an environmental *B. subtilis* strain previously isolated from European seabass gut, with probiotic characteristics (Serra et al., 2019). From IPNV, we choose the VP2 protein, an antigen that was used for the development of the commercially available injectable vaccine against the disease, but also for the experimental development of oral vaccines (Dhar et al., 2014; Min et al., 2012). Concerning the bacterial antigen, we chose the outer membrane protein OmpK, a shared antigen to several species of *Vibrio*, that has already been used as a subunit experimental vaccine with promising results (L. Li et al., 2019; Nguyen et al., 2018).

Our initial attempt was to display the VP2 protein at the spores' surface by creating a recombinant protein that consisted in a fusion between VP2 and the coat proteins CotB or CotC. These two coat proteins have been successfully used as carriers of both bacterial and viral proteins (Hinc et al., 2010; Jiang et al., 2019; Sun et al., 2018). In a study comparing the two carriers, a fusion with CotB resulted in the display of the target protein while the fusion with CotC resulted in a most efficient expression of the target protein (Hinc et al., 2010). Unfortunately, we were not able to achieve the CotB-VP2 and CotC-VP2 fusion at the spores' surface since we could not obtain a correct structure in the case of pGG1.

A second attempt was carried on using another strategy based on specifically dedicated plasmid vectors (Bartels et al., 2018) to display the VP2 antigen at the surface of *B. subtilis* spores. From the available sporovectos, using different coat proteins as carriers we chose CotY, a crust protein, since it was reported to give similar fluorescence intensity when GFP was fused C-terminally or N-terminally (Bartels et al., 2018). We use both p1CSV-CotY-C and p1CSV-CotY-N as plasmid vectors as the success of protein display at the surface of the spores is protein-specific and highly variable whether it is C- or N-terminally fused. We were able to transform *B. subtilis* 168 and obtain C-terminal and N-terminal translational fusions between VP2 and CotY. The obtained colonies were selected trough their resistance to chloramphenicol (the antibiotic resistance marker incorporated in the constructions) and their loss in the capacity to degrade starch, as a proof of integration at the *amyE* locus. Negative colonies do not grow in chloramphenicol plates and have the *amyE* gene intact allowing for the degradation of starch through the production of an α-amylase. If the chromosomal integration occurred correctly, the *amyE* gene is interrupted and therefore the colony is not able to degrade the starch. Two strains were obtained in the *B. subtilis* 168 background, CRS206 (CotY-VP2) and CRS208 (VP2-CotY), and the corresponding CotY-VP2 recombinant proteins were apparently detected in purified spores resolved by SDS-PAGE with an anti-VP2 antibody. Although a band with the expected size of 74 KDa, corresponding to the sum of the MWs of CotY (18 KDa) and VP2 (56 KDa) could be detected in the recombinant strains CRS206 and CRS208 and not in the parental strain *B. subtilis* 168, this detection by western blot was not always consistent. Different reasons might explain such result: i) the antibody was a very old one, kept since 1982 at -80ºC, and doubts about its integrity/stability were raise during the development of this work; ii) the epitope recognized by the anti-VP2 antibody might be out of reach, due to conformational changes that hide it iii) CotY can form clusters with other crust proteins (Bartels et al., 2019; J. Zhang et al., 1993), which can ultimately influence either the display of our target proteins in the surface of the spore or its detection. Thus, these highly cross-linked proteins structures made it possible that the recombinant proteins were not even entering the gel. To try to rule-out this hypothesis we resolved spore proteins in lower % acrylamide gels (reducing from the 15% to 10%) and used higher % of reducing (e.g. DTT) and denaturing (e.g. in-gel urea) agents to guarantee proper denaturing conditions. Despite all the different approaches, inconsistency in the detection of recombinant CotY-VP2 at the surface of the spores remained, leading us to seek alternative detection methods.

We chose to add one tag of 6 histidines at the N-terminal ends of the viral protein VP2 and the bacterial protein OmpK, to be able to detect the recombinant proteins using a

commercial antibody with established specificity and efficaccy. A fusion with GFP was also included as a technical control (since the display, if successful, is visible by microscopy) and to clarify if we could display a functional protein at the surface of the spores. Two fusions for each target protein were obtained in the *B. subtilis* 168 background, CRS216 (CotY-H6-VP2), CRS217 (H6-VP2-CotY), CRS218 (CotY-H6-GFP), CRS219 (H6-GFP-CotY), CRS220 (CotY-H6-OmpK) and CRS221 (H6-OmpK-CotY). The anti-HisTag antibody recognized intense bands of the expected sizes in the case of the C-terminal fusions CotY-6H-GFP and CotY-6H-OmpK, but no specific bands were detected in the case of both fusions with VP2 and in the N-terminal fusions of GFP and OmpK. These results did not clarify our doubts relative to the display of VP2 at the surface of *B. subtilis* spores. Again, the CotY-VP2 recombinant proteins can acquire a conformation that hides the 6His-tag epitope avoiding its recognition by the antibody, or it can form highly crosslinked clusters with other crust proteins (Bartels et al., 2019; J. Zhang et al., 1993), affecting either its display at the surface of the spore or its detection. We were not able to clarify it. These reasons might also explain why there was not detection of the recombinant CotY-OmpK and CotY-GFP proteins in the N-terminal versions as the successful display of the proteins at the surface of the spores depends not only in the nature of each protein, the type of fusion and the spatial and chimeric interactions with other proteins of the spores coat (Isticato et al., 2014; H. Wang et al., 2017).

Nevertheless, observation under the microscope showed that spores of strains bearing both C-ter and N-ter fusion of CotY-GFP (CRS218 and CRS219) could exhibit green fluorescence, showing that we were able not only to display GFP (as indicated by the western results in the case of the C-ter CRS218) but also to display a functional GFP protein at the surface of *B. subtilis* spores. Moreover, we could confirm that both strains produced mature spores: phase-bright under phase-contrast microscopy, indicative of heat-resistance, and impermeable to DAPI DNA staining, since the coat of the spores resists the entry of this agent, as opposing to the blue coloration observed in vegetative and sporulating cells. Curiously, spores harboring the C-terminal fusion CotY-H6-GFP (the only one detected by western blot analysis) exhibited higher intensity of fluorescence, as if the display was more efficient in this version.

All the recombinant strains exhibited a pattern of bacterial growth similar to the parental strain *B. subtilis* 168, initiating the process of sporulation approximately 4 hours after the initial inoculation, which corresponds to the beginning of the stationary phase (Errington, 2003). Although presenting a lower percentage of sporulation in comparison with the WT strain, all recombinant strains were able to originate heat and lysozyme resistant spores,

which indicated that the overall spores' structure was not affected whilst expressing the viral immunogenic protein VP2, the common Vibrio-antigen OmpK and the green fluorescence protein GFP. The reasons for the diminished sporulation % remain so far unknown, and its influence on other resistance characteristics of the resulting spores must be evaluated in future studies. This might be important in the context of the harsh gut ecosystem as well as for the industrial applications of the spores, namely for feed incorporation.

A preliminary toxicity test in zebrafish larvae indicated that we could expose the larvae to $10^8$ cfu per milliliter of a suspension of spores from *B. subtilis* 168, which was the maximum yield we obtained, without any visible harmful effect. Zebrafish larvae were then exposed to a suspension of purified spores from strains bearing the CotY-OmpK fusions (CRS220 and CRS221) three days before being infected with *V. anguillarum* and *V. parahaemolyticus,* as an attempt to evaluate their vaccine potential against vibriosis. Larvae "vaccinated" with spores displaying the C-terminal fusion CotY-H6-OmpK significantly increase the percentage of survival of larvae challenged with *V. anguillarum* and *V. parahaemolyticus*. The survival of unvaccinated larvae or of larvae "vaccinated" with spores of the WT parental strain (not carrying the CotY-OmpK) did not show significant improvement. These results indicate that spores displaying the immunogenic protein OmpK at their surface were able to protect zebrafish larvae from 2 different *Vibrio* pathogens and are thus promising vaccine vehicles against vibriosis in aquaculture.

# 5. Conclusions and future work

In this work, we were able to display two immunogenic proteins – VP2 from IPNV and OmpK from Vibrio – and the green fluorescence protein GFP, at the surface of *B. subtilis* 168 spores, using the crust protein CotY as carrier. Although the sequencing of the target genomic region indicated that all fusions were successfully integrated into *B. subtilis* 168 chromosome via a double cross-over event at the *amyE* locus, we were not able to detect by western blot analysis, the N-terminal versions of OmpK and GFP and have doubts on both VP2 fusions at the surface of the spores. On contrary, the C- terminal versions of OmpK and GFP were successfully detected, by western blot. GFP display at the spores' surface was further confirmed by fluorescence microscopy in both derivatives. Recombinant strains obtained were able to originate heat and lysozyme resistant spores, which is essential to their application as oral antigen delivery vehicles, as spores have to resist the harsh environment of the fish gastrointestinal tract. Our preliminary vaccination tests indicated that spores carrying the bacterial antigen OmpK can have a protective effect in zebrafish larvae when challenged with *V. anguillarum* and *V. parahaemolyticus*. Our work shows that spores have potential to be used as oral vaccines in aquaculture, namely against fish vibriosis. These tests are however preliminary and vaccination potential of recombinant spores should also be evaluated in animals of other ages, including adults. Toxicity tests should also be carried out with the recombinant OmpK strains, in a similarly way to what was done with WT *B. subtilis* spores, being zebrafish larvae the ideal systems of toxicity evaluation (Nishimura et al., 2016).

Ultimately, we were not able to transform the probiotic FI99, thus failing to fulfill our objective of constructing a ProbioSporoVaccine. The low competence associated with undomesticated strains and the fact that available laboratory methods of transformation are optimized for laboratory domesticated strains, like *B. subtilis* 168, might explain our difficulties. Other transformation methods should be tested in the strain FI99, namely electroporation (Duitman et al., 2007). This isolate has probiotic effects, and it would be interesting to assess how these characteristics influence the potential protective effect that recombinant spores have in zebrafish larvae.

# References

Ahmadivand, S., Soltani, M., M., B., Evensen, O., Alirahimi, E., Hassanzadeh, R., & Soltani, E. (2017). Oral DNA vaccines based on CS-TPP nanoparticles and alginate microparticles confer high protection against infectious pancreatic necrosis virus (IPNV) infection in trout. *Dev Comp Immunol, 74*, 178-189. doi:10.1016/j.dci.2017.05.004

Assefa, A., & Abunna, F. (2018). Maintenance of Fish Health in Aquaculture: Review of Epidemiological Approaches for Prevention and Control of Infectious Disease of Fish. *Veterinary Medicine International, 2018*. doi:10.1155/2018/5432497

Austin, B., & Austin, D. A. (2016). Chapter 1 Introduction. In *Bacterial Fish Pathogens* (pp. 1-19).

Balasuriya, U. B. R., Barratt-Boyes, S., Beer, M., Bird, B., Brownlie, J., Cullen, J. M., Delhon, G. A., Donis, R. O., Gardner, I., Gilkerson, J., Golde, W. T., Hartley, C., Heidner, H., Herden, C., & Kirkland, P. (2017). Chapter 16 - *Birnaviridae and Picobirnaviridae*. In N. J. MacLachlan & E. J. Dubovi (Eds.), *Fenner's Veterinary Virology* (pp. 319-325): Academic Press.

Banerjee, G., & Ray, A. K. (2017). The advancement of probiotics research and its application in fish farming industries. *Res Vet Sci, 115*, 66-77. doi:10.1016/j.rvsc.2017.01.016

Bartels, J., Bluher, A., Lopez Castellanos, S., Richter, M., Gunther, M., & Mascher, T. (2019). The *Bacillus subtilis* endospore crust: protein interaction network, architecture and glycosylation state of a potential glycoprotein layer. *Mol Microbiol, 112*(5), 1576-1592. doi:10.1111/mmi.14381

Bartels, J., Lopez Castellanos, S., Radeck, J., & Mascher, T. (2018). Sporobeads: The Utilization of the *Bacillus subtilis* Endospore Crust as a Protein Display Platform. *ACS Synth Biol, 7*(2), 452-461. doi:10.1021/acssynbio.7b00285

Bayliss, S. C., Verner-Jeffreys, D. W., Bartie, K. L., Aanensen, D. M., Sheppard, S. K., Adams, A., & Feil, E. J. (2017). The Promise of Whole Genome Pathogen Sequencing for the Molecular Epidemiology of Emerging Aquaculture Pathogens. *Front Microbiol, 8*, 121. doi:10.3389/fmicb.2017.00121

Caruffo, M., Navarrete, N. C., Salgado, O. A., Faundez, N. B., Gajardo, M. C., Feijoo, C. G., Reyes-Jara, A., Garcia, K., & Navarrete, P. (2016). Protective Yeasts Control *V. anguillarum* Pathogenicity and Modulate the Innate Immune Response of

Challenged Zebrafish (*Danio rerio*) Larvae. *Front Cell Infect Microbiol, 6*, 127. doi:10.3389/fcimb.2016.00127

Crane, M., & Hyatt, A. (2011). Viruses of fish: an overview of significant pathogens. *Viruses, 3*(11), 2025-2046. doi:10.3390/v3112025

Cutting, S. M., B. P. Vander-Horn. (1990). Genetic analysis. In C. R. Harwood & S. M. Cutting (Eds.), *Molecular biological methods for Bacillus* (pp. 27-74). Chichester, United Kingdom: John Wiley & Sons Ltd.

Dai, X., Liu, M., Pan, K., & Yang, J. (2018). Surface display of OmpC of *Salmonella* serovar *Pullorum* on *Bacillus subtilis* spores. *PLoS One, 13*(1), e0191627. doi:10.1371/journal.pone.0191627

Das, K., Thomas, T., Garnica, O., & Dhandayuthapani, S. (2016). Recombinant *Bacillus subtilis* spores for the delivery of *Mycobacterium tuberculosis* Ag85B-CFP10 secretory antigens. *Tuberculosis (Edinb), 101S*, S18-S27. doi:10.1016/j.tube.2016.09.016

de Hoon, M. J., Eichenberger, P., & Vitkup, D. (2010). Hierarchical evolution of the bacterial sporulation network. *Curr Biol, 20*(17), R735-745. doi:10.1016/j.cub.2010.06.031

Deng, Y., Xu, L., Chen, H., Liu, S., Guo, Z., Cheng, C., Ma, H., & Feng, J. (2020). Prevalence, virulence genes, and antimicrobial resistance of *Vibrio* species isolated from diseased marine fish in South China. *Sci Rep, 10*(1), 14329. doi:10.1038/s41598-020-71288-0

Dhar, A. K., Manna, S. K., & Thomas Allnutt, F. C. (2014). Viral vaccines for farmed finfish. *Virusdisease, 25*(1), 1-17. doi:10.1007/s13337-013-0186-4

Duc, L. H., Hong, H. A., Atkins, H. S., Flick-Smith, H. C., Durrani, Z., Rijpkema, S., Titball, R. W., & Cutting, S. M. (2007). Immunization against anthrax using *Bacillus subtilis* spores expressing the anthrax protective antigen. *Vaccine, 25*(2), 346-355. doi:10.1016/j.vaccine.2006.07.037

Duc, L. H., Hong, H. A., Fairweather, N., Ricca, E., & Cutting, S. M. (2003). Bacterial spores as vaccine vehicles. *Infect Immun, 71*(5), 2810-2818. doi:10.1128/iai.71.5.2810-2818.2003

Duitman, E. H., Wyczawski, D., Boven, L. G., Venema, G., Kuipers, O. P., & Hamoen, L. W. (2007). Novel methods for genetic transformation of natural *Bacillus subtilis* isolates used to study the regulation of the mycosubtilin and surfactin synthetases. *Appl Environ Microbiol, 73*(11), 3490-3496. doi:10.1128/AEM.02751-06

Errington, J. (1993). *Bacillus subtilis* Sporulation: Regulation of Gene Expression and Control of Morphogenesis. *Microbiological Reviews, 57*(1).

Errington, J. (2003). Regulation of endospore formation in *Bacillus subtilis*. *Nat Rev Microbiol, 1*(2), 117-126. doi:10.1038/nrmicro750

Errington, J., Murray, H., & Wu, L. J. (2005). Diversity and redundancy in bacterial chromosome segregation mechanisms. *Philos Trans R Soc Lond B Biol Sci, 360*(1455), 497-505. doi:10.1098/rstb.2004.1605

FAO. (2020). The State of World Fisheries and Aquaculture 2020. Sustainability in action. In *The State of World Fisheries and Aquaculture (SOFIA)* Rome, Italy.

Fečkaninová, A., Koščová, J., Mudroňová, D., Popelka, P., & Toropilová, J. (2017). The use of probiotic bacteria against *Aeromonas* infections in salmonid aquaculture. *Aquaculture, 469*, 1-8. doi:10.1016/j.aquaculture.2016.11.042

Frans, I., Michiels, C. W., Bossier, P., Willems, K. A., Lievens, B., & Rediers, H. (2011). *Vibrio anguillarum* as a fish pathogen: virulence factors, diagnosis and prevention. *J Fish Dis, 34*(9), 643-661. doi:10.1111/j.1365-2761.2011.01279.x

Girard, L. (2019). Quorum sensing in *Vibrio* spp.: the complexity of multiple signalling molecules in marine and aquatic environments. *Crit Rev Microbiol, 45*(4), 451-471. doi:10.1080/1040841X.2019.1624499

Gudding, R., & Van Muiswinkel, W. B. (2013). A history of fish vaccination: science-based disease prevention in aquaculture. *Fish Shellfish Immunol, 35*(6), 1683-1688. doi:10.1016/j.fsi.2013.09.031

Henriques, A. O., & Moran, C. P., Jr. (2007). Structure, assembly, and function of the spore surface layers. *Annu Rev Microbiol, 61*, 555-588. doi:10.1146/annurev.micro.61.080706.093224

Higgins, D., & Dworkin, J. (2012). Recent progress in *Bacillus subtilis* sporulation. *FEMS Microbiol Rev, 36*(1), 131-148. doi:10.1111/j.1574-6976.2011.00310.x

Hill, C., Guarner, F., Reid, G., Gibson, G. R., Merenstein, D. J., Pot, B., Morelli, L., Canani, R. B., Flint, H. J., Salminen, S., Calder, P. C., & Sanders, M. E. (2014). Expert consensus document. The International Scientific Association for Probiotics and Prebiotics consensus statement on the scope and appropriate use of the term probiotic. *Nat Rev Gastroenterol Hepatol, 11*(8), 506-514. doi:10.1038/nrgastro.2014.66

Hinc, K., Isticato, R., Dembek, M., Karczewska, J., Iwanicki, A., Peszynska-Sularz, G., De Felice, M., Obuchowski, M., & Ricca, E. (2010). Expression and display of

UreA of *Helicobacter acinonychis* on the surface of *Bacillus subtilis* spores. *Microb Cell Fact, 9*, 2. doi:10.1186/1475-2859-9-2

Ina-Salwany, M. Y., N., A.-S., A., M., Mursidi, F. A., Mohd-Aris, A., Amal, M. N. A., Kasai, H., Mino, S., Sawabe, T., & Zamri-Saad, M. (2019). Vibriosis in Fish: A Review on Disease Development and Prevention. *J Aquat Anim Health, 31*(1), 3-22. doi:10.1002/aah.10045

Isticato, R., & Ricca, E. (2014). Spore Surface Display. *Microbiology Spectrum, 2*(5). doi:10.1128/microbiolspec

Isticato, R., Sirec, T., Treppiccione, L., Maurano, F., De Felice, M., Rossi, M., & Ricca, E. (2013). Non-recombinant display of the B subunit of the heat labile toxin of *Escherichia coli* on wild type and mutant spores of *Bacillus subtilis*. *Microbial Cell Factories, 12*(98).

Isticato R., C. G., De Felice M., Ricca E. (2004). Display of Molecules on the Spore Surface. In H. A. Ricca E, Cutting SM (Ed.), *Bacterial spore formers: probiotics and emerging applications.* (pp. 193–200). Norfolk, UK: Horizon Biosience.

Jiang, H., Bian, Q., Zeng, W., Ren, P., Sun, H., Lin, Z., Tang, Z., Zhou, X., Wang, Q., Wang, Y., Wang, Y., Wu, M. X., Li, X., Yu, X., & Huang, Y. (2019). Oral delivery of *Bacillus subtilis* spores expressing grass carp reovirus VP4 protein produces protection against grass carp reovirus infection. *Fish Shellfish Immunol, 84*, 768-780. doi:10.1016/j.fsi.2018.10.008

Jun, L., & Woo, N. Y. S. (2003). Pathogenicity of vibrios in fish: An overview. *Journal of Ocean University of Qingdao, 2*(2), 117-128. doi:10.1007/s11802-003-0039-7

Kibenge, F. S. (2019). Emerging viruses in aquaculture. *Curr Opin Virol, 34*, 97-103. doi:10.1016/j.coviro.2018.12.008

Kuebutornye, F. K. A., Abarike, E. D., & Lu, Y. (2019). A review on the application of *Bacillus* as probiotics in aquaculture. *Fish Shellfish Immunol, 87*, 820-828. doi:10.1016/j.fsi.2019.02.010

Kunst, F., Ogasawara, N., Moszer, I., Albertini, A. M., Alloni, G., Azevedo, V., Bertero, M. G., Bessieres, P., Bolotin, A., Borchert, S., Borriss, R., Boursier, L., Brans, A., Braun, M., Brignell, S. C., Bron, S., Brouillet, S., Bruschi, C. V., Caldwell, B., Capuano, V., Carter, N. M., Choi, S. K., Cordani, J. J., Connerton, I. F., Cummings, N. J., Daniel, R. A., Denziot, F., Devine, K. M., Dusterhoft, A., Ehrlich, S. D., Emmerson, P. T., Entian, K. D., Errington, J., Fabret, C., Ferrari, E., Foulger, D., Fritz, C., Fujita, M., Fujita, Y., Fuma, S., Galizzi, A., Galleron, N., Ghim, S. Y., Glaser, P., Goffeau, A., Golightly, E. J., Grandi, G., Guiseppi, G.,

Guy, B. J., Haga, K., Haiech, J., Harwood, C. R., Henaut, A., Hilbert, H., Holsappel, S., Hosono, S., Hullo, M. F., Itaya, M., Jones, L., Joris, B., Karamata, D., Kasahara, Y., Klaerr-Blanchard, M., Klein, C., Kobayashi, Y., Koetter, P., Koningstein, G., Krogh, S., Kumano, M., Kurita, K., Lapidus, A., Lardinois, S., Lauber, J., Lazarevic, V., Lee, S. M., Levine, A., Liu, H., Masuda, S., Mauel, C., Medigue, C., Medina, N., Mellado, R. P., Mizuno, M., Moestl, D., Nakai, S., Noback, M., Noone, D., O'Reilly, M., Ogawa, K., Ogiwara, A., Oudega, B., Park, S. H., Parro, V., Pohl, T. M., Portelle, D., Porwollik, S., Prescott, A. M., Presecan, E., Pujic, P., Purnelle, B., Rapoport, G., Rey, M., Reynolds, S., Rieger, M., Rivolta, C., Rocha, E., Roche, B., Rose, M., Sadaie, Y., Sato, T., Scanlan, E., Schleich, S., Schroeter, R., Scoffone, F., Sekiguchi, J., Sekowska, A., Seror, S. J., Serror, P., Shin, B. S., Soldo, B., Sorokin, A., Tacconi, E., Takagi, T., Takahashi, H., Takemaru, K., Takeuchi, M., Tamakoshi, A., Tanaka, T., Terpstra, P., Togoni, A., Tosato, V., Uchiyama, S., Vandebol, M., Vannier, F., Vassarotti, A., Viari, A., Wambutt, R., Wedler, H., Weitzenegger, T., Winters, P., Wipat, A., Yamamoto, H., Yamane, K., Yasumoto, K., Yata, K., Yoshida, K., Yoshikawa, H. F., Zumstein, E., Yoshikawa, H., & Danchin, A. (1997). The complete genome sequence of the gram-positive bacterium *Bacillus subtilis*. *Nature, 390*(6657), 249-256. doi:10.1038/36786

Lam, S. H., Chua, H. L., Gong, Z., Lam, T. J., & Sin, Y. M. (2004). Development and maturation of the immune system in zebrafish, *Danio rerio*: a gene expression profiling, in situ hybridization and immunological study. *Developmental & Comparative Immunology, 28*(1), 9-28. doi:10.1016/s0145-305x(03)00103-4

Lanzilli, M., Donadio, G., Fusco, F. A., Sarcinelli, C., Limauro, D., Ricca, E., & Isticato, R. (2018). Display of the peroxiredoxin Bcp1 of *Sulfolobus solfataricus* on probiotic spores of *Bacillus megaterium*. *N Biotechnol, 46*, 38-44. doi:10.1016/j.nbt.2018.06.004

Lega, T., Weiher, P., Obuchowski, M., & Nidzworski, D. (2016). Presenting Influenza A M2e Antigen on Recombinant Spores of *Bacillus subtilis*. *PLoS One, 11*(11), e0167225. doi:10.1371/journal.pone.0167225

Li, L., Meng, H., Gu, D., Li, Y., & Jia, M. (2019). Molecular mechanisms of *Vibrio parahaemolyticus* pathogenesis. *Microbiol Res, 222*, 43-51. doi:10.1016/j.micres.2019.03.003

Li, N., Yang, Z., Bai, J., Fu, X., Liu, L., Shi, C., & Wu, S. (2010). A shared antigen among *Vibrio* species: outer membrane protein-OmpK as a versatile Vibriosis vaccine

candidate in Orange-spotted grouper (*Epinephelus coioides*). *Fish Shellfish Immunol, 28*(5-6), 952-956. doi:10.1016/j.fsi.2010.02.010

Lin, P., Yuan, H., Du, J., Liu, K., Liu, H., & Wang, T. (2020). Progress in research and application development of surface display technology using *Bacillus subtilis* spores. *Appl Microbiol Biotechnol, 104*(6), 2319-2331. doi:10.1007/s00253-020-10348-x

Liu, H., Yang, S., Wang, X., & Wang, T. (2019). Production of trehalose with trehalose synthase expressed and displayed on the surface of *Bacillus subtilis* spores. *Microb Cell Fact, 18*(1), 100. doi:10.1186/s12934-019-1152-7

Lucas, J. (2015). Aquaculture. *Curr Biol, 25*(22), R1064-1065. doi:10.1016/j.cub.2015.08.013

Lvov, D. K., Shchelkanov, M. Y., Alkhovsky, S. V., & Deryabin, P. G. (2015). Double-Stranded RNA Viruses. In *Zoonotic Viruses in Northern Eurasia* (pp. 113-133).

Ma, J., Bruce, T. J., Jones, E. M., & Cain, K. D. (2019). A Review of Fish Vaccine Development Strategies: Conventional Methods and Modern Biotechnological Approaches. *Microorganisms, 7*(11). doi:10.3390/microorganisms7110569

Mauriello, E. M., Duc le, H., Isticato, R., Cangiano, G., Hong, H. A., De Felice, M., Ricca, E., & Cutting, S. M. (2004). Display of heterologous antigens on the *Bacillus subtilis* spore coat using CotC as a fusion partner. *Vaccine, 22*(9-10), 1177-1187. doi:10.1016/j.vaccine.2003.09.031

McKenney, P. T., Driks, A., & Eichenberger, P. (2013). The *Bacillus subtilis* endospore: assembly and functions of the multilayered coat. *Nat Rev Microbiol, 11*(1), 33-44. doi:10.1038/nrmicro2921

Min, L., Li-Li, Z., Jun-Wei, G., Xin-Yuan, Q., Yi-Jing, L., & Di-Qiu, L. (2012). Immunogenicity of *Lactobacillus*-expressing VP2 and VP3 of the infectious pancreatic necrosis virus (IPNV) in rainbow trout. *Fish Shellfish Immunol, 32*(1), 196-203. doi:10.1016/j.fsi.2011.11.015

Mohamad, N., Amal, M. N. A., Ina-Salwany, M. Y., Saad, M. Z., Nasruddin, N. S., Al-saari, N., Mino, S., & Sawabe, T. (2019). Vibriosis in cultured marine fishes: a review. *Aquaculture, 512*. doi:10.1016/j.aquaculture.2019.734289

Nayak, S. K. (2020). Multifaceted applications of probiotic *Bacillus* species in aquaculture with special reference to *Bacillus subtilis*. *Reviews in Aquaculture*. doi:10.1111/raq.12503

Newaj-Fyzul, A., Al-Harbi, A. H., & Austin, B. (2014). Review: Developments in the use of probiotics for disease control in aquaculture. *Aquaculture, 431*, 1-11. doi:10.1016/j.aquaculture.2013.08.026

Nguyen, H. T., Nguyen, T. T. T., Chen, Y. C., Vu-Khac, H., Wang, P. C., & Chen, S. C. (2018). Enhanced immune responses and effectiveness of refined outer membrane protein vaccines against *Vibrio harveyi* in orange-spotted grouper (*Epinephelus coioides*). *J Fish Dis, 41*(9), 1349-1358. doi:10.1111/jfd.12828

Nishimura, Y., Inoue, A., Sasagawa, S., Koiwa, J., Kawaguchi, K., Kawase, R., Maruyama, T., Kim, S., & Tanaka, T. (2016). Using zebrafish in systems toxicology for developmental toxicity testing. *Congenit Anom (Kyoto), 56*(1), 18-27. doi:10.1111/cga.12142

Oidtmann, B., Dixon, P., Way, K., Joiner, C., & Bayley, A. E. (2018). Risk of waterborne virus spread - review of survival of relevant fish and crustacean viruses in the aquatic environment and implications for control measures. *Reviews in Aquaculture, 10*(3), 641-669. doi:10.1111/raq.12192

Olmos, J., Acosta, M., Mendoza, G., & Pitones, V. (2019). *Bacillus subtilis*, an ideal probiotic bacterium to shrimp and fish aquaculture that increase feed digestibility, prevent microbial diseases, and avoid water pollution. *Arch Microbiol*. doi:10.1007/s00203-019-01757-2

Oyarbide, U., Iturria, I., Rainieri, S., & Pardo, M. A. (2015). Use of gnotobiotic zebrafish to study *Vibrio anguillarum* pathogenicity. *Zebrafish, 12*(1), 71-80. doi:10.1089/zeb.2014.0972

Plomp, M., Monroe, A. C., Setlow, P., & Malkin, A. J. (2014). Architecture and Assembly of the *Bacillus subtilis* Spore Coat. *PLOS One, 9*(9). doi:10.1371/journal.pone.0108560.t001

Potot, S., Serra, C. R., Henriques, A. O., & Schyns, G. (2010). Display of recombinant proteins on *Bacillus subtilis* spores, using a coat-associated enzyme as the carrier. *Appl Environ Microbiol, 76*(17), 5926-5933. doi:10.1128/AEM.01103-10

Raszl, S. M., Froelich, B. A., Vieira, C. R., Blackwood, A. D., & Noble, R. T. (2016). *Vibrio parahaemolyticus* and *Vibrio vulnificus* in South America: water, seafood and human infections. *J Appl Microbiol, 121*(5), 1201-1222. doi:10.1111/jam.13246

Rendueles, O., Ferrieres, L., Fretaud, M., Begaud, E., Herbomel, P., Levraud, J. P., & Ghigo, J. M. (2012). A new zebrafish model of oro-intestinal pathogen colonization reveals a key role for adhesion in protection by probiotic bacteria. *PLoS Pathog, 8*(7), e1002815. doi:10.1371/journal.ppat.1002815

Reyes, M., Ramirez, C., Nancucheo, I., Villegas, R., Schaffeld, G., Kriman, L., Gonzalez, J., & Oyarzun, P. (2017). A novel "in-feed" delivery platform applied for oral DNA vaccination against IPNV enables high protection in Atlantic salmon (*Salmon salar*). *Vaccine, 35*(4), 626-632. doi:10.1016/j.vaccine.2016.12.013

Serra, C. R., Almeida, E. M., Guerreiro, I., Santos, R., Merrifield, D. L., Tavares, F., Oliva-Teles, A., & Enes, P. (2019). Selection of carbohydrate-active probiotics from the gut of carnivorous fish fed plant-based diets. *Sci Rep, 9*(1), 6384. doi:10.1038/s41598-019-42716-7

Setlow, P. (2006). Spores of *Bacillus subtilis*: their resistance to and killing by radiation, heat and chemicals. *J Appl Microbiol, 101*(3), 514-525. doi:10.1111/j.1365-2672.2005.02736.x

Setlow, P. (2014). Spore Resistance Properties. *Microbiol Spectrum, 2*(5:TBS-0003-2012). doi:doi:10.1128/microbiolspec.TBS-0003-2012

Silva, Y. J., Costa, L., Pereira, C., Mateus, C., Cunha, A., Calado, R., Gomes, N. C., Pardo, M. A., Hernandez, I., & Almeida, A. (2014). Phage therapy as an approach to prevent *Vibrio anguillarum* infections in fish larvae production. *PLoS One, 9*(12), e114197. doi:10.1371/journal.pone.0114197

Singh, K., Kallali, B., Kumar, A., & Thaker, V. (2011). Probiotics: A review. *Asian Pacific Journal of Tropical Biomedicine, 1*(2), S287-S290. doi:10.1016/s2221-1691(11)60174-3

Sirec, T., Strazzulli, A., Isticato, R., De Felice, M., Moracci, M., & Ricca, E. (2012). Adsorption of β-galactosidase of *Alicyclobacillus acidocaldarius* on wild type and mutants spores of *Bacillus subtilis*. *Microbial Cell Factories, 11*(100).

Steil, L., Serrano, M., Henriques, A. O., & Volker, U. (2005). Genome-wide analysis of temporally regulated and compartment-specific gene expression in sporulating cells of *Bacillus subtilis*. *Microbiology (Reading), 151*(Pt 2), 399-420. doi:10.1099/mic.0.27493-0

Sun, H., Lin, Z., Zhao, L., Chen, T., Shang, M., Jiang, H., Tang, Z., Zhou, X., Shi, M., Zhou, L., Ren, P., Qu, H., Lin, J., Li, X., Xu, J., Huang, Y., & Yu, X. (2018). *Bacillus subtilis* spore with surface display of paramyosin from *Clonorchis sinensis* potentializes a promising oral vaccine candidate. *Parasit Vectors, 11*(1), 156. doi:10.1186/s13071-018-2757-0

Takemura, A. F., Chien, D. M., & Polz, M. F. (2014). Associations and dynamics of Vibrionaceae in the environment, from the genus to the population level. *Front Microbiol, 5*, 38. doi:10.3389/fmicb.2014.00038

Tam, N. K., Uyen, N. Q., Hong, H. A., Duc le, H., Hoa, T. T., Serra, C. R., Henriques, A. O., & Cutting, S. M. (2006). The intestinal life cycle of *Bacillus subtilis* and close relatives. *J Bacteriol, 188*(7), 2692-2700. doi:10.1128/JB.188.7.2692-2700.2006

Tan, I. S., & Ramamurthi, K. S. (2014). Spore formation in *Bacillus subtilis*. *Environ Microbiol Rep, 6*(3), 212-225. doi:10.1111/1758-2229.12130

Thompson, F. L., Iida, T., & Swings, J. (2004). Biodiversity of vibrios. *Microbiol Mol Biol Rev, 68*(3), 403-431, table of contents. doi:10.1128/MMBR.68.3.403-431.2004

Toranzo, A. E., Magariños, B., & Romalde, J. L. (2005). A review of the main bacterial fish diseases in mariculture systems. *Aquaculture, 246*(1-4), 37-61. doi:10.1016/j.aquaculture.2005.01.002

Varas, M., Farina, A., Diaz-Pascual, F., Ortiz-Severin, J., Marcoleta, A. E., Allende, M. L., Santiviago, C. A., & Chavez, F. P. (2017). Live-cell imaging of *Salmonella Typhimurium* interaction with zebrafish larvae after injection and immersion delivery methods. *J Microbiol Methods, 135*, 20-25. doi:10.1016/j.mimet.2017.01.020

Wang, F., Song, T., Jiang, H., Pei, C., Huang, Q., & Xi, H. (2019). *Bacillus subtilis* Spore Surface Display of Haloalkane Dehalogenase DhaA. *Curr Microbiol, 76*(10), 1161-1167. doi:10.1007/s00284-019-01723-7

Wang, H., Wang, Y., & Yang, R. (2017). Recent progress in *Bacillus subtilis* spore-surface display: concept, progress, and future. *Appl Microbiol Biotechnol, 101*(3), 933-949. doi:10.1007/s00253-016-8080-9

Zhang, J., Fitz-James, P. C., & Aronson, A. I. (1993). Cloning and Characterization of a Cluster of Genes Encoding Polypeptides Present in the Insoluble Fraction of the Spore Coat of *Bacillus subtilis*. *Journal of Bacteriology, 175*, 3757-3766.

Zhang, L., & Orth, K. (2013). Virulence determinants for *Vibrio parahaemolyticus* infection. *Curr Opin Microbiol, 16*(1), 70-77. doi:10.1016/j.mib.2013.02.002

Zhang, L., Tian, X., Kuang, S., Liu, G., Zhang, C., & Sun, C. (2017). Antagonistic Activity and Mode of Action of Phenazine-1-Carboxylic Acid, Produced by Marine Bacterium *Pseudomonas aeruginosa* PA31x, Against *Vibrio anguillarum* In vitro and in a Zebrafish In vivo Model. *Front Microbiol, 8*, 289. doi:10.3389/fmicb.2017.00289

Zhang, X. H., He, X., & Austin, B. (2020). *Vibrio harveyi*: a serious pathogen of fish and invertebrates in mariculture. *Mar Life Sci Technol*, 1-15. doi:10.1007/s42995-020-00037-z

Zhu, L., Wang, X., Wang, K., Yang, Q., He, J., Qin, Z., Geng, Y., Ouyang, P., & Huang, X. (2017). Outbreak of infectious pancreatic necrosis virus (IPNV) in farmed rainbow trout in China. *Acta Trop, 170*, 63-69. doi:10.1016/j.actatropica.2017.02.025

Zhu, Z., Dong, C., Weng, S., & He, J. (2019). Identification of outer membrane protein TolC as the major adhesin and potential vaccine candidate for *Vibrio harveyi* in hybrid grouper, *Epinephelus fuscoguttatus* x *E. lanceolatus*. *Fish Shellfish Immunol, 86*, 143-151. doi:10.1016/j.fsi.2018.11.037

# Supplementary material


**Figure S1.** Schematic representation of the translational fusion of *cotY* and *vp2* in pGG3.The sequence of the represented region was successfully confirmed in pGG3 and CRS206.


**Figure S2.** Schematic representation of the translational fusion of *cotY* and *vp2* in pGG4.The sequence of the represented region was successfully confirmed in pGG4 and CRS208.


**Figure S3.** Schematic representation of the translational fusion of *cotY* and *6His-vp2* in pGG5. The sequence of the represented region was successfully confirmed in pGG5 and CRS216,


**Figure S4.** Schematic representation of the translational fusion of *cotY* and *6His-vp2* in pGG6. The sequence of the represented region was successfully confirmed in pGG6 and CRS217.

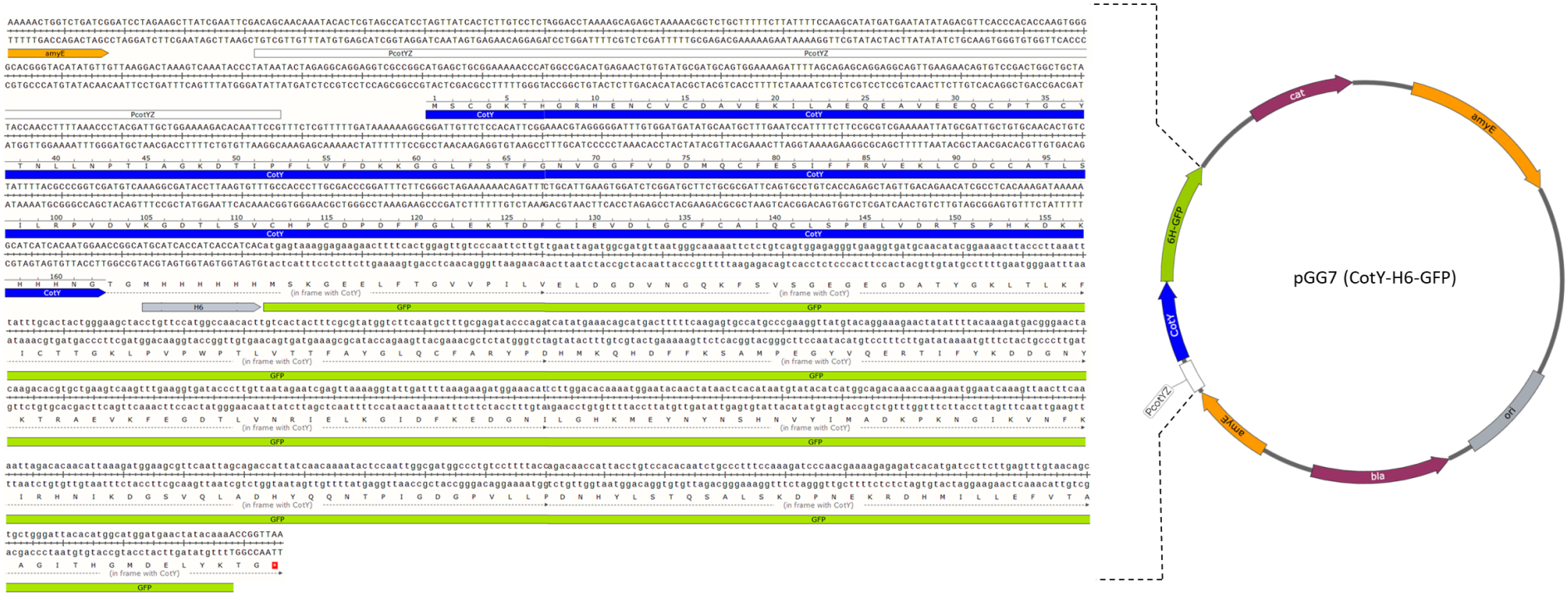


**Figure S5.** Schematic representation of the translational fusion of *cotY* and *6His-gfp* in pGG7. The sequence of the represented region was successfully confirmed in pGG7 and CRS218.

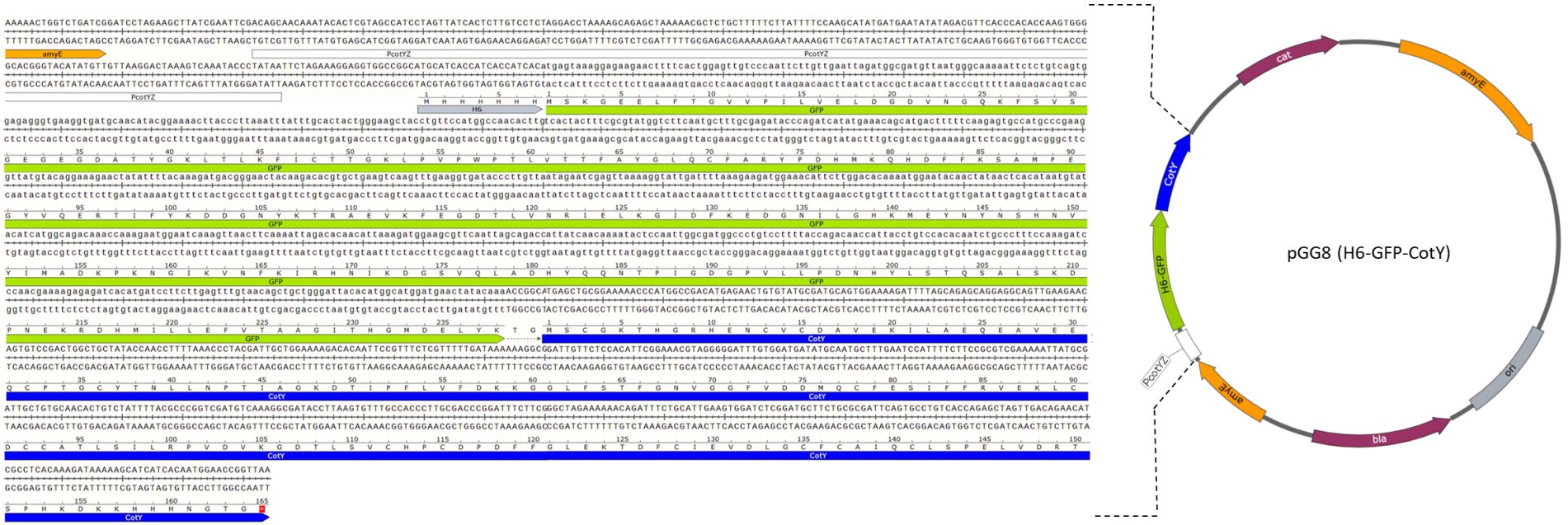


**Figure S6.** Schematic representation of the translational fusion of *cotY* and *6His-gfp* in pGG8. The sequence of the represented region was successfully confirmed in pGG8 and CRS219.

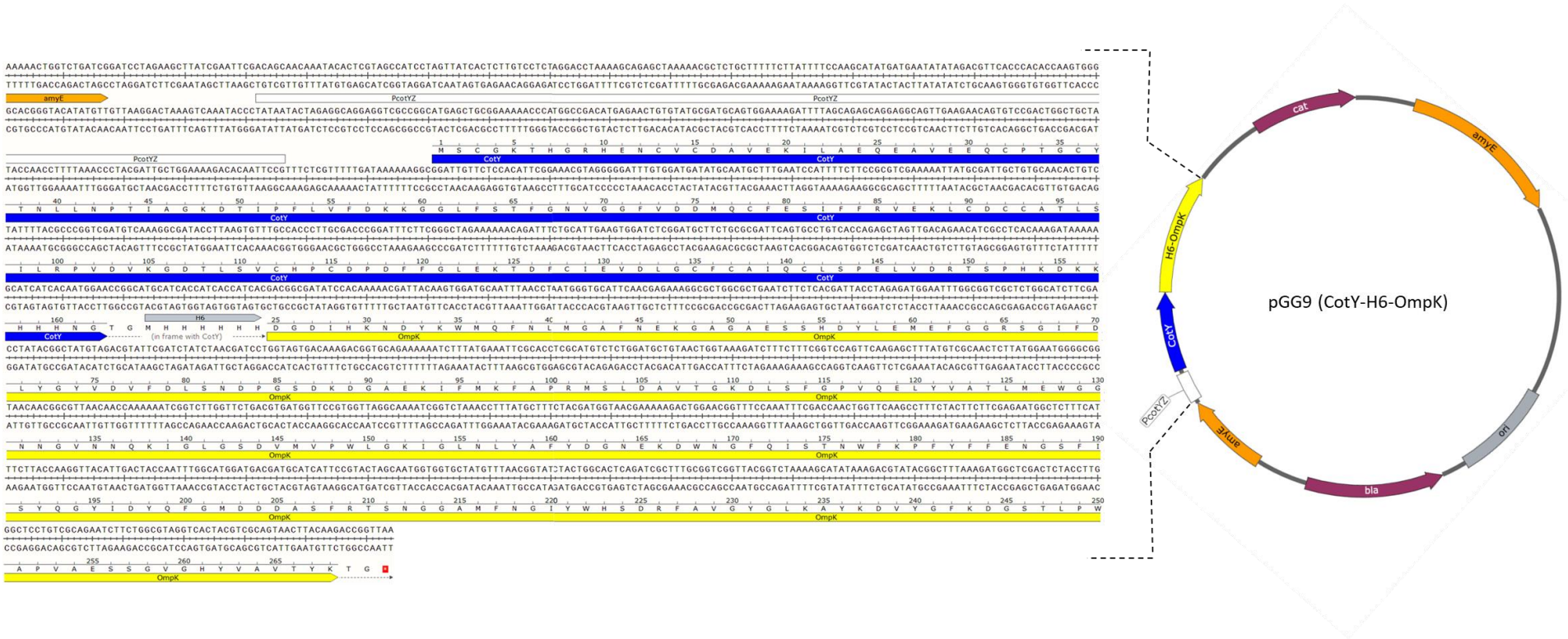


**Figure S7.** Schematic representation of the translational fusion of *cotY* and *6His-ompK* in pGG9. The sequence of the represented region was successfully confirmed in pGG9 and CRS220.


**Figure S8.** Schematic representation of the translational fusion of *cotY* and *6His-ompK* in pGG10. The sequence of the represented region was successfully confirmed in pGG10 and CRS221.